



AMERICAN UNIVERSITY OF BEIRUT

MODEL-BASED INVESTIGATION OF GAS  
EXCHANGE IN PULMONARY CAPILLARIES  
DUE TO VARIOUS SCENARIOS OF LUNG  
ABNORMALITIES AND TREATMENTS

by

ELIAS GEORGES MKANNA

A thesis

submitted in partial fulfillment of the requirements  
for the degree of Master of Engineering  
to the Department of Mechanical Engineering  
of the Faculty of Engineering and Architecture  
at the American University of Beirut

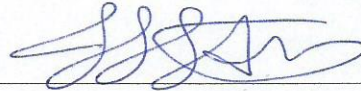
Beirut, Lebanon  
December 2015

AMERICAN UNIVERSITY OF BEIRUT

MODEL-BASED INVESTIGATION OF GAS  
EXCHANGE IN PULMONARY CAPILLARIES  
DUE TO VARIOUS SCENARIOS OF LUNG  
ABNORMALITIES AND TREATMENTS

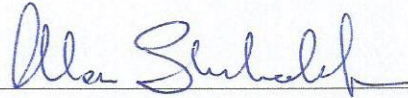
by  
ELIAS GEORGES MKANNA

Approved by:



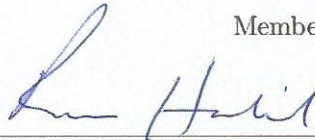
Prof. Issam Lakkis, Associate Professor  
Mechanical Engineering

Advisor



Prof. Alan Shihadeh, Professor  
Mechanical Engineering

Member of Committee



Prof. Robert Habib, Professor  
Internal Medicine

Member of Committee

Date of thesis defense: December 14, 2015

# AMERICAN UNIVERSITY OF BEIRUT

## THESIS, DISSERTATION, PROJECT RELEASE FORM

Student Name: Mkanna Elias Georges  
Last First Middle

Master's Thesis       Master's Project       Doctoral Dissertation

I authorize the American University of Beirut to: (a) reproduce hard or electronic copies of my thesis, dissertation, or project; (b) include such copies in the archives and digital repositories of the University; and (c) make freely available such copies to third parties for research or educational purposes.

I authorize the American University of Beirut, **three years after the date of submitting my thesis, dissertation, or project**, to: (a) reproduce hard or electronic copies of it; (b) include such copies in the archives and digital repositories of the University; and (c) make freely available such copies to third parties for research or educational purposes.

[Signature]  
Signature

December 16<sup>th</sup> 2015  
Date



# Acknowledgements

I am very grateful to all the people who helped me complete this work:

Prof. ISSAM LAKKIS, my thesis advisor, who supported me all along my work. He was my true mentor during my masters program at AUB. He was always available to help me manage my time and critically think about a complication to dissolve it correctly. I didn't have the chance to take a course with Dr. Lakkis in my undergraduate studies, so I had the determination to work with him in my graduate studies. And I am so lucky to have joined his research group this year.

Prof. ALAN LOUIS SHIHADAH, who always listens carefully to my progress during group meetings, and provides constructive advise to help improve the quality of the work.

Prof. ROBERT HABIB, from whom I learned a lot on lung physiology and HFOV treatment in clinical practice. His input in group meetings was always helpful to know that the lung model is on the right tracks.

Prof. SALAH ZEIN-EL-DINE, who enriched me with his deep knowledge on lung abnormalities and treatments in clinical practice.



# An Abstract of the Thesis of

Elias Georges Mkanna for Master of Engineering  
Major: Mechanical Engineering

Title: Model-Based Investigation of Gas Exchange in Pulmonary Capillaries Due to Various Scenarios of Lung Abnormalities and Treatments

Lung diseases (IRDS, lung obstructive diseases, apnea, lung interstitial emphysema, etc.) are a serious threat to human beings of all ages and typically lead to malfunctioning of the respiratory system that could cause death. The physical mechanisms behind clinical therapies that rely on various modalities of lung ventilation such as high frequency oscillatory ventilation (HFOV), are not yet fully understood. This is, in part, due to the limitations associated with in vivo measurements. The aim of this work is to present a physically-based lung model to investigate the effect of lung abnormalities and treatment scenarios on exchange of gases with the blood. This model builds on a previous model to accurately predict exchanges of  $O_2$  and  $CO_2$  with blood in the pulmonary capillaries. The previous model couples lung mechanics, gas transport in the airways and the alveoli, and blood oxygenation through diffusion of gases across the alveolar membrane. However, it was built for the purpose of studying the effect of Bubble CPAP on preterm infants. The current model will enhance the previous one by estimating lung parameters over a span of height, age, gender, and body weight to cover a wide variety of individuals. Not only the model will be generalized, it will also add the distribution of carbon dioxide in the respiratory system,



improve the numerical cost of the solution by efficiently coupling the air and blood side, and implement the dissociation curves to relate concentrations and partial pressures of gases in blood through the binding property of hemoglobin. Unlike lumped models in literature, the model takes into account the dynamics of the spatial distribution of respiratory gases in the airways and within individual alveoli, which leads to more accurate prediction of gases transport. Gas exchange is investigated with the variation of respiration frequency, pressure amplitude, tissue compliance, and airway resistance. The results show altered gas exchange in the case of lung abnormalities, justified by the solution of lung mechanics. Taking a scenario of a sick preterm infant, the physical mechanisms behind undergoing HFOV treatment are clarified in terms of gas exchange and lung mechanics. The ultimate goal of optimizing HFOV treatment parameters for severely sick preterm infants is achieved.

# Contents

<b>Acknowledgements</b>	<b>v</b>
<b>Abstract</b>	<b>vii</b>
<b>Nomenclature</b>	<b>xxi</b>
<b>1 Introduction</b>	<b>1</b>
1.1 Motivation for lung modeling . . . . .	2
1.2 Significance and impact . . . . .	3
1.3 Thesis' specific aims . . . . .	3
<b>2 Background and literature review</b>	<b>5</b>
2.1 Background . . . . .	5
2.1.1 Respiration mechanics . . . . .	6
2.1.2 The pulmonary membrane, the area of gases exchange . . . . .	10
2.1.3 Oxygen . . . . .	13
2.1.4 Carbon dioxide . . . . .	16
2.2 Models in literature . . . . .	18
2.2.1 Lung mechanics models . . . . .	19
2.2.2 Pulmonary system models . . . . .	20
2.3 The built model . . . . .	22
<b>3 Elements of the model</b>	<b>25</b>
3.1 Lung mechanics . . . . .	25

3.1.1	Frequency of respiration . . . . .	25
3.1.2	Lung volumes . . . . .	26
3.1.3	Nominal compliance and airway resistance . . . . .	30
3.1.4	Surfactant fraction . . . . .	31
3.1.5	The lung mechanics model . . . . .	32
3.1.6	Characteristic frequency . . . . .	37
3.2	Gases transport in the airways . . . . .	40
3.2.1	Modeling the airways . . . . .	40
3.2.2	Governing equations in the airways . . . . .	43
3.3	Gases reaching the alveoli . . . . .	44
3.3.1	Modeling the alveoli . . . . .	44
3.3.2	Governing equations in the alveoli . . . . .	45
3.4	Gas exchange and blood perfusion model . . . . .	46
3.4.1	The pulmonary membrane . . . . .	46
3.4.2	Getting the mixed boundary coefficients . . . . .	49
3.4.3	The dissociation curves . . . . .	50
3.4.4	Model and governing equations . . . . .	53
<b>4</b>	<b>Solution Approach and Validation</b>	<b>57</b>
4.1	Iterative solution . . . . .	57
4.2	Model Description . . . . .	58
4.2.1	input needed . . . . .	59
4.2.2	output generated . . . . .	60
4.3	Validation . . . . .	61
4.3.1	Compliance and airway resistance . . . . .	61
4.3.2	Lung mechanics in normal breathing . . . . .	62
4.3.3	Tuning contact area and getting the blood volume . . . . .	63
4.3.4	gases transport in normal breathing . . . . .	65
<b>5</b>	<b>Sensitivity Analysis</b>	<b>69</b>
5.1	Frequency sweep plots . . . . .	69

5.1.1	Preterm infant . . . . .	70
5.1.2	Adult male . . . . .	72
5.2	Parameter variation . . . . .	73
5.2.1	Pressure amplitude . . . . .	73
5.2.2	Compliance . . . . .	75
5.2.3	Airway resistance . . . . .	77
5.3	Derived Tidal Volume . . . . .	79
<b>6</b>	<b>Scenario investigation</b>	<b>83</b>
6.1	Lack of surfactant in preterm infants . . . . .	83
6.2	High frequency oscillatory ventilation . . . . .	86
6.3	Optimal frequency of oscillation . . . . .	87
6.4	Effect on gas exchange . . . . .	91
<b>7</b>	<b>Conclusion</b>	<b>95</b>
7.1	Effective summary . . . . .	95
7.2	Future directions . . . . .	96
<b>A</b>	<b>An overview on lung diseases</b>	<b>99</b>
<b>B</b>	<b>Detailed derivation of the ODC</b>	<b>103</b>



# List of Figures

2-1	The respiratory system and its components, and gas exchange between an alveolus and a capillary . . . . .	6
2-2	The interaction of respiratory muscles during expiration (left) and inspiration (right) . . . . .	7
2-3	Diffusion of oxygen and carbon dioxide through the different components of the pulmonary membrane between an alveolus and a capillary	11
2-4	Oxygen partial pressure build-up with distance traveled by the blood in the pulmonary capillaries . . . . .	13
2-5	The oxygen-hemoglobin dissociation curve shown as hemoglobin saturation (left axis) or oxygen concentration (right axis) as a function of oxygen partial pressure . . . . .	15
2-6	Carbon Dioxide partial pressure drop, with distance traveled by the blood, in the pulmonary capillaries . . . . .	17
2-7	The carbon dioxide dissociation curve, shown as the concentration of carbon dioxide versus its partial partial in the blood . . . . .	19
3-1	Plot of the lung volume versus the airway pressure depicting the static model for a preterm infant (girl), the lung volume is zero before the 5 cmH <sub>2</sub> O open pressure . . . . .	33
3-2	The symmetric pressure signal representing the oscillation of the gauge airway pressure, the frequency of the signal is that of a preterm infant (45 breaths per minute or 0.75 Hz) . . . . .	34

3-3	Schematic showing the electric equivalence of the small signal dynamic model, $\delta P(t) = -P_{ip}(t)$ . . . . .	36
3-4	Characteristic frequency versus tissue compliance for a preterm infant, the red lines show the nominal value . . . . .	39
3-5	Characteristic frequency versus airway resistance for a preterm infant, the red lines show the nominal value . . . . .	39
3-6	Characteristic frequency versus pressure amplitude for a preterm infant, the red lines show the nominal value . . . . .	40
3-7	A simple schematic showing an airway tube with a particle of oxygen crossing to reach the alveoli. The particle of oxygen is subject to a Poiseuille flow . . . . .	42
3-8	Schematic showing an airway tube with an appropriate control volume to derive the advection-diffusion equation . . . . .	43
3-9	Section of the airways from figure 3-8, showing an alveolus and the components of the alveolar governing equation . . . . .	46
3-10	Plot of the oxygen dissociation curve as hemoglobin saturation versus oxygen partial pressure for typical values of carbon dioxide partial pressure. The magnification shows the Bohr effect, a leftward shift with lower partial pressure of carbon dioxide . . . . .	52
3-11	Plot of the carbon dioxide dissociation curve as concentration versus partial pressure for typical values hemoglobin saturation with oxygen. The Haldane effect is shown, a leftward shift with lower hemoglobin saturation. . . . .	53
3-12	schematic showing the control volume taken to derive the advection diffusion equation for oxygen in the pulmonary capillary . . . . .	55
4-1	Calculated airway resistance versus age from a preterm infant to a 20 years old adult . . . . .	62

4-2	Lung mechanics results for a normal breathing case of a preterm infant (girl) and a 20 years old male. The plots on the left show the intrapleural pressure signal (blue), the alveolar pressure signal (green), and the airways' pressure signal (magenta). The plots in middle show the lung volume with the nominal values of FRC (blue) and tidal volume (red). The plots on the right show the pressure versus volume hysteresis curves. 2 respiration cycles are shown. . . . .	63
4-3	The variation of contact area $CA$ for optimal gas exchange, with age and gender. $CA$ is a controlled input of the model, and the data point plotted are the fine-tuned values of $CA$ to yield in an optimal gas exchange. . . . .	64
4-4	The variation of blood volume $V_b$ with age. The plot is similar for both genders . . . . .	65
4-5	The spatial distribution of oxygen (red) and carbon dioxide (blue) in the airways (left plot) and the capillaries (middle and right plots) at the beginning of an inspiration and the beginning of the following expiration for a preterm infant (girl). The third respiration cycle is considered.	66
4-6	The variation of oxygen mean partial pressure $P_{O_{2,b}}$ (red) and carbon dioxide mean partial pressure $P_{CO_{2,b}}$ (blue) with time, coupled with the lung volume variation (two similar top plots) for a preterm infant (girl). 10 respiration cycles are shown. . . . .	67
5-1	Dependence of oxygenation and ventilation on the frequency of respiration for a preterm infant, at nominal values of pressure amplitude, compliance, and resistance. The black curve is the ratio of the tidal volume to the dead space volume (right vertical axis) as a function of the frequency. The dashed horizontal line indicate a tidal volume equal to the dead space volume . . . . .	70



5-2	Dependence of oxygenation and ventilation on the frequency of respiration for a 20 years old male, at nominal values of the pressure amplitude, the compliance, and the resistance. The black curve is the ratio of the tidal volume to the dead space volume (right vertical axis) as a function of the frequency. The dashed horizontal line indicate a tidal volume equal to the dead space volume . . . . .	72
5-3	Sensitivity of oxygenation on the pressure amplitude over a frequency sweep at nominal values of compliance, and resistance, for an adult male (20 years old). . . . .	74
5-4	Sensitivity of ventilation on the pressure amplitude over a frequency sweep at nominal values of compliance, and resistance, for an adult male (20 years old). . . . .	75
5-5	Sensitivity of oxygenation on the tissue compliance over a frequency sweep, at nominal values of pressure amplitudes and resistance, for an adult male (20 years old). . . . .	76
5-6	Sensitivity of ventilation on the tissue compliance over a frequency sweep, at nominal values of pressure amplitudes and resistance, for an adult male (20 years old). . . . .	76
5-7	Sensitivity of oxygenation on the airway resistance over a frequency sweep, at nominal values of pressure amplitude and compliance, for an adult male (20 years old). . . . .	77
5-8	Sensitivity of ventilation on the airway resistance over a frequency sweep, at nominal values of pressure amplitude and compliance, for an adult male (20 years old). . . . .	78
5-9	The characteristic frequency versus the pressure amplitude for an adult male. the red lines indicate the characteristic frequency at 5 cmH <sub>2</sub> O and 3 cmH <sub>2</sub> O. . . . .	81
5-10	The characteristic frequency versus the tissue compliance for an adult male. The red lines indicate the characteristic frequency at nominal compliance, 10 % decrease, and 50 % decrease. . . . .	81

5-11	The characteristic frequency versus the airway resistance for an adult male. The red lines indicate the characteristic frequency at nominal resistance, 50 % increase, and 200 % increase. . . . .	82
6-1	The implemented surfactant model. The left plot shows the open pressure (solid line) and the needed minimum airway pressure (line with circles) versus the surfactant fraction. The right plot shows the decrease in compliance with surfactant fraction (the nominal compliance level is at 3.05 mL/cmH2O). . . . .	84
6-2	The implemented P-V model for the cases of normal presence of surfactant ( $SF=1$ ) and absence of surfactant ( $SF=0$ ). Sick Preterm infants have a higher open pressure equal to 5 cmH2O + $MAP$ , and a lower compliance shown in the flatter violet curve. . . . .	85
6-3	Plot showing the pressure amplitude as a function of frequency to yield an optimal gas exchange (proper oxygenation and ventilation) for the sick preterm infant. $MAP=10.7$ cmH2O $f_{i,O_2}=21$ % . . . . .	88
6-4	Plot showing the pressure amplitude as a function of frequency to yield an optimal gas exchange for several compliance levels. $MAP=10.7$ cmH2O $f_{i,O_2}=21$ % . . . . .	89
6-5	Plot showing the ratio of tidal volume to dead space volume as a function of frequency to yield an optimal gas exchange for several compliance levels. $MAP=10.7$ cmH2O $f_{i,O_2}=21$ % . . . . .	90
6-6	Plot showing the mean airway pressure as a function of frequency to yield an optimal gas exchange for several compliance levels. $MAP=10.7$ cmH2O $f_{i,O_2}=21$ % . . . . .	90
6-7	The effect of the pressure amplitude (x-axis), frequency (legends) and breathed fraction of oxygen (legend) on oxygenation, for a sick preterm infant (-32 % $C_{tissue}$ ), with $MAP=10.7$ cmH2O. The black dashed line indicates the oxygen level of the sick infant . . . . .	92

6-8 The effect of the pressure amplitude (x-axis), frequency (legends) and  
breathed fraction of oxygen (legend) on ventilation, for a sick preterm  
infant (-32 %  $C_{tissue}$ ), with  $MAP=10.7$  cmH<sub>2</sub>O. The black dashed line  
indicates the carbon dioxide level of the sick infant . . . . . 93

# List of Tables

B.1	Concentration definition for the derivation of the ODC . . . . .	103
B.2	Chemical reactions and balance equations in the blood . . . . .	104



# Nomenclature

Symbol	Units	Description
$A_d$	$m^2$	Area of diffusion
$A$	years	Age
$A_p$	$m^2$	Airway pipe cross sectional area
$A_{tube}$	$m^2$	Airway tube cross sectional area
$A_{CA}$	$m^2$	Alveolar-capillary contact area
$A_{cap}$	$m^2$	Capillary cross sectional area
$BW$	$kg$	Body weight
$\beta$	–	Static model constant
$C_{aq}$	$mol/m^3$	Concentration of a gas in an aqueous medium
$C_{NOM}$	$m^3/Pa$	Nominal tissue compliance
$C_{surfactant}$	$m^3/Pa$	Compliance due to lack of surfactant
$C_{tissue}$	$m^3/Pa$	Tissue compliance
$CO_2(x, t)$	$mol/m^3$	Carbon dioxide concentration in the airways
$\bar{CO}_2(t)$	$mol/m^3$	Mean carbon dioxide concentration in the alveoli
$CO_{2,b}(t)$	$mol/m^3$	Mean carbon dioxide concentration in the blood
$CA$	%	Percent alveolar-capillary contact area
$\Delta p$	Pa	Pressure difference across alveolar membrane
$d$	m	Distance of diffusion
$DR$	$mol/s.m^2$	Net rate of diffusion
$D$	$mol/Pa.s.m$	Diffusion coefficient for a pressure difference
$\mathfrak{D}$	$m^2/s$	Diffusion coefficient for a concentration difference
$DV$	$m^3$	Dead space volume

<b>Symbol</b>	<b>Units</b>	<b>Description</b>
$\delta P(t)$	Pa	Applied pressure signal
$\Delta P$	Pa	Pressure amplitude
$D_{cap}$	m	Capillary diameter
$ERV$	$m^3$	Expiratory reserve volume
$FRC$	$m^3$	Functional residual capacity
$f$	Hz	Frequency of respiration
$f^*$	Hz	Characteristic frequency
$\gamma_{water}$	Pa.m	Water surface tension
$he$	cm	Height
$H$	m	Height
$h^0$	m	Nominal thickness of the alveolar membrane
$h$	m	Thickness of the alveolar membrane
$IRV$	$m^3$	Inspiratory reserve volume
$IC$	$m^3$	Inspiratory capacity
$k_H$	Pa. $m^3$ /mol	Henry's constant
$k_H^{pc}$	Pa. $m^3$ /mol	Henry's constant pressure to concentration
$k_H^{cc}$	–	Henry's constant concentration to concentration
$L^*$	m	Characteristic airway length
$L_{pipe}$	m	Airway pipe length
$L_{tube}$	m	Airway tube length
$L_{cap}$	m	Capillary length around an alveolus
$MW$	kg/mol	Molecular weight of a gas
$\mu$	Pa.s	Air dynamic viscosity
$MAP$	Pa	Minimum airway pressure
$N_{tube}$	–	Number of airway tubes
$N_{alv}$	–	Number of alveoli
$N_{cap}^{alv}$	–	Number of capillaries per alveolus
$O_2(x, t)$	mol/ $m^3$	Oxygen concentration in the airways
$\bar{O}_2(t)$	mol/ $m^3$	Mean oxygen concentration in the alveoli

<b>Symbol</b>	<b>Units</b>	<b>Description</b>
$O_{2,pm}$	$\text{mol}/m^3$	oxygen concentration in the pulmonary membrane
$O_{2,b}(t)$	$\text{mol}/m^3$	Mean oxygen concentration in the blood
$P_a$	Pa	Partial pressure of a gas in air
$P_{ip,max}$	Pa	Maximum intrapleural pressure
$P_{ip,min}$	Pa	Minimum intrapleural pressure
$P_{open}$	Pa	Excess pressure to open the alveoli
$P_{MAX}$	Pa	Maximum open pressure
$P_{MIN}$	Pa	Minimum open pressure
$\bar{P}_{aw}$	Pa	Mean airway pressure
$p_{tr}$	Pa	Transition pressure
$P_{alv}$	Pa	Alveolar pressure
$\bar{P}_{O_2}(t)$	Pa	Mean oxygen partial pressure in the alveoli
$\bar{P}_{CO_2}(t)$	Pa	Mean carbon dioxide partial pressure in the alveoli
$P_{O_{2,b}}(t)$	Pa	Mean oxygen partial pressure in the blood
$P_{CO_{2,b}}(t)$	Pa	Mean carbon dioxide partial pressure in the blood
$P_{mean}$	Pa	HFOV mean airway pressure
$q$	$\text{mol}/s.m^2$	Flux of a gas across the alveolar membrane
$RV$	$m^3$	Residual volume
$R_{alv}^0$	$m^3$	Nominal alveolar radius
$R_{AW}$	$m^3$	Airway resistance
$R_{tube}$	$m^3$	Airway tube radius
$R$	$\text{Pa}.m^3/\text{mol}.K$	Universal gas constant
$So$	$\text{mol}/m^3$	Solubility of a gas in water
$SF$	—	Surfactant concentration fraction
$S$	%	Hemoglobin saturation with oxygen
$TV_{nom}$	$m^3$	Nominal tidal volume
$TLC$	$m^3$	Total lung capacity
$\tau_{RC}$	s	Time constant for RC model
$\tau_{diff}$	s	Diffusion time scale across the alveolar membrane



<b>Symbol</b>	<b>Units</b>	<b>Description</b>
$T$	K	Body temperature
$t_{res}$	s	Resident time of the blood in the pulmonary capillaries
$TV$	$m^3$	Tidal volume
$\vec{u}$	m/s	Velocity vector in airways
$U(t)$	m/s	Mean velocity in airways
$U_b(t)$	m/s	Mean velocity in the blood
$VC$	$m^3$	Vital capacity
$V$	$m^3$	Lung volume
$V_0$	$m^3$	Lung volume at ambient pressure
$V_{tube}$	$m^3$	Airway tube volume
$\dot{V}$	$m^3/s$	Air volume flow rate
$V_{alv}^0$	$m^3$	Nominal alveolar volume
$V_{membrane}^0$	$m^3$	Nominal volume of alveolar membrane
$V_b$	$m^3$	Blood volume entering pulmonary capillaries
$\dot{V}_b$	$m^3/s$	Blood volume flow rate
$Z_C$	Pa.s/ $m^3$	Lung impedance

# Chapter 1

## Introduction

Mechanical Engineering is a discipline of many diverse fields including automotive, aerospace, energy conversion, biotechnology, automation, and manufacturing to state few. Put in a simpler way, a mechanical engineer deals with everything in motion. Probably, one of the most complex machines that has been the subject of investigation over centuries, is the human body.

Indeed, the human body is assimilated to a complex machine of numerous systems that need to operate properly. The work of this thesis is concerned with innovations in the respiratory system. From microscopic to macroscopic scale, a mechanical engineer's duty is to bring into life ideas that will make the world a better living place. The key idea in this work is to couple respiration physiology with engineering knowledge to partially dissolve the complexity of this humongous machine.

Stating the idea and elaborating on it, is mind-enriching yet useless without the effort of bringing it to life. After all, isn't engineering about finding straightforward, applicable solutions to otherwise complicated problems? This work heads towards designing a state-of-the-art physically based lung model, that mimics respiratory behavior of individuals.

This chapter elucidates the motivation behind lung modeling, its significance and impact, and the aims to be achieved for implementing the idea successfully. The following chapters will explain the needed background for respiration physiology and lung modeling, the building blocks of the designed models, the testing and validation

of the model, sensitivity analysis, and a simulated abnormality-treatment scenario.

## 1.1 Motivation for lung modeling

Normal breathing can be altered by several respiratory abnormalities. These include disorders that affect the mechanical operation of the lungs by either increasing the resistance to entering air or decreasing the lung's capability to open, disorders that affect the gas exchange region, and disorders related to the blood flow in the pulmonary capillaries and hemoglobin (main carrier of oxygen). Further details and examples of these disorders is explained in appendix A. Even with fully functional respiratory systems, abnormal breathing can be caused by cases such as insufficient oxygen levels in the atmosphere, and carbon monoxide poisoning.

Treatment of the aforementioned abnormalities is possible as long as the respiratory disorder is clearly understood. Clinical therapies usually rely on various modalities of lung ventilation such as oxygen therapy, continuous positive airway pressure (CPAP), or high frequency oscillatory ventilation (HFOV). For example, an insufficient oxygen intake can be easily treated with oxygen therapy by putting the patient in a highly oxygenated room. CPAP and HFOV consist of aiding a patient suffering from various scenarios of difficult breathing, by applying a pressure signal at the opening of the respiratory passageways. A patient facing brief breathing cessations when asleep due to airway obstruction, can wear a CPAP mask that ensures permanent opening of the airways.

Unfortunately, not all cases are simple to treat. Clinical practice faces some difficulties related to in vivo measuring and understanding the physical mechanisms underlying the several abnormalities and treatments. This motivated the construction of a physically-based lung model to answer questions related to parameter changes for several scenarios of lung abnormalities and treatments. The lung model, once properly functional and validated, has the potential to simulate a wide variety of abnormalities no matter how complicated they might be, thus solving the need of in vivo measurements and experimentation. The results obtained can also help clinicians

predict the effectiveness of various treatments to specific pulmonary disorders, so that the optimal choice can be ultimately done.

## 1.2 Significance and impact

Once the model is complete, and the simulations display respiration parameters that are fairly close to actual physiological ones, it will serve as an important tool for the following purposes:

1. Investigation of the dynamics of various modalities of ventilation in a wide range of lung abnormality scenarios. This is the main reason that motivated the work. Knowing what respiratory parameters actually change in a certain lung disease is the key to understand what treatment to undergo.
2. Potential use in clinical practice. A simulation interface can be easily done in a user-friendly manner especially for clinicians and doctors who will be able to easily enter physiological parameters and investigate a breathing performance in terms of lung volumes, pulmonary pressures, and blood partial pressure of oxygen and carbon dioxide.
3. Academic tutorial on lung performance. The interface is also useful for students to learn respiratory physiology and easily practice and analyze different simulation scenarios.

## 1.3 Thesis' specific aims

A previous lung model was built to investigate blood oxygenation in preterm infants treated by Bubble-Nasal CPAP [3]. The model covers relations between volume and pressure in the lung tissue (lung mechanics), oxygen distribution in the airways and alveoli during respiration, and oxygen uptake by the pulmonary capillaries (oxygenation). The current work takes the previous model as a starting point and improves it

to come up with a generalized breathing simulator that is able to monitor the breathing of a human being and the ways it can be altered due to various lung abnormalities and corresponding treatments. In order to do so, here are specific aims that need to be achieved for this thesis:

1. Estimating lung parameters such as number of alveoli, blood volume entering the lungs, tidal volume, and many more, over a span of age, height, and body weight to generalize the model from preterm infants to any human being.
2. Including carbon dioxide in the model. From the onset of inspiration, until gas exchange, then expiration, carbon dioxide distribution needs to be solved in parallel with oxygen distribution for a more realistic model.
3. Improving gas exchange across the alveolar-capillary membrane by integrating oxygen and carbon dioxide dissociation curves. Oxygen and carbon dioxide concentrations and partial pressures are interrelated during the exchange through these curves.
4. Accounting for the concentration of surfactant in estimating the lung compliance. The surfactant is a chemical substance that prevents the alveoli from collapsing; its absence leads to a reduced compliance and is an indicator of diseases such as the infant respiratory distress syndrome (IRDS).
5. Testing the model and fine tuning it to get physiological values of oxygen and carbon dioxide content in the blood.
6. Investigating oxygenation and carbon dioxide removal over a sweep of respiration frequencies for preterm infants and adults, and performing sensitivity analysis of various key parameters to understand their impact on gas exchange.
7. Simulating a scenario of a preterm infant with a respiratory distress syndrome, and understanding the reason behind using HFOV as a treatment. Doing so will help clinical practice understand some physical dynamics underlying the treatment by HFOV.

# Chapter 2

## Background and literature review

In this chapter, a brief background will be given on respiration physiology starting on the air side, then moving to gas exchange with the blood side. The background is highly referenced by [14]. Afterwards, light will be shed on previous research and modeling in lung physiology to put the current work in context.

### 2.1 Background

As human beings, we are composed of about 100 trillion cells that carry different functions in our organism. A single cell can live and fulfill its functions only if the right amount of oxygen is provided. A cell will not be able to live, if it is not supplied with oxygen. This complex human body that scientists have been discovering for ages owes its supply of oxygen to the respiratory system. Through respiration, a human being is capable of procuring oxygen for all his cells and getting rid of debris gases such as carbon dioxide. Starting from the mouth or the nasal passageways, air rich in oxygen is inspired to the trachea, then bronchi to reach the two lungs. Within one lung, the bronchi divides into several bronchioles that end up with the smallest and most important elements of respiration, the alveoli. It is within these elements that oxygen will be transported to blood and thereafter distributed to the organism's tissues. Moreover, these alveoli will receive carbon dioxide from the blood, and will expel it out of the system through expiration. This is the simplest way to explain the

operation of the respiratory system that can be seen in figure 2-1.

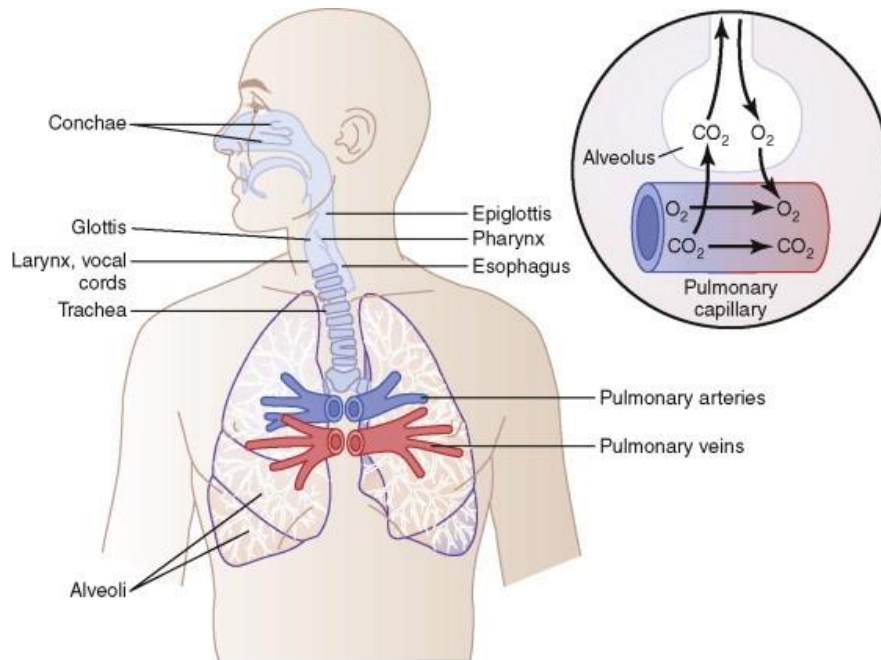


Figure 2-1: The respiratory system and its components, and gas exchange between an alveolus and a capillary

### 2.1.1 Respiration mechanics

For a proper respiration, there is an organized interaction between the lungs' inflation/deflation and the different respiratory pressures and muscles.

#### The lungs' operation

The lungs are spongy-like elements that are protected by the thoracic cage. They can be easily assimilated to two balloons that change in volume through the process of filling or emptying them from air. While breathing, the movement of the lungs within the thoracic cavity is lubricated by the pleural fluid, and actuated by the interaction of the following muscles:

- The diaphragm that contracts downward during inspiration to increase the longitudinal lung space for entering air, and relaxes upward during expiration to help the expulsion of air out of the respiratory system.

- The internal and external intercostal muscles that relax and contract respectively during inspiration to increase the antero-posterior lung space for entering air, then act in the opposite direction during expiration.

Figure 3-7 below helps visualize the operation of the above muscles.

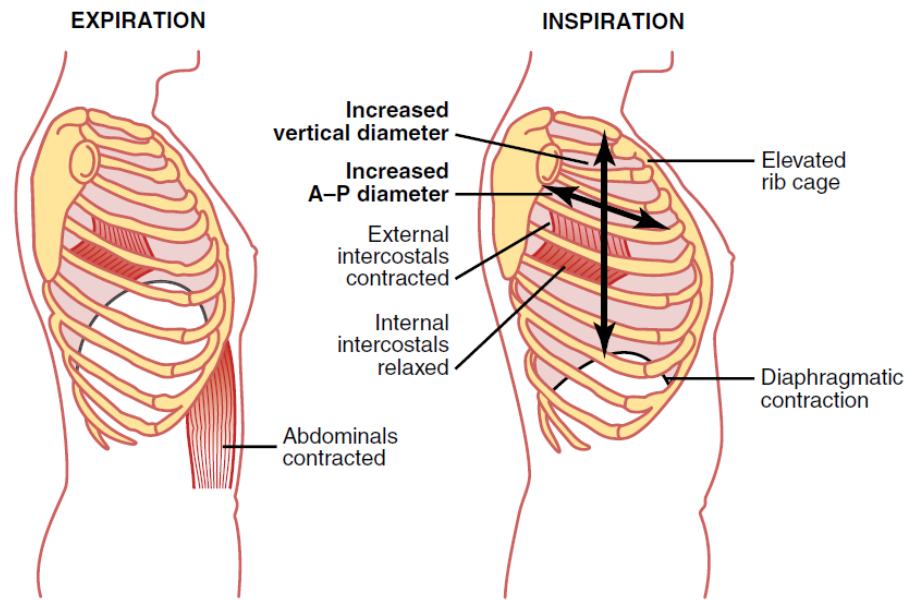


Figure 2-2: The interaction of respiratory muscles during expiration (left) and inspiration (right)

The interaction of the respiratory muscles is directly related to the pulmonary pressures, namely, the intrapleural pressure and the alveolar pressure. The former is the pressure of the lubricating pleural fluid between the lungs and the thoracic cage, and the latter is the pressure build-up in the alveoli.

- The intrapleural pressure is normally a suction pressure that is about -5 cmH<sub>2</sub>O at the onset of inspiration. When the chest cavity expands, it becomes more negative (-10 cmH<sub>2</sub>O) thus helping air to enter the lungs. The pressure then increases to its initial suction level during expiration.
- The alveolar pressure oscillates between -1 and 1 cmH<sub>2</sub>O. The minimum value is reached when the air is sucked into the alveoli during inspiration. The maximum value is reached when the alveoli are filled with air at the beginning of expiration.



## Lung volumes and capacities

To study lung mechanics, one needs to look into the expansion and contraction of the lungs. In other words, one needs to see to what extent are the lungs filled during inspiration, and how much can they be emptied during expiration. Lung volumes have been defined in a suitable manner to help measure the respiration performance of an individual. They are as follows:

- the tidal volume ( $TV$ ) defined as the volume of air that is inspired or expired during normal breathing at rest.
- the inspiratory reserve volume ( $IRV$ ) defined as the maximum excess air that an individual can fill the lungs with, if he inspires with full force.
- the expiratory reserve volume ( $ERV$ ) defined as the maximum excess air that an individual can empty from his lungs, if he expires at full force.
- the residual volume ( $RV$ ) defined as the air that stays in the lungs after a full force expiration. Obviously, one cannot totally empty the lungs from air or else they would collapse and become dysfunctional.

From these lung volumes, lung capacities are defined being more efficient to clinicians, in assessing an individual's performance:

- the inspiratory capacity ( $IC$ ), measuring the volume of air that can be inspired during a forceful inspiration.

$$IC = TV + IRV$$

- the functional residual capacity ( $FRC$ ), measuring the volume of air that remains in the lungs just after a normal expiration.

$$FRC = RV + ERV$$

- the vital capacity ( $VC$ ), measuring the volume of air that can be expelled from the lungs with a full force inspiration and expiration.

$$VC = IRV + TV + ERV$$

- the total lung capacity ( $TLC$ ), measuring the volume of air that can fill the lung after a full force inspiration.

$$TLC = IRV + TV + ERV + RV$$

### The dead space volume

The air entering the lungs is rich in oxygen, it fills the alveoli for gas exchange with the blood in the pulmonary capillaries. However, not all the inspired air reaches the alveoli, a part gets trapped in some regions of the airways where gas exchange doesn't occur. This volume of air is called the dead space volume. It is very important to account for this volume since not all inspired air necessarily reaches the alveoli for gas exchange.

### **Lung compliance and airway resistance**

The lung compliance is a quantity that relates the lung volume to the pressure. It is exactly the amount of volume by which the lung can increase per unit pressure differential. Knowing that, during an inspiration, the intrapleural pressure in a normal subject goes from -5 to -10 cmH<sub>2</sub>O, we can find a nominal value for the compliance if the volume of inspired air is given (See section 3.1). Lung compliance is an important parameter to judge whether a lung is healthy or diseased; some lung abnormalities such as constrictive diseases or respiratory distress syndromes usually tend to decrease the lung tissue compliance leading to difficulties in breathing and gas exchange.

The airway resistance is a quantity that measures the extent to which the airway channels can block the flow of air. As air is inspired from the mouth or nose, it will enter the respiratory passageways that ramify to channels of finer size. From the

knowledge of fluid mechanics, the resistance to a flow is highly sensitive to the size of a channel: the smaller the channel, the larger the flow resistance. Therefore, the airway resistance is significant in respiration mechanics. Similar to the compliance, airway resistance is also an important parameter that enters in the identification of lung abnormalities such as the cases of obstructive lung diseases like asthma.

### **2.1.2 The pulmonary membrane, the area of gases exchange**

The pulmonary membrane is the barrier that separates the air entering or leaving the lungs from the respiratory passageways, and the blood entering or leaving the lungs from the pulmonary artery or vein respectively. It is the medium through which the respiratory gases can cross from the air to the blood and reciprocally. The alveoli are the respiratory elements where gas exchange occurs, so the pulmonary membrane is the space in between an alveolus and a pulmonary capillary. Two lungs contain many millions of alveoli, each alveolus is surrounded by many capillaries so as to make a "sheet" of blood flowing through the lungs. This leads to an estimated pulmonary membrane area of  $70\text{ m}^2$  in an adult subject, equivalent to the area of a living room! From the alveoli to the blood, the pulmonary membrane consists of the surfactant layer that has the main role of preventing alveolar collapse (see subsection 3.1.4), the alveolar epithelium and basement membrane, the interstitial space, and the capillary basement and endothelium membrane. The membrane's size is  $0.6\ \mu\text{m}$  on average, but can vary in size due to the accumulation of edema fluid in the interstitial space, in some abnormal cases. The pulmonary membrane is clearly shown in figure 2-3 below.

#### **Gases exchange through diffusion**

Gas exchange across the pulmonary membrane can only happen through diffusion. As a definition, diffusion is a random movement of molecules through a membrane caused by the kinetic energy of the molecules. The pulmonary membrane is formed by a lipid bilayer. Some molecules are not soluble in lipids and cannot therefore diffuse

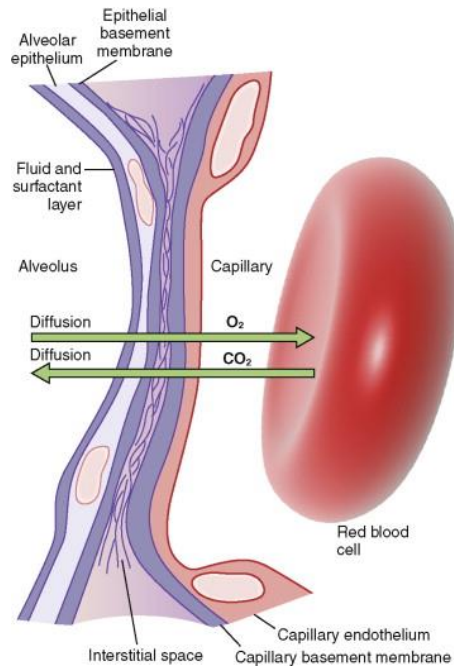


Figure 2-3: Diffusion of oxygen and carbon dioxide through the different components of the pulmonary membrane between an alveolus and a capillary

through the membrane unless through a certain channel or through protein carriers. However, oxygen and carbon dioxide, the main gases of respiration, are able to diffuse into a lipid bilayer. The principle fluid medium in the body is water (about 70 to 85 % in cells), therefore dissolved gases in the fluid of the pulmonary membrane can be considered to be dissolved in water. The driving force which determines the direction of net diffusion in the gas exchange area, is the pressure difference. For instance, the alveolar pressure of oxygen (pressure inside the alveoli) is higher than the partial pressure of oxygen in the blood, so the net diffusion of oxygen is from the alveolar air to the blood. The partial pressure of carbon dioxide in the blood is higher than the alveolar pressure of carbon dioxide, so the net diffusion of carbon dioxide is from the blood to the alveolar air.

The partial pressure of a gas in air can be related to its concentration in a water medium by Henry's Law. It states that, at constant temperature, the amount of gas that dissolves in a liquid is directly proportional to the partial pressure of that gas in equilibrium with the liquid:

$$P_a = k_H C_{aq} \quad (2.1)$$

Where  $P_a$  is the partial pressure of the gas in air,  $C_{aq}$  is the concentration of the gas in the aqueous medium, and  $k_H$  is Henry's constant. Henry's law is useful in the model to relate the partial pressures of oxygen and carbon dioxide to their concentrations in the pulmonary membrane.

Net diffusion also depends on parameters other than the pressure difference  $\Delta p$ . It increases with a higher diffusion area  $A_d$ , a higher solubility  $S_o$  of a gas in water, a lower distance of diffusion  $d$ , and a lower molecular weight of the gas species  $MW$ . The net rate of diffusion  $DR$  is therefore a quantity proportional to the aforementioned parameters:

$$DR \propto \frac{\Delta p A_d S_o}{d \sqrt{MW}} \quad (2.2)$$

The solubility and the molecular weight are the only parameters that are characteristics of a specific respiratory gas. They can be lumped to form the relative diffusion coefficients  $D \propto \frac{S_o}{\sqrt{MW}}$ . It follows from equation 2.2 that the flux of a gas  $q$  across the pulmonary membrane can be written as a function of a pressure gradient, taking  $\hat{n}$  to be the normal direction along diffusion.

$$q = D \frac{\partial P}{\partial n} \quad (2.3)$$

Alternatively, net diffusion can be thought of, as driven by a concentration gradient  $\frac{\partial C}{\partial n}$ , thus writing a species' flux as follows, with  $\mathfrak{D}$  being the diffusion coefficient of a species in  $m^2/s$

$$q = \mathfrak{D} \frac{\partial C}{\partial n} \quad (2.4)$$

In respiration physiology, we are interested in the net diffusion of oxygen and carbon dioxide: the main respiratory gases that needs to be exchanged between the alveoli and the pulmonary capillaries. In the following, We explain how these gases are transported in the blood to reach the exchange area in the lungs.

### 2.1.3 Oxygen

After inspiration, oxygenated air fills the alveoli, and the partial pressure of oxygen reaches 104 mmHg. The arterial blood entering the lungs has given all its oxygen to the body tissues and is qualified as poor in oxygen with a partial pressure of 40 mmHg. Therefore, the net diffusion occurs from the alveolar air to the blood with a pressure difference of 64 mmHg. The blood acquires an oxygen partial pressure equivalent to the alveolar pressure after crossing one third of the distance (see figure 2-4). Nevertheless, The oxygen partial pressure in the blood is at slightly lower values at the exit of the lungs. In fact, 2% of the blood has a purpose of nourishing the lung tissue. It will leave the lungs poor in oxygen and will mix up with the oxygenated blood thus decreasing its partial pressure.

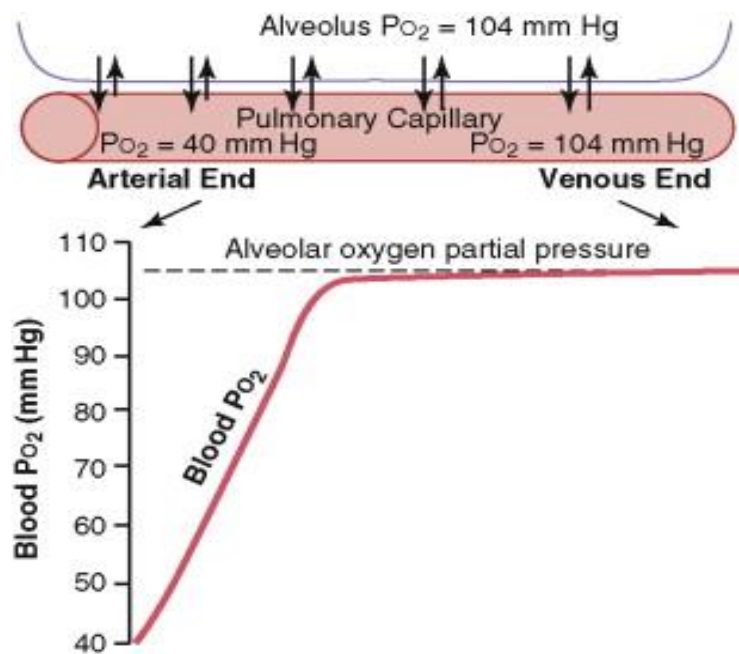


Figure 2-4: Oxygen partial pressure build-up with distance traveled by the blood in the pulmonary capillaries

#### Ways of transport

There is two ways of transport for oxygen in the blood stream. It is mainly transported from the lungs to the various tissues of the body through 25 trillion red blood cells,

or it can also be transported in the interstitial fluid between the red blood cells called the plasma:

- The red blood cells contain a chemical substance known for its ability to bind to the respiratory gases: the hemoglobin. Oxygen is transported in the blood through its combination with hemoglobin in the red blood cells, to form the oxy-hemoglobin complex. In the lungs, the poor oxygen content of the blood, stimulates the hemoglobin molecules to bind to oxygen molecules being diffused from the alveoli, until the red blood cells saturate with oxygen. The saturation level occur at 97 %, or, in other words, 97 % of the oxygen molecules that diffuse into the blood, are bound to hemoglobin in the red blood cells. It follows that the transport of oxygen through binding to hemoglobin, is the determining factor for oxygen concentration and partial pressure in the blood. Besides this, hemoglobin has an oxygen buffering function due to its chemical affinity to oxygen. It can control oxygen content in the blood as follows: when there is enough oxygen in the tissue, the hemoglobin will seize to release oxygen, and when the tissues lack oxygen, the hemoglobin will immediately release oxygen.
- 60% of an adult human body is constituted of fluid, one third of which fills the space between the cells. The extracellular fluid that circulates in the blood (or the plasma) ensures the transport of the other 3% of the oxygen molecules in the dissolved state. It is difficult for oxygen molecules to dissolve in the plasma due to their low solubility coefficient in water. The lower the solubility, the higher the partial pressure exerted by the gas for it to dissolve. Furthermore, oxygen that binds to hemoglobin exerts no pressure implying that only 3% dissolved oxygen is needed to raise the partial pressure of oxygen from 40 mmHg to the alveolar level of 104 mmHg. From here, we can see the importance of oxygen transport with hemoglobin.

## Oxygen-Hemoglobin dissociation curve

Since oxygen is mainly transported in the blood via hemoglobin, its partial pressure can be related to hemoglobin saturation through the oxygen-hemoglobin dissociation curve. It is the variation of hemoglobin saturation in oxygen as a function of the oxygen partial pressure. The dissociation curves are constructed based on empirical data from respiration physiology. The oxygen dissociation curve has a sigmoidal shape and is shown in figure 2-5 below.

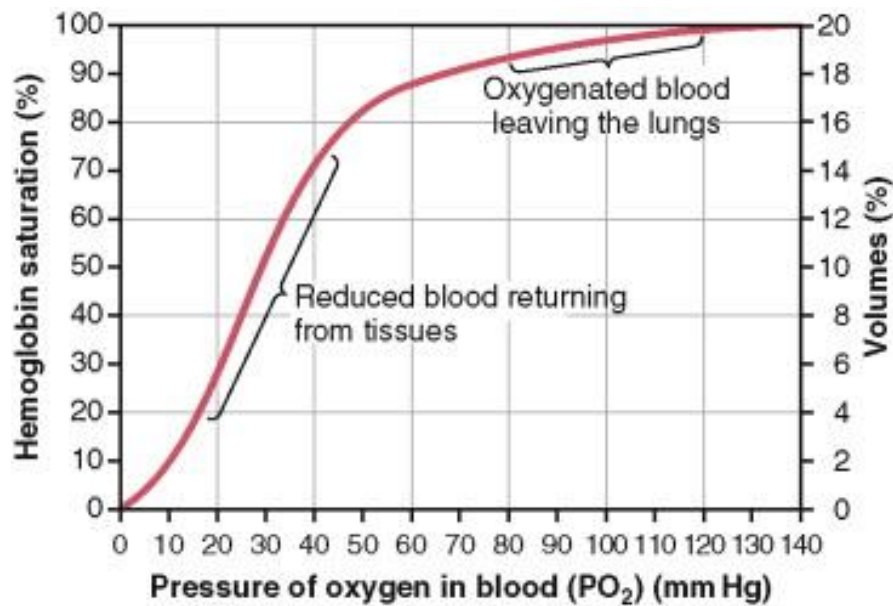


Figure 2-5: The oxygen-hemoglobin dissociation curve shown as hemoglobin saturation (left axis) or oxygen concentration (right axis) as a function of oxygen partial pressure

Blood leaving the lungs has about 100 mmHg partial pressure in oxygen. From figure 2-5, the hemoglobin is at 97 % saturation. Arterial blood entering the lungs has 40 mmHg partial pressure in oxygen, thus the hemoglobin is at 75 % saturation. The hemoglobin saturation can be converted to a concentration in oxygen (the right y-axis of figure 2-5) through the following explanation: In a normal person, the blood contains 15 grams of hemoglobin per 100 mL of blood. Each gram of hemoglobin can bind with 1.34 mL of oxygen at maximum. So 100 % hemoglobin saturation corresponds to carrying 20 mL of oxygen in 100 mL of blood (or 20 volumes percent).



The oxygen-hemoglobin dissociation curve can be shifted to the left or right by the impact of several factors during the transport of oxygen. The curve shown in figure 2-5 is for normal blood. The factors that shift the dissociation curve to the left are listed below:

- An increase in the pH of the blood or decrease in hydrogen ions concentration
- A decrease in Carbon dioxide concentration
- A decrease in Blood temperature
- A decrease in the concentration of 2,3-biphosphoglycerate (BPG), a metabolic compound for blood

One can see that carbon dioxide content in the blood can affect oxygen content; This is captured by the Bohr effect: In the lungs, when carbon dioxide diffuses into the alveolar air, its concentration in the blood decreases. Consequently, the dissociation curve shifts upward to the left leading to more bound oxygen to hemoglobin, at the oxygen partial pressure of 100 mmHg. In the tissues, The Bohr Effect operates reciprocally to stimulate the release of oxygen.

#### **2.1.4 Carbon dioxide**

The arterial blood entering the lungs is rich in carbon dioxide with a partial pressure of 45 mmHg. The alveolar carbon dioxide partial pressure after inspiration is 40 mmHg. Notice that the pressure difference is much smaller than in the case of oxygen. But net diffusion is still important from the blood to the alveoli because carbon dioxide has a much higher solubility than oxygen in water (20 times higher), and a higher solubility yields in a higher diffusion coefficient ( $D \propto \frac{S_o}{\sqrt{MW}}$ ). Therefore, carbon dioxide will be diffused to the alveolar air, and then expiration occurs to expel it out of the body. The partial pressure of carbon dioxide in the blood reaches the alveolar pressure (40 mmHg) at one third the distance traveled by the blood (see figure 2-6).

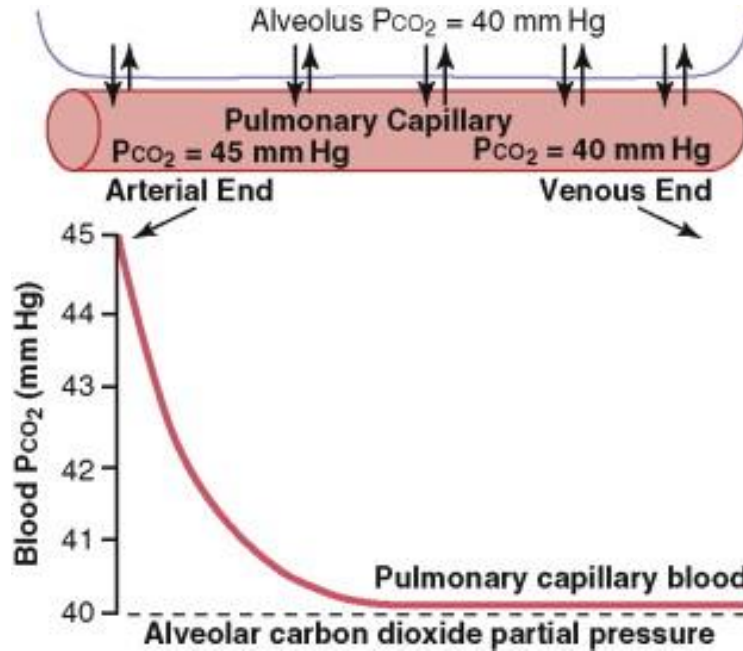


Figure 2-6: Carbon Dioxide partial pressure drop, with distance traveled by the blood, in the pulmonary capillaries

### Ways of transport

The transport of carbon dioxide occurs in three different ways in the blood. Since carbon dioxide has a much higher solubility than oxygen, it can be transported easily in a dissolved state. Therefore, a lower percent will be bound to hemoglobin.

- The hemoglobin can also bind to carbon dioxide to form the carbamino-hemoglobin complex. In the lungs, the hemoglobin is capable of releasing carbon dioxide for the gas exchange. 30 % of carbon dioxide is transported by the hemoglobin
- The main way of transport for carbon dioxide is in the ionic form. Carbon dioxide can be transported in the form of bicarbonate ions ( $\text{HCO}_3^-$ ). Carbon dioxide can react rapidly with water in the blood to form the carbonic acid through the action of the carbonic anhydrase, an enzyme that is abundant in the red blood cells. Carbonic acid ( $\text{H}_2\text{CO}_3$ ) dissociates then into hydrogen ions and bicarbonate ions. Hydrogen ions combine to hemoglobin (playing the role of acid-base buffer here), and bicarbonate ions are dissolved in the plasma of the blood to transport carbon dioxide. Chloride ions diffuse into the red blood

cells to compensate the absence of bicarbonate ions thus maintaining a neutral charge distribution). In the lungs, the reverse chemical reactions occur to reform the carbon dioxide molecules that need to diffuse to the alveoli.

- 7 % of the carbon dioxide molecules are directly dissolved in the plasma of the blood.

### **Carbon dioxide dissociation curve**

The carbon dioxide dissociation curve is defined as the variation of the concentration of carbon dioxide as a function of its partial pressure in the blood. As can be seen from figure 2-7 below, the physiological range of operation is pretty narrow. However, the carbon dioxide dissociation curve is significantly affected by oxygen partial pressure by what is called the Haldane Effect: As oxygen combines to hemoglobin in the lungs, the hemoglobin will become a strong acid, removing the carbon dioxide from the blood into the alveoli. The Haldane Effect promotes carbon dioxide transport more importantly than the Bohr Effect promotes oxygen transport, this will be seen clearly in the implementation of the dissociation curves in our model in chapter 3.4.3.

This was a brief look on the background needed for the construction of the physically based lung model. In the coming sections of this chapter, we will go over previous works on lung modeling and state the uniqueness of the built model.

## **2.2 Models in literature**

The literature review focuses on two main parts of lung modeling: the first part is the lung mechanics which indicates the relationship between pressure and volume covering the viscoelastic nature of the lungs, and the second part is the pulmonary system which goes over modeling the several respiratory elements such as the airways, the exchange barrier, and the blood, with an emphasis on gas exchange.

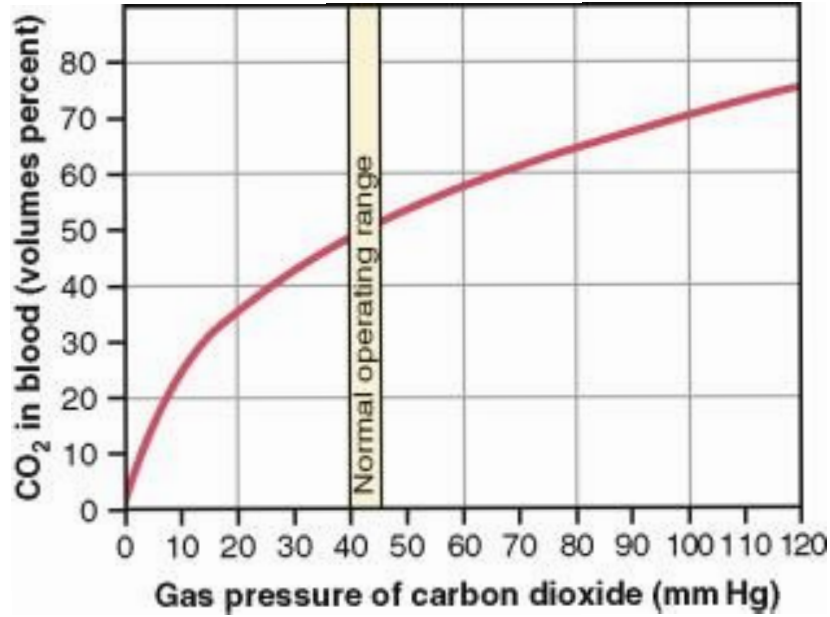


Figure 2-7: The carbon dioxide dissociation curve, shown as the concentration of carbon dioxide versus its partial partial in the blood

### 2.2.1 Lung mechanics models

Hildebrandt *et al* [15], 1969, presented a constant phase model for the lung, providing an empirical equation of lung tissue stress relaxation based on the statistical nature of the tissues at a molecular basis. The resulted pressure response of a lung tissue due to a unit step input of volume is given by  $P = V(a - b \ln t)$ . Hildebrandt also studied the hysteresis area of the P-V curve and found it to be independent of frequency. In a related study, he determined the relation between pressure and volume in a rubber balloon that is found to be  $P = V(at^{-\beta} + b)$ .

Bogaard *et al* [2], 1995, measured the static relationship between pressure and volume for patients in chronic obstructive pulmonary disease. They did an exponential fit of the resulted data ( $V = a + bP$  and  $V = V_{max}(1 - e^{-k(P-P_0)})$  for small and large volumes respectively.)

Athanasiades *et al* [1], 1999, provided a nonlinear equation that describes the

viscoelasticity of lungs. The lung tissue static elastic recoil is given by  $P = ae^{kV} + b$ . They also determined the P-V dynamic relationship  $P = P(V, \dot{V})$ .

Van Genderingen *et al* [29], 2001, modeled the lung as a capacitor that accounts for the compliance of the lung and as a resistor that accounts for both the flow resistance and the tissue resistance. He determined the dynamic relation between the mean airway pressure and the volume of the lung by solving the circuit equivalent problem  $(P = R\dot{V} + \frac{V}{C})$ . He calculated the resistance and the compliance of neonatal lung and provided the linear relationship between pressure and volume for moderate values of volume, and the exponential relationship for over-extended lungs.

Freed *et al* [11], 2012, determined a hypoelastic model for the alveoli. The experiments allows the determination of tissue shape response, tissue dilatation and tissue deformation covariance.

### 2.2.2 Pulmonary system models

Flumerfelt *et al* [10], 1968, modeled the capillary bed across the alveoli as a set of distributed-parameter flow-forced diffusional tubes with the dominant diffusion across the pulmonary membrane. Blood is considered as a quasi-homogeneous fluid in which the red blood cells are uniformly distributed. Concentrations and partial pressures of oxygen and carbon dioxide were found in the blood by including empirical dissociation curves. The model used both constant and pulsatile blood flow and concluded that damping the pulsatile flow through the capillaries enhances gas exchange.

Liu *et al* [18], 1998, studied the mechanics of airways. They modeled the lung as a single unit: single alveolar region connected to a single tube that represents the airways. The modeled airway tube was divided into three parts: upper airways, collapsible airways and small airways each having a specific resistance and compliance. They did an electrical equivalent model of the lungs and calculated the pressure of

oxygen at different locations in the airways, alveoli, and capillaries.

Niranjan *et al* [21], 1999, considered exchange of gases by diffusion through a lumped exchange barrier with the assumption of instantaneous chemical reactions in the single phase blood. Physiological blood shunt is neglected. The blood flow is also a lumped model composed of an artery compartment that branches into two capillary compartments and ends up with a vein compartment. Each compartment is described by its resistance and compliance. Constant pressure sources define the entry of blood in the artery and its exit in the vein.

Lu *et al* [19], 2002, presented a lumped parameter model for gas exchange with a single cylindrical tube capillary perfectly mixed radially, and discretized into small segments. A molar balance was solved on each segment to come up with a concentration distribution along the capillary. The concentrations were then converted to partial pressures through the dissociation curves.

Whiteley *et al* [30], 2003, presented a model of a single red blood cell moving at constant velocity in the pulmonary capillaries, surrounded by the plasma, and bounded by the pulmonary membrane. They allowed spatial variation of partial pressures and concentrations, and accurate diffusion modeling. All equations were based on the diffusion process. The governing partial differential equations of oxygen and carbon dioxide in the plasma included convection, and the equations that represent the binding of the gases to hemoglobin included chemical reactions. The model's output was oxygen and carbon dioxide partial pressures, concentration of hydrogen and bicarbonate ions, and oxy-hemoglobin and carbamino-hemoglobin saturation.

Chbat *et al* [4], 2009, divided the respiratory system responsible of gas exchange into three compartments: the dead space, the alveoli, and the capillary with a portion shunted from exchange. This model is a part of a bigger cardiovascular model in which the blood flow in arteries, capillaries and veins is characterized by inertia (for

large arteries), resistances for energy loss, and capacitances for blood volume storage.

Ionescu *et al* [16], 2010, studied the structural geometry of the lung. They divided the airway into 24 generations, starting from the trachea ending with the alveolar mouth, where each airway in a given generation was divided into two branches in the next generation. Each branch was modeled as a tube. Data was provided about the length and the diameter of the tubes for each generation.

Gaudenzi *et al* [12], 2013, modeled the blood flow in the arteries as a simple Poiseuille flow where inertia is neglected and flow rate is proportional to the pressure difference.

## 2.3 The built model

The lung mechanics models in literature focus only on the pressure volume relationship of the lung tissue without coupling to a complete pulmonary model. Furthermore, the compliance and resistance are obtained from experimental fits and clinical studies, and not derived from the underlying physics of the model. The built model calculates the lung tissue compliance and the airway flow resistance from the physics of respiration, and integrates them in the model of Van Genderingen *et al* [29], to get the lung volume oscillation with the oscillating intrapleural pressure during a respiration cycle. The model also allows the input of any pressure signal at the entry of the respiratory airways in case of a treatments like CPAP or HFOV.

As for modeling the whole pulmonary system, none of the above models presents a comprehensive physically-based lung model in which oxygen and carbon dioxide's spatial and temporal distribution are calculated in the airways, the alveoli, and the blood, to accurately predict gas exchange. The advection-diffusion equation from fluid mechanics is used to compute the distribution of the respiratory gases in the airways. Non-steady conservation of gases' concentration is solved inside the alveoli.

Regarding the blood models in literature, they are part of cardiovascular models and none of them is coupled to a complete pulmonary model. In the built model, the concentrations of oxygen and carbon dioxide in the blood are calculated by following a parcel of blood traveling at a uniform speed through the pulmonary capillaries. This parcel is subject to an entering flux of oxygen and exiting flux of carbon dioxide across the pulmonary membrane. The gas fluxes are calculated from the gases distribution in the alveoli and airways. In respiration physiology, the gases contents in the blood are expressed in terms of partial pressure in mmHg. The calculated concentrations are converted to partial pressures by incorporating explicit relations of the dissociation curves to the model. This was a brief outlook of the model constructed in this thesis, the next chapter will go into further details concerning all the building blocks.





# Chapter 3

## Elements of the model

### 3.1 Lung mechanics

When the negative intrapleural pressure increases with inspiration, air enters the airways to fill the alveoli. An alveolus is a viscoelastic element that changes in volume as air enters. When millions of alveoli are filled with air, the lungs will inflate. Lung mechanics is an essential part of the model that treats the interdependence between pulmonary pressures and lung volume as a human being is breathing. This section explains the building blocks needed, states the used lung mechanics model with its solution, and analyzes its implication on the frequency of respiration and gas exchange.

#### 3.1.1 Frequency of respiration

As it will be explained in section 4.2, the lung model allows the simulation of either normal breathing or imposed breathing. In the former, the subject breathes at the natural nominal rate, in the latter, the frequency of respiration can be controlled. Therefore, we need to model the frequency of respiration for the normal breathing part. The respiration frequency has a significant impact on the lung mechanics model for it directly affect the tidal volume entering the lungs. In other words, higher respiration rates are accompanied with smaller volume intakes. A preterm infant

naturally breathes at frequencies higher than an adult. The frequency of respiration depends on age as follows [7]:

- Newborns: 30-60 Breaths per minute
- 6 months old: 25-40 Breaths per minute
- 3 years old: 20-30 Breaths per minute
- 6 years old: 18-25 Breaths per minute
- 10 years old: 17-23 Breaths per minute
- Adults: 12-18 Breaths per minute

The lung model combines linear interpolations based on the above ranges to get the mean frequency of respiration versus age. For later reference in this thesis, a preterm infant breathes naturally at the rate of 45 breaths per minute, equivalent to 0.75 Hz, and an adult (20 years old) breathes naturally at the rate of 15 breaths per minutes, equivalent to 0.25 Hz.

### **3.1.2 Lung volumes**

Nominal values for the lung volumes explained in chapter 2, are needed to get many important parameters such as the nominal lung compliance and the volume of the lung at the open pressure which is normally the maximum intrapleural pressure (5 cmH<sub>2</sub>O). Nominal lung volumes and capacities also locate the oscillation of the tidal volume versus time between physiological values, which helps in assessing the validity of a simulation.

#### **The tidal volume**

It is very important not to confuse between the nominal tidal volume and the simulated tidal volume. The former is found based on literature and used to calculate the nominal compliance as will be seen shortly. The latter is the amplitude of the volume

signal that is solution of the lung mechanics model stated in subsection 3.1.5. At normal respiration frequencies, the simulated tidal volume should be equal or close to the nominal tidal volume. The nominal tidal volume is usually measured per unit body weight and is estimated to be 4-5 mL/Kg in newborn babies, increasing to about 7 mL/Kg in adults. The following function can be established to model the nominal tidal volume  $TV_{nom}$  in mL, as a function of age  $A$  in years and body weight  $BW$  in Kg:

$$TV_{nom} = [4.5 + \min(\frac{2.5A}{18}, 2, 5)] * BW \quad (3.1)$$

### **Residual volume, functional residual capacity, and total lung capacity**

RV, FRC, and TLC are usually measured experimentally for individuals of different ages, weights, heights, and sex. Since these lung volumes and capacities require at most an entry of 4 parameters which might be tedious for frequent running of the model, it is convenient to couple the weight and height of an individual to the age. This is done by implementing growth charts into the model for both males and females from the age of few days till the age of 20. The growth charts are based on the USA population, they take the age and sex as input and output the weight and height at various percentiles [9]. For our purposes, the 50th percentile is taken as an acceptable value. Note that if one wishes to study ages higher than 20 years, the height and weight must be specified.

Back to lung volumes, models for RV, FRC and TLC exist in literature over a span of age, weight, and height and for both genders [22] [24] [27]. Note that in the following equations,  $A$  is the age in years,  $BW$  is the weight in Kg,  $he$  is the height in cm, and  $H$  is the height in m.

#### Residual Volume RV in mL

- For infants (0-5 years)

$$RV = 18.1BW \quad (3.2)$$

- For children and adolescent (5-18 years)

For boys,

$$RV = 0.162he^{3.099}10^{-3} \quad (3.3)$$

For girls,

$$RV = 0.320he^{2.972}10^{-3} \quad (3.4)$$

- For adults and elderly (18-72 years)

For men,

$$RV = 1310H + 22A - 1230 \quad (3.5)$$

For women,

$$RV = 1810H + 16A - 2000 \quad (3.6)$$

#### Functional Residual Capacity FRC in mL

- For infants (0-5 years)

$$FRC = 0.0036he^{2.531} \quad (3.7)$$

- For children and adolescent (5-18 years)

For boys,

$$FRC = 0.125he^{3.298}10^{-3} \quad (3.8)$$

For girls,

$$FRC = 0.286he^{3.136}10^{-3} \quad (3.9)$$

- For adults and elderly (18-72 years)

For men,

$$FRC = 2340H + 9A - 1090 \quad (3.10)$$

For women,

$$FRC = 2240H + A - 1000 \quad (3.11)$$

#### Total lung capacity TLC in mL

- For infants (0-2 years)

$$TLC = -381.41 + 11.68he \quad (3.12)$$

- For children and adolescent (5-18 years)

For boys,

$$TLC = 0.95he^{3.039}10^{-3} \quad (3.13)$$

For girls,

$$TLC = 1.698he^{2.909}10^{-3} \quad (3.14)$$

- For adults and elderly (18-72 years)

For men,

$$TLC = 7990H - 7080 \quad (3.15)$$

For women,

$$TLC = 6600H - 5790 \quad (3.16)$$

### **Expiratory and inspiratory reserve volumes**

Using the models above, we can easily calculate IRV and ERV in mL, through the following equations:

$$ERV = FRC - RV \quad (3.17)$$

$$IRV = TLC - RV - TV - ERV \quad (3.18)$$

The remaining lung capacities, namely, the inspiratory capacity and the vital capacity, can be also calculated.

### **Dead space volume**

The dead space volume is the measure of the region where no gas exchange occurs. In the case of our model, gas exchange happens only across the alveoli, henceforth, the dead space volume is equivalent to the volume of the airways. In general, the

dead space volume  $DV$  in mL, is correlated with height [6]:

$$DV = 7.585he^{2.363}10^{-4} \quad (3.19)$$

### 3.1.3 Nominal compliance and airway resistance

The components that form the skeleton of lung mechanics are the compliance and resistance of the airways and the lung tissue. The airways are modeled as a set of parallel tubes that relate the inlet of the mouth to the inlet of the alveoli. The airway model will be further explained in section 3.2. The airways are assumed to have a negligible compliance by arguing that the walls of the respiratory tubes are rigid and do not expand or contract with air flowing through them. The lung tissue is assumed to have a negligible resistance to air flow in the current model, because the alveoli are spherical shaped elements with a radius much larger than the airways', and have the primary role of expanding or collapsing based on entering or exiting air. Therefore, the two key parameters in lung mechanics are the lung tissue compliance  $C_{tissue}$  and the airway resistance  $R_{AW}$ . The nominal value of the tissue compliance is calculated next whereas the airway resistance is calculated after the lung mechanics model is solved in subsection 3.1.5.

#### Nominal lung tissue compliance

As defined previously, the compliance is the response of the lung volume per unit pressure differential. In other words, the compliance of the tissue is a measure of how much the lungs inflate with a given pressure difference in the chest cavity. Thus, one can simply calculate a nominal value for this compliance since, during a normal inspiration, the human being intakes the nominal tidal volume, at a difference of 5 cmH2O in intrapleural pressure. Put in a mathematical equation:

$$C_{NOM} = \frac{TV_{nom}}{P_{ip,max} - P_{ip,min}} \quad (3.20)$$

The maximum and minimum intrapleural pressures are fixed in the model at -5 cmH<sub>2</sub>O and -10 cmH<sub>2</sub>O respectively, so the nominal compliance varies with age based on the variation of the nominal tidal volume in equation 3.1.

### 3.1.4 Surfactant fraction

With lack of surfactant in the linings of the alveoli, surface tension forces will exert a pressure that tends to collapse the alveoli, leading to a reduced overall compliance of the lungs. To be able to model diseases that are directly correlated to the lack of surfactant, especially the infant respiratory distress syndrome (IRDS) developed in preterm infants, a surfactant model is needed to account for the reduced compliance.

The electricity equivalence of the model corresponds to two capacitors in series. The first one models the nominal compliance  $C_{NOM}$  found previously, and the second one models the compliance  $C_{surfactant}$  arising from the excess pressure build up due to insufficient surfactant. The surfactant concentration enters into the picture as the surfactant fraction  $SF$  which is a real number between 0 and 1. Assuming a spherical shape of the alveolus with nominal radius  $R_{alv}^0$ , we can use the knowledge of surface tension in fluid mechanics to calculate  $P_{open}$ , the pressure needed to open the alveoli.

- When  $SF = 0$ , the linings of the alveoli consist of pure water:

$$P_{open} = P_{MAX} = \frac{2\gamma_{water}}{R_{alv}^0} \quad (3.21)$$

- When  $SF = 1$ , the surfactant content of the alveoli is normal and the alveoli are open at the existant intrapleural pressure:

$$P_{open} = P_{MIN} = 5cmH2O \quad (3.22)$$

- when  $0 < SF < 1$ , The open pressure needed is modeled as a linear profile between  $P_{MIN}$  and  $P_{MAX}$  as follows:

$$P_{open} = P_{MIN} + (1 - SF)(P_{MAX} - P_{MIN}) \quad (3.23)$$



Now,  $C_{surfactant}$  can be calculated from the ratio of the initial lung volume  $FRC$  over the portion of the open pressure that arises from lack of surfactant, in other words,  $P_{open} - P_{MIN}$ .

$$C_{surfactant} = \frac{FRC}{P_{open} - P_{MIN}} \quad (3.24)$$

Finally, the operating compliance of an individual with lack of surfactant is the equivalent compliance of the two series capacitors:

$$C_{tissue} = \frac{1}{\frac{1}{C_{NOM}} + \frac{1}{C_{surfactant}}} \quad (3.25)$$

It is important to mention that the reduced compliance is accompanied with an increased open pressure, that needs to be compensated with a correspondent continuous positive airway pressure (CPAP), to keep the lungs open. The surfactant model will be put in use when taking the case of a preterm infant suffering from IRDS in chapter 6.

### 3.1.5 The lung mechanics model

The lung mechanics model is one that captures the relationship between an applied pressure signal and the resulting lung volume response. Starting with a static  $p - V$  model, we move then to the dynamic model and solve it in the small pressure signal region. The model is based on Van Genderingen et.al [29].

#### The static model

The static model shows the relationship between the lung volume and a continuous pressure signal that doesn't vary with time, applied on the lungs:

$$\begin{aligned} V &= 0 & \text{for } \bar{p}_{aw} < p_{open} \\ V &= C_{tissue}\bar{p}_{aw} + V_0 & \text{for } p_{open} < \bar{p}_{aw} < p_{tr} \\ V &= p_{tr}C_{tissue} \left( (1 + \beta) - \beta e^{-\frac{\bar{p}_{aw} - p_{tr}}{\beta p_{tr}}} \right) + V_0 & \text{for } \bar{p}_{aw} > p_{tr} \end{aligned} \quad (3.26)$$

where  $\beta = \frac{1}{2}$ ,  $p_{tr} = 20$  cmH2O,  $p_{open} = 5$  cmH2O,  $V_0$  is the volume of the open lungs at ambient pressure. As it can be seen, at airway pressures higher than 20 cmH2O, we start having a non-linear relationship between the pressure and volume which leads to a decrease in the compliance. However, the p-V relationship of the built model will only consider the linear region meaning that the tissue compliance remains constant with the increase of  $\bar{P}_{aw}$  (see figure 3-1).

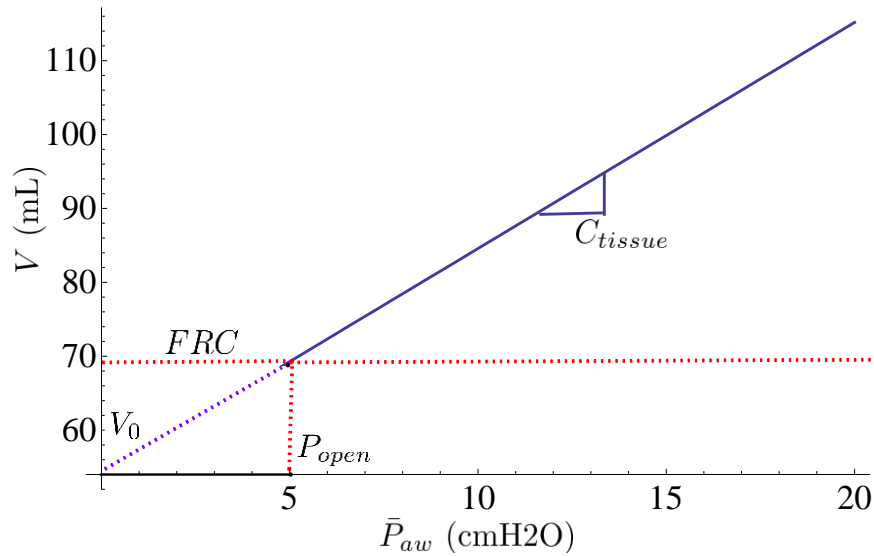


Figure 3-1: Plot of the lung volume versus the airway pressure depicting the static model for a preterm infant (girl), the lung volume is zero before the 5 cmH2O open pressure

The minimum pressure needed to open the lungs is equivalent to  $-P_{ip,max} = 5$  cmH2O. At this pressure, the volume of the lungs is the functional residual capacity  $FRC$ . Then, as the pressure increases, the lung volume increases with a constant rate of  $C_{tissue}$ . Below 5 cmH2O, the lungs collapse yielding in a zero lung volume.  $V_0$  is about 53 mL but is not relevant to the model.

### The small signal dynamic model

For the static model defined in figure 3-1, the dynamic  $p - V$  model can be expressed as:

$$\delta P(t) = R_{AW} \frac{dV}{dt} + \frac{V}{C_{tissue}} \quad (3.27)$$

In an electric equivalent analysis, the model consists of a resistor  $R_{AW}$  in series with a capacitor  $C_{tissue}$  with a dynamic signal input  $\delta P(t)$  (see figure 3-3).

The model can be solved for a sinusoidal pressure signal that mimics the respiration process of an individual at a frequency of respiration  $f$  and a pressure amplitude  $\Delta P$  with an inspiration to expiration ratio of unity (figure 3-2)

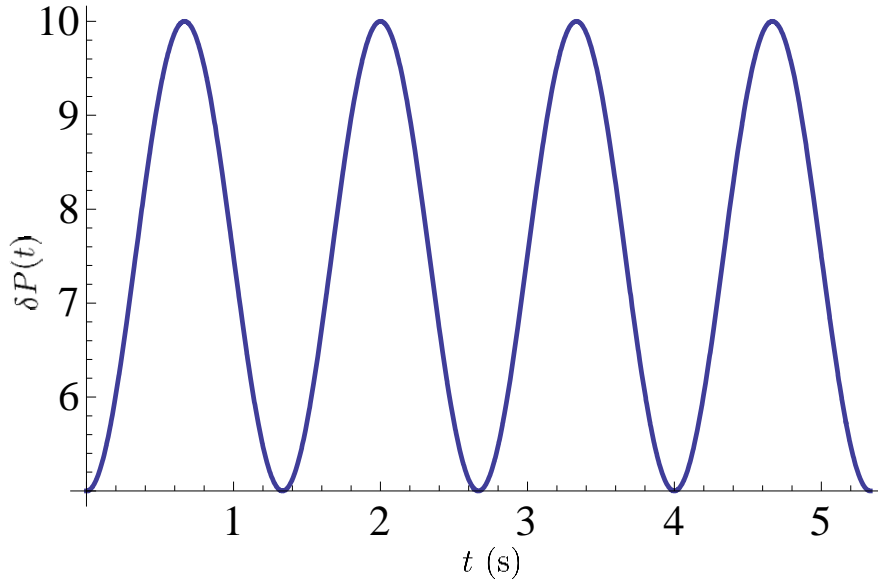


Figure 3-2: The symmetric pressure signal representing the oscillation of the gauge airway pressure, the frequency of the signal is that of a preterm infant (45 breaths per minute or 0.75 Hz)

$$\delta P(t) = -P_{ipmax} + \Delta P \sin^2(\pi f t) \quad (3.28)$$

Equation 3.27 can be rewritten as:

$$\frac{dV}{dt} + \frac{V}{R_{AW} C_{tissue}} = \frac{\delta P(t)}{R_{AW}} \quad (3.29)$$

Define  $g(t) = e^{\frac{t}{R_{AW}C_{tissue}}}$

$$\frac{1}{g(t)} \frac{d(Vg(t))}{dt} = \frac{dV}{dt} + \frac{V}{g(t)} \frac{dg(t)}{dt} = \frac{dV}{dt} + \frac{V}{R_{AW}C_{tissue}} = \frac{\delta P(t)}{R_{AW}} \quad (3.30)$$

Then

$$\frac{d(Vg(t))}{dt} = \frac{\delta P(t)}{R_{AW}} g(t) \quad (3.31)$$

Integration along time from 0 to  $t$  yields:

$$V(t)g(t) - V(t=0)g(0) = \int_0^t \frac{\delta P(\tau)}{R_{AW}} g(\tau) d\tau \quad (3.32)$$

The initial time  $t = 0$  is associated to just before inspiration, therefore  $V(t = 0) = FRC$

$$V(t)g(t) - FRC = \int_0^t \frac{\delta P(\tau)}{R_{AW}} g(\tau) d\tau \quad (3.33)$$

Replacing  $g(t)$  and rearranging the equation gives the following expression for the lung volume:

$$V(t) = FRC e^{\frac{-t}{R_{AW}C_{tissue}}} + \frac{1}{R_{AW}} \int_0^t e^{\frac{-(t-\tau)}{R_{AW}C_{tissue}}} \delta P(\tau) d\tau \quad (3.34)$$

The solution of the model can be replaced in equation 3.29 to obtain the following expression for the volume flow rate of air in the airways:

$$\frac{dV}{dt}(t) = \frac{\delta P(t)}{R_{AW}} - \frac{1}{R_{AW}C_{tissue}} \left( FRC e^{\frac{-t}{R_{AW}C_{tissue}}} + \frac{1}{R_{AW}} \int_0^t e^{\frac{-(t-\tau)}{R_{AW}C_{tissue}}} \delta P(\tau) d\tau \right) \quad (3.35)$$

This volume flow rate expression will be used to compute a characteristic frequency beyond which air will not reach the alveoli to aerate them (subsection 3.1.6).

## Airway resistance

The airway resistance is calculated from the time constant of the small signal dynamic model

$$\tau_{RC} = R_{AW}C_{tissue}$$

$C_{tissue}$  is already found, the time constant is still needed to get the airway resistance. From the background of respiration physiology, we know that the pressure in the alveoli oscillates between -1 and 1 cmH<sub>2</sub>O. Therefore, using the solution of the lung mechanics, we can calculate  $P_{alv}$  the pressure in the alveoli, and find a time constant  $\tau_{RC}^*$  such that  $|P_{alv}| < 1$ . Figure 3-3 below helps visualize the lung mechanics model.

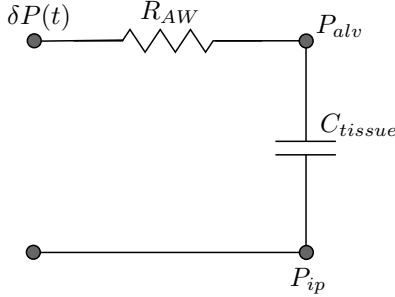


Figure 3-3: Schematic showing the electric equivalence of the small signal dynamic model,  $\delta P(t) = -P_{ip}(t)$

Taking a quasi-steady respiration, we can get an expression for  $P_{alv}$  in terms of the model solution (equation 3.34)

$$P_{alv} = \frac{V(t)}{C_{tissue}}$$

$$P_{alv} = \frac{1}{\tau_{RC}} \int_0^t e^{-\frac{(t-\tau)}{\tau_{RC}}} \delta P(\tau) d\tau \quad (3.36)$$

After finding  $\tau_{RC}^*$  such that  $P_{alv}$  is bounded between -1 and 1, we easily get a value of the airway resistance:

$$R_{AW} = \frac{\tau_{RC}^*}{C_{tissue}} \quad (3.37)$$

### 3.1.6 Characteristic frequency

The solution of the  $p - V$  dynamic model is used here to prove that there is a characteristic frequency beyond which, air will not reach the alveoli. This frequency helps in the analysis of gas exchange in later chapters. The expected behavior is an alteration in gas exchange (lower oxygenation and lower carbon dioxide removal or ventilation).

The first step is to evaluate the integral in equation 3.35 and simplify the terms by setting to zero, all the negative exponential terms so as to consider the quasi-steady behavior of respiration. Using an efficient mathematical tool, the result is as follows:

$$\frac{dV}{dt}(t) = \frac{C_{tissue}\Delta P(-4f^2\pi^2\tau_{RC}\cos 2\pi ft + 2\pi f\sin 2\pi ft)}{2 + 8\pi^2 f^2\tau_{RC}^2} \quad (3.38)$$

To get a characteristic airway length  $L^*$  we integrate the volume rate in equation 3.38 over a complete period of inspiration and then we divide by the cross sectional area of the airway pipe  $A_p$ :

$$L^* = \frac{\int_{insp} \frac{dV}{dt} dt}{A_p}$$

$$L^* = \frac{C_{tissue}\Delta P}{\sqrt{1 + 4\pi^2 f^2\tau_{RC}^2} A_p} \quad (3.39)$$

To make sure that the air reaches the alveoli properly for good gas exchange, the characteristic length  $L^*$  must be larger than the actual length of the airway pipe  $L_{pipe}$

$$L^* > L_{pipe}$$

Solving for the frequency we get the following:

$$f < f^*$$

$$f < \frac{1}{2} \frac{\sqrt{(C_{tissue}\Delta P)^2 - (A_p L_{pipe})^2}}{\pi A_p L_{pipe} \tau_{RC}} \quad (3.40)$$

We can further simplify  $f^*$  by replacing  $A_p L_{pipe}$  by  $V_{pipe}$  which is the dead space volume  $DV$ . For a normal breathing case, we also have  $TV = C_{tissue} \Delta P$ , then:

$$f^* = \frac{1}{2} \frac{\sqrt{(TV)^2 - (DV)^2}}{\pi DV \tau_{RC}} \quad (3.41)$$

$$\tau_{RC} = R_{AW} C_{tissue}$$

If we replace all the parameters by their nominal values for a preterm infant, from the models above, we get a characteristic frequency  $f_{infant}^* = 4.17$  Hz whereas if we do it for an adult male (20 years old), we get a lower characteristic frequency  $f_{adult}^* = 2.4$  Hz. This suggests that gas exchange should be altered in adults at lower respiration frequency than in infants.

Now, if we go back to equation 3.40, and consider a preterm infant, we can plot the behavior of the characteristic frequency  $f_{infant}^*$  when the tissue compliance, airway resistance, and pressure amplitude are swept near physiological ranges. From figure 3-4, the characteristic frequency starts by slightly decreasing with lower compliance, but then decreases faster at very low compliances. From figure 3-5, the characteristic frequency decreases with higher airway resistance. A decrease in tissue compliance or an increase in the airway resistance are both indicators of lung abnormalities and disease. So the results imply that a diseased subject has a lower characteristic frequency which will cause a disruption in gas exchange at lower frequencies of respiration than in a normal subject. The good news is that the pressure amplitude can be increased to enhance the characteristic frequency as can be seen in figure 3-6. Therefore, increasing the pressure amplitude of the signal to a value higher than the nominal 5 cmH<sub>2</sub>O, can be helping in the case of lung disease. But unfortunately, the pressure amplitude can't go indefinitely higher because this can lead to the destruction of the sick lung tissue. This analysis, obtained from solving the lung mechanics model, will be useful in explaining alterations of gas exchange with lung abnormalities, in later chapters.

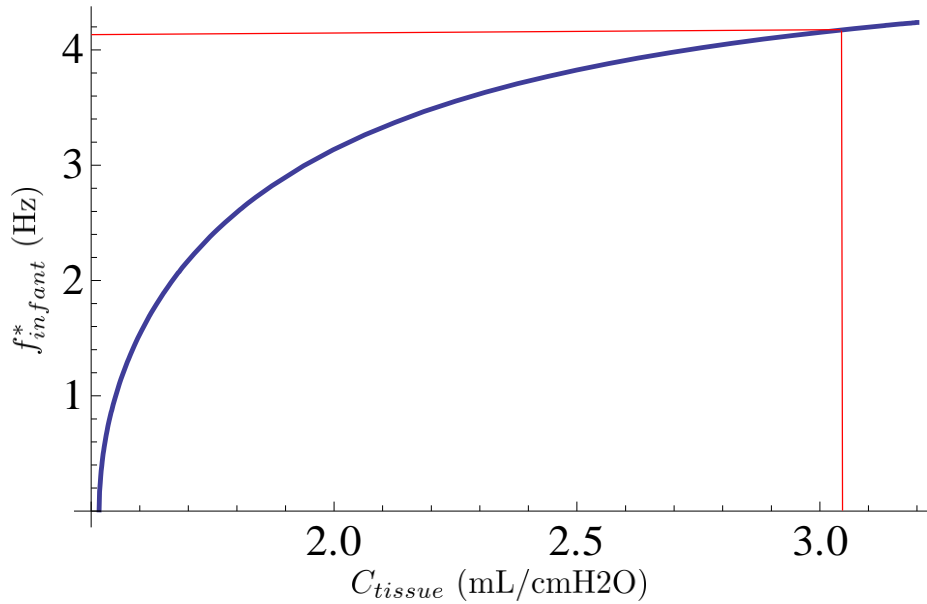


Figure 3-4: Characteristic frequency versus tissue compliance for a preterm infant, the red lines show the nominal value

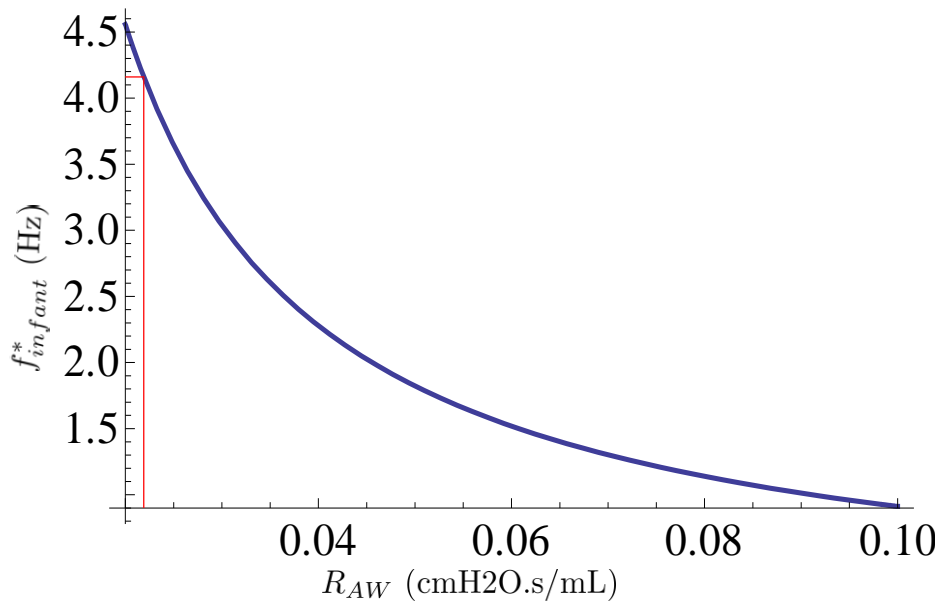


Figure 3-5: Characteristic frequency versus airway resistance for a preterm infant, the red lines show the nominal value



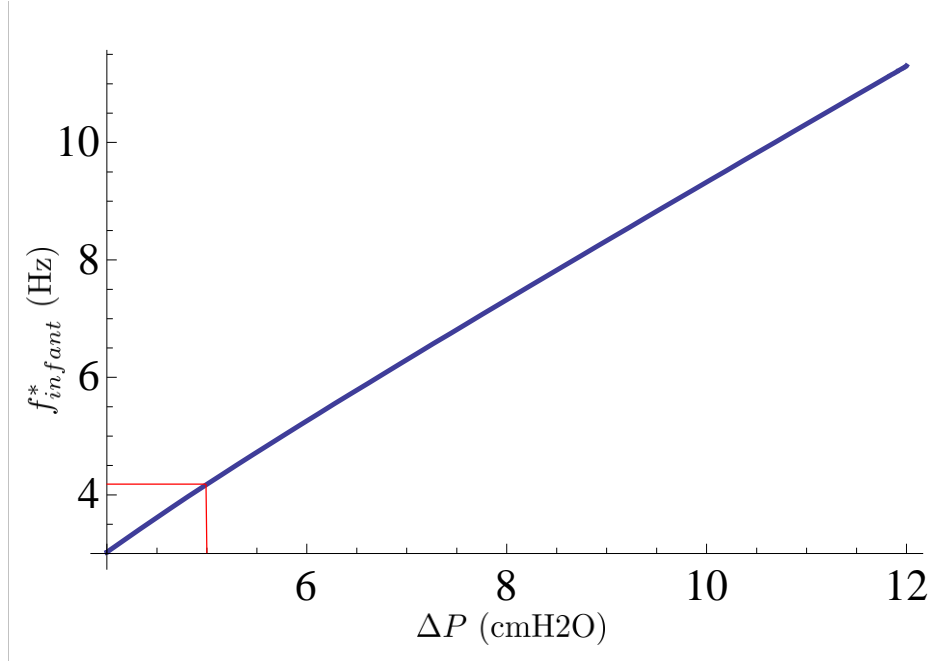


Figure 3-6: Characteristic frequency versus pressure amplitude for a preterm infant, the red lines show the nominal value

## 3.2 Gases transport in the airways

### 3.2.1 Modeling the airways

The main respiratory airways consist of the trachea, that branches into two bronchi, ramifying into several bronchioles at the end of which sacs of alveoli are reached. So air flows in different channels to fill the alveoli. The current airway model is composed of a set of parallel identical tubes  $N_{tube}$ , each of which has a radius  $R_{tube}$  and a length  $L_{tube}$  [3]. The parameters of this model are calculated by conserving the length, volume, and resistance of the actual airways as follows:

Conservation of airway length: The actual airway length is considered to be a percentage of body height. Taking actual measurement of the pipe length assumed to be roughly the distance between the bottom of the chin and the lower chest, this percentage is estimated to be about 20%. The length of the airway pipe in meters is then  $L_{pipe} \approx 0.20H$ . To conserve the airway length, the tube must have a length equivalent to the pipe length.

$$L_{tube} = L_{pipe} \quad (3.42)$$

Conservation of airway volume: The actual airway volume is the volume of air that doesn't reach the alveoli for gas exchange. This volume is equivalent to the dead space volume  $DV$  found previously in equation 3.19. The volume of the set of parallel tubes is  $V_{tube}$ , leading to:

$$DV = V_{tube} = N_{tube}\pi R_{tube}^2 L_{tube} \quad (3.43)$$

Conservation of airway resistance: An expression of the airway resistance can be found by applying the knowledge acquired in fluid mechanics on one of the airway tubes. Basically, air flowing in one airway tube can be looked at as a pressure driven air flow in a channel. The driving force of this flow is then the difference between the maximum and minimum intrapleural pressure  $\delta P$ .

The Navier-Stokes equation in its most general form is written as:

$$\frac{\partial \vec{u}}{\partial t} + \vec{u} \cdot \nabla \vec{u} = -\nabla P + \mu \nabla^2 \vec{u} \quad (3.44)$$

Let  $\hat{x}$  be the direction along the airway tube in a cylindrical coordinate system  $(x, r, \theta)$ . Assuming a fully-developed steady flow in one dimension along the tube, the Navier-Stokes equation reduces to the following:

$$0 = -\frac{\partial P}{\partial x} + \frac{\mu}{r} \frac{\partial}{\partial r} \left( r \frac{\partial u}{\partial r} \right) \quad (3.45)$$

Then the flow is taken to be a Poiseuille flow and has a parabolic profile as shown in schematic 3-7 below. The considered airway tube is of radius  $R_{tube}$  and length  $L_{pipe}$ .

The volume flow rate for a Poiseuille flow is typically calculated by integrating the velocity profile, solution of equation 3.45, over the radius of the airway tube. It will result in the following equation:

$$\dot{V} = \frac{\pi R_{tube}^4 \Delta P}{8\mu L_{pipe}} \quad (3.46)$$

Equation 3.46 can be written in terms of the resistance to the flow in the tube:

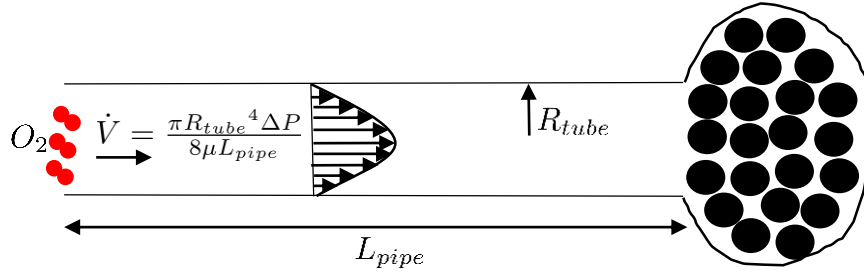


Figure 3-7: A simple schematic showing an airway tube with a particle of oxygen crossing to reach the alveoli. The particle of oxygen is subject to a Poiseuille flow

$$\dot{V} = \frac{\Delta P}{R} \quad (3.47)$$

Therefore one airway tube has the following resistance:

$$R = \frac{8\mu L_{pipe}}{\pi R_{tube}^4} \quad (3.48)$$

To get the total airway resistance, we need to calculate the equivalent resistance for  $N_{tube}$  tubes in parallel, of resistance  $R$ , where  $N_{tube}$  is the number of airway tubes that the airway model contains.

$$R_{AW} = \frac{R}{N_{tube}} = \frac{8\mu L_{pipe}}{\pi R_{tube}^4 N_{tube}} \quad (3.49)$$

The parameters  $L_{pipe}$ ,  $R_{tube}$ , and  $N_{tube}$  of the airway model, can now be calculated using the derived equations 3.42, 3.43, and 3.49, making sure all units are in S.I:

$$L_{tube} = L_{pipe} \quad (3.50)$$

$$R_{tube} = \sqrt{\frac{8\mu L_{tube}^2}{R_{AW} DV}} \quad (3.51)$$

$$N_{tube} = \frac{DV}{\pi R_{tube}^2 L_{tube}} \quad (3.52)$$

### 3.2.2 Governing equations in the airways

After calculating the parameters of the airway model, we consider one tube from the airways (figure 3-8 below). The transport of oxygen and carbon dioxide in this tube, is governed by the unsteady advection-diffusion equations along the tube (direction  $\hat{x}$ ) derived from a taken control volume of length  $dx$  in the tube.  $U(t)$  is the air speed in the tube and can be found by dividing the volume flow rate expression in equation 3.35 with the tube area  $A_{tube}$ .  $O_{2,in}$  and  $CO_{2,in}$  are the concentrations of oxygen and carbon dioxide respectively, at the inlet of the mouth (based on the atmospheric composition of these gases).

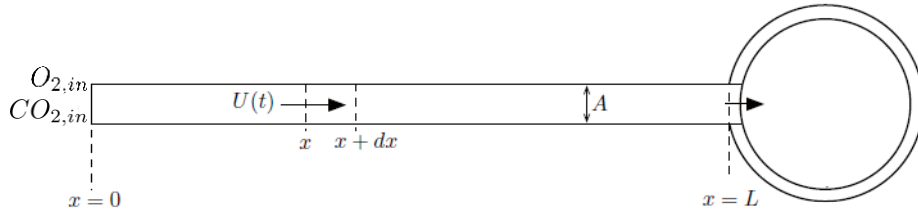


Figure 3-8: Schematic showing an airway tube with an appropriate control volume to derive the advection-diffusion equation

The derived advection -diffusion equations are written in terms of concentrations of oxygen  $O_2$  and carbon dioxide  $CO_2$ , where  $\mathfrak{D}_{O_2,air}$  and  $\mathfrak{D}_{CO_2,air}$  are the oxygen and carbon dioxide diffusion coefficients in air respectively.

$$\frac{\partial O_2}{\partial t} + U(t) \frac{\partial O_2}{\partial x} = \mathfrak{D}_{O_2,air} \frac{\partial^2 O_2}{\partial x^2} \quad (3.53)$$

$$\frac{\partial CO_2}{\partial t} + U(t) \frac{\partial CO_2}{\partial x} = \mathfrak{D}_{CO_2,air} \frac{\partial^2 CO_2}{\partial x^2} \quad (3.54)$$

Equations 3.53 and 3.54 are solved with the Dirichlet's boundary condition at  $x = 0$  and the mixed boundary condition at  $x = L$

$$\underline{x = 0}$$

$$O_2 = O_{2,in}$$

$$CO_2 = CO_{2,in}$$

$x = L$  where  $k_i$ ,  $h_i$ , and  $f_i$  are mixed boundary coefficients derived from the governing equations of the alveoli (refer to subsection 3.4.2)

$$k_{O_2}(t) \frac{\partial O_2}{\partial x} + h_{O_2}(t) O_2 = f_{O_2}(t)$$

$$k_{CO_2}(t) \frac{\partial CO_2}{\partial x} + h_{CO_2}(t) CO_2 = f_{CO_2}(t)$$

### 3.3 Gases reaching the alveoli

#### 3.3.1 Modeling the alveoli

The alveolus is the smallest element of the respiratory system where gas exchange between the air and blood occurs. Therefore, modeling the alveoli serves as a link between the respiratory gases content in the airways from one side, and their content in the blood from the other side. The alveoli are considered to be spherically-shaped elements that change in volume with time, based on the lung mechanics model. The number of alveoli is an important parameter that needs to be found for the complete model. According to Thurlbeck [28], 1982, the number of alveoli follows a logarithmic growth with age and depends on gender, with males having slightly more alveoli than females at a certain age. The number of alveoli  $N_{alv}$  in millions, is correlated as follows:

for boys

$$N_{alv} = 311.2 + 62.79 \ln(A) \tag{3.55}$$

for girls

$$N_{alv} = 269.4 + 55.49 \ln(A) \tag{3.56}$$

This correlation suggests that the number of alveoli grows importantly from an infant to an adult: A preterm infant has about 30 million alveoli whereas a 20 years old adult has about 500 million alveoli. From the onset of 20 years, the increase in the

number of alveoli becomes insignificant.

Having  $N_{alv}$ , the initial volume of a single alveolus, just before inspiration can be calculated as follows:

$$V_{alv}^0 = \frac{FRC}{N_{alv}} \quad (3.57)$$

From this volume, one can get a nominal value of  $R_{alv}$ , the radius of an open, spherically-shaped alveolus:

$$R_{alv}^0 = \sqrt[3]{\frac{3V_{alv}^0}{4\pi}} \quad (3.58)$$

The alveolar radius is not constant during respiration. The lungs are compliant elements that change in volume with every respiration cycle. For example, during inspiration, the alveoli are filled with air and increase in volume, leading to a higher alveolar radius.  $R_{alv}^0$  will be used in subsection 3.4.1 to get the variation of the pulmonary membrane's thickness with time  $h(t)$

### 3.3.2 Governing equations in the alveoli

The governing equations in the alveoli are non-steady conservation of oxygen and carbon dioxide concentrations. The non-steady term accounts for the species accumulation in the alveoli with time. For instance, carbon dioxide has a much higher concentration in the alveoli than in the atmosphere. Figure 3-9 helps visualize the formulation of the equation.

$$\frac{d(\bar{O}_2(t)V(t))}{dt} = O_2(L)Q_{in} - A_{CA}q_{O_2 \rightarrow blood} - \mathfrak{D}_{O_2,air}A_{tube} \frac{\partial O_2}{\partial x}(L) \quad (3.59)$$

In the equation above,  $Q_{in} = \frac{dV}{dt}(t)$ , is the volume flow rate in the airways,  $q_{O_2 \rightarrow blood}$  is the flux of oxygen to the blood, an expression of which will be derived in section 3.4, and  $A_{CA}$  is the contact area between the alveoli and the capillaries also derived in section 3.4. The concentration of oxygen entering the alveoli  $O_2(L)$  is a good estimate for  $\bar{O}_2$  since the alveoli is a very small element. Simplifying the left side term and

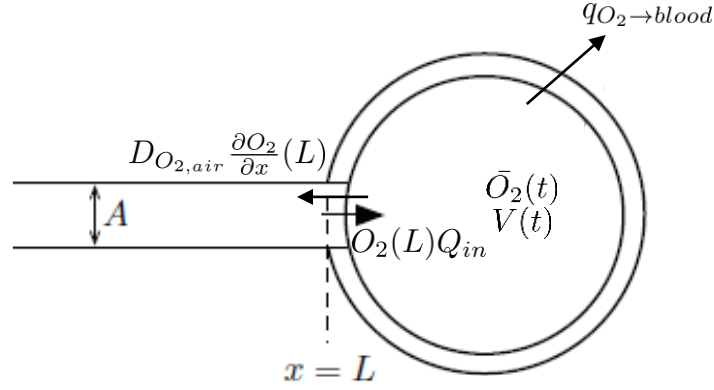


Figure 3-9: Section of the airways from figure 3-8, showing an alveolus and the components of the alveolar governing equation

adjusting the terms, equation 3.59 can be rewritten as follows:

$$\frac{d\bar{O}_2}{dt} = -\frac{A_{CA}}{V(t)} q_{O_2 \rightarrow \text{blood}} - \mathfrak{D}_{O_2, \text{air}} \frac{A_{\text{tube}}}{V(t)} \frac{\partial O_2}{\partial x}(L) \quad (3.60)$$

The analysis is similar for carbon dioxide:

$$\frac{d\bar{C}O_2}{dt} = -\frac{A_{CA}}{V(t)} q_{CO_2 \leftarrow \text{blood}} - \mathfrak{D}_{CO_2, \text{air}} \frac{A_{\text{tube}}}{V(t)} \frac{\partial CO_2}{\partial x}(L) \quad (3.61)$$

Note that the flux term for  $CO_2$  is from the blood to the alveoli, but the signs don't need to be changed because the solution of the equations will determine the direction of the fluxes by itself. Equations 3.60 and 3.61 are very important in linking oxygen and carbon dioxide content between the air and the blood. We now move to the last building block that completes the lung model.

## 3.4 Gas exchange and blood perfusion model

### 3.4.1 The pulmonary membrane

The only barrier that fully prevents the mixing of air with blood along the respiratory system is the pulmonary membrane. This very thin membrane is permeable to oxygen

and carbon dioxide, and allows exchange by diffusion. The initial thickness of an alveolus is taken to be the nominal thickness of the pulmonary membrane ( $h^0 \approx 0.5\mu m$ ). However the thickness of the pulmonary membrane is not constant at all times; During inspiration, an alveolus will increase in volume leading to a thinner membrane. The conserved quantity here is the pulmonary membrane volume  $V_{membrane}$  calculated using the initial alveolar radius  $R_{alv}^0$ :

$$V_{membrane}^0 = \frac{4}{3}\pi(R_{alv}^0 + h^0)^3 - \frac{4}{3}\pi(R_{alv}^0)^3 = V_{membrane}(t) \quad (3.62)$$

Therefore, we can get an expression for the thickness of the pulmonary membrane  $h(t)$  as a function of time:

$$h(t) = \sqrt[3]{\frac{3}{4\pi}[V_{membrane}^0 + \frac{4}{3}\pi R_{alv}^3(t)]} - R_{alv}(t) \quad (3.63)$$

The pulmonary membrane is assumed to be a thin body of water ( $h(t) \ll L_x$  where  $L_x$  is in the blood flow direction). The governing equation of diffusion across the membrane can be written in terms of molar concentration  $C$  with  $\hat{n}$  being the direction along the thickness:

$$\frac{\partial C}{\partial t} = \mathfrak{D}_{water} \frac{\partial^2 C}{\partial n^2} \quad (3.64)$$

Performing an order of magnitude analysis, the diffusion time scale is:

$$\tau_{diff} = \frac{(h^0)^2}{\mathfrak{D}_{water}} \quad (3.65)$$

Typical values of  $\mathfrak{D}_{water}$  for oxygen is  $0.21 \cdot 10^{-8} m^2/s$  leading to  $\tau_{diff} \approx 0.00017s$ . We can see that the diffusion time scale across the pulmonary membrane is very small compared the respiration time scale (1.5 to 4 second). Henceforth, it is safe to assume a steady diffusion process, leading to a constant flux of oxygen and carbon dioxide at a given time. Since it is of interest to express the content of oxygen and carbon dioxide in terms of partial pressures in the blood, the fluxes are shown below in terms



of a pressure difference, using  $D$  as a diffusion coefficient.  $\bar{P}_{O_2}$  and  $\bar{P}_{CO_2}$  are the mean partial pressures in the alveoli,  $P_{O_{2,b}}$  and  $P_{CO_{2,b}}$  are the mean partial pressures in the blood.

$$q_{O_2 \rightarrow \text{blood}} = D_{O_2, \text{water}} \frac{\bar{P}_{O_2} - P_{O_{2,b}}}{h(t)} \quad (3.66)$$

$$q_{CO_2 \leftarrow \text{blood}} = D_{CO_2, \text{water}} \frac{\bar{P}_{CO_2} - P_{CO_{2,b}}}{h(t)} \quad (3.67)$$

The diffusion coefficients of oxygen and carbon dioxide are available in literature based on a concentration difference:  $\mathfrak{D}_{O_2, \text{water}}$  and  $\mathfrak{D}_{CO_2, \text{water}}$  in  $m^2/s$ . Henry's law and the ideal gas law in air, are used to transform the fluxes in equations 3.66 and 3.67 above. Let  $O_{2,pm}$  be the oxygen concentration within the pulmonary membrane near the alveolar air, then through Henry's law:

$$k_H^{pc} = \frac{\bar{P}_{O_2}}{O_{2,pm}} \quad (3.68)$$

Henry's law can be also expressed as the ratio of concentrations:

$$k_H^{cc} = \frac{\bar{O}_2}{O_{2,pm}} \quad (3.69)$$

Using the ideal gas law, the partial pressure and concentration of a gas are simply related in the alveoli with  $T$  being the temperature in Kelvin and  $R$  being the universal ideal gas constant:

$$\frac{k_H^{cc}}{k_H^{pc}} = \frac{\bar{O}_2}{\bar{P}_{O_2}} = \frac{1}{RT} \quad (3.70)$$

Note that the exact same relations can be established for carbon dioxide. Using equation 3.68, we can transform the fluxes to concentration difference:

$$q_{O_2 \rightarrow \text{blood}} = \mathfrak{D}_{O_2, \text{water}} \frac{O_{2,pm} - \frac{P_{O_{2,b}}}{k_H^{pc}}}{h(t)} \quad (3.71)$$

$$q_{CO_2 \leftarrow blood} = \mathfrak{D}_{CO_2, water} \frac{CO_{2, pm} - \frac{PCO_{2, b}}{k_H^{bc}}}{h(t)} \quad (3.72)$$

The fluxes can be further adjusted using equations 3.69 and 3.70:

$$q_{O_2 \rightarrow blood} = \frac{\mathfrak{D}_{O_2, water}}{k_H^{cc}} \frac{\bar{O}_2 - \frac{PO_{2, b}}{RT}}{h(t)} \quad (3.73)$$

$$q_{CO_2 \leftarrow blood} = \frac{\mathfrak{D}_{CO_2, water}}{k_H^{cc}} \frac{C\bar{O}_2 - \frac{PCO_{2, b}}{RT}}{h(t)} \quad (3.74)$$

It is clearly seen that  $\frac{PO_{2, b}}{RT} \neq \bar{O}_{2, b}$  and  $\frac{PCO_{2, b}}{RT} \neq C\bar{O}_{2, b}$ . In fact the concentrations and partial pressures in the blood are related through the dissociation curves. Explicit relations for the dissociation curves will be presented in subsection 3.4.3.

### 3.4.2 Getting the mixed boundary coefficients

Consider the so far derived equations for oxygen. Replacing the expression of the flux, equation 3.73, in the governing equation of the alveolar space, equation 3.60, and rearranging the expression, we get:

$$\mathfrak{D}_{O_2, air} \frac{A}{V(t)} \frac{\partial O_2}{\partial x}(L) + \frac{ACA \mathfrak{D}_{O_2, water}}{V(t) k_H^{cc} h(t)} \bar{O}_2 = \frac{ACA \mathfrak{D}_{O_2, water}}{V(t) k_H^{cc} h(t) RT} PO_{2, b} - \frac{d\bar{O}_2}{dt} \quad (3.75)$$

The mixed boundary condition at the end of the airways is written as follows:

$$k_{O_2}(t) \frac{\partial O_2}{\partial x} + h_{O_2}(t) O_2 = f_{O_2}(t) \quad (3.76)$$

Comparing equations 3.75 and 3.76, we get the mixed boundary coefficient to solve the advection-diffusion equation in the airways:

$$k_{O_2}(t) = \mathfrak{D}_{O_2, air} \frac{A}{V(t)}$$

$$h_{O_2}(t) = \frac{ACA \mathfrak{D}_{O_2, water}}{V(t) k_H^{cc} h(t)}$$

$$f_{O_2}(t) = \frac{A_{CA} \mathfrak{D}_{O_2, water}}{V(t) k_H^{cc} h(t) RT} P_{O_2, b} - \frac{dO_2}{dt}$$

The exact same analysis can be done for carbon dioxide:

$$k_{CO_2}(t) = \mathfrak{D}_{CO_2, air} \frac{A}{V(t)}$$

$$h_{CO_2}(t) = \frac{A_{CA} \mathfrak{D}_{CO_2, water}}{V(t) k_H^{cc} h(t)}$$

$$f_{CO_2}(t) = \frac{A_{CA} \mathfrak{D}_{CO_2, water}}{V(t) k_H^{cc} h(t) RT} P_{CO_2, b} - \frac{dCO_2}{dt}$$

It follows that the governing equation in the alveolar space is nothing but the mixed boundary condition of the advection-diffusion equation in the airways. Furthermore, the blood partial pressure of gases appears in the alveolar equation. Therefore, the airways, the alveoli, and the blood are all coupled in the solution.

### 3.4.3 The dissociation curves

#### Oxygen

The oxygen-hemoglobin dissociation curve (ODC) relates the saturation of hemoglobin with oxygen (which can be transformed to an oxygen concentration) to the oxygen partial pressure in the blood. As already said, these curves are constructed from empirical data. However, some work in literature developed an explicit relation of these curves for easier integration in modeling. The first explicit expression was done by Hill (1910) and has the form:

$$\frac{C_1}{H} = \frac{kp_1^n}{1 + kp_1^n}$$

$C_1$  is the oxyhemoglobin concentration,  $H$  is the total hemoglobin content,  $p_1$  is the oxygen partial pressure,  $k$  and  $n$  are constants.

The research afterwards conserved the form of the explicit relation, but showed an explicit dependence of the dissociation curve on carbon dioxide partial pressure and pH. Sharan *et al* [26], 1989, proposed a mathematical model that explicitly

shows the variation of the ODC with pH and carbon dioxide content. This model is summarized as follows: The reduced form of hemoglobin is  $HbNH_2$ , the oxygenated form of Hemoglobin is  $O_2HbNH_2$ , and carbaminohemoglobin is present in the ionic form  $HbNHCOO^-$ ,  $H^+$ . Oxygen, carbon dioxide, and hydrogen ions (indicative of pH) all enter in reaction with hemoglobin in the blood. The ODC relation is derived from a kinetic study of the several chemical reactions between the respiratory gases and hemoglobin. The ODC expression is written as follows:

$$S = 100 \frac{K_0 P_{O_2,b}^n}{1 + K_0 P_{O_2,b}^n} \quad (3.77)$$

$$K_0 = \frac{(1 + 10^{-pH} K_2 + \frac{\gamma^{K_6} P_{CO_2,b}}{10^{-pH}}) K 10^{l pH}}{1 + 10^{-pH} K_1 + \frac{\gamma^{K_5} P_{CO_2,b}}{10^{-pH}}} \quad (3.78)$$

$S$  is the hemoglobin saturation in %,  $P_{O_2,b}$  and  $P_{CO_2,b}$  are the oxygen and carbon dioxide partial pressures respectively. All other parameter are defined and explained in appendix B.

Figure 3-10 below plots the ODC for two characteristic values of  $P_{CO_2,b}$  in the blood. We can see that as  $P_{CO_2,b}$  increases, the ODC shifts to the left. Therefore the model mimics the Bohr effect correctly.

The saturation of hemoglobin can be written as an oxygen concentration:

$$O_{2,b} = \frac{S}{100} O_{2,b|S=100\%} = \frac{S}{100} 0.201$$

Leading to:

$$O_{2,b} = f(P_{O_2,b}, P_{CO_2,b}) = 0.201 \frac{K_0 P_{O_2,b}^n}{1 + K_0 P_{O_2,b}^n} \quad (3.79)$$

## Carbon dioxide

The carbon dioxide dissociation curve relates directly the carbon dioxide concentration to its partial pressure in the blood. Meade *et al* [20], 1972, developed an explicit relation for the carbon dioxide dissociation, using best fitting on the experimental results of Comroe (1963). The relation covers a wide range of carbon dioxide partial

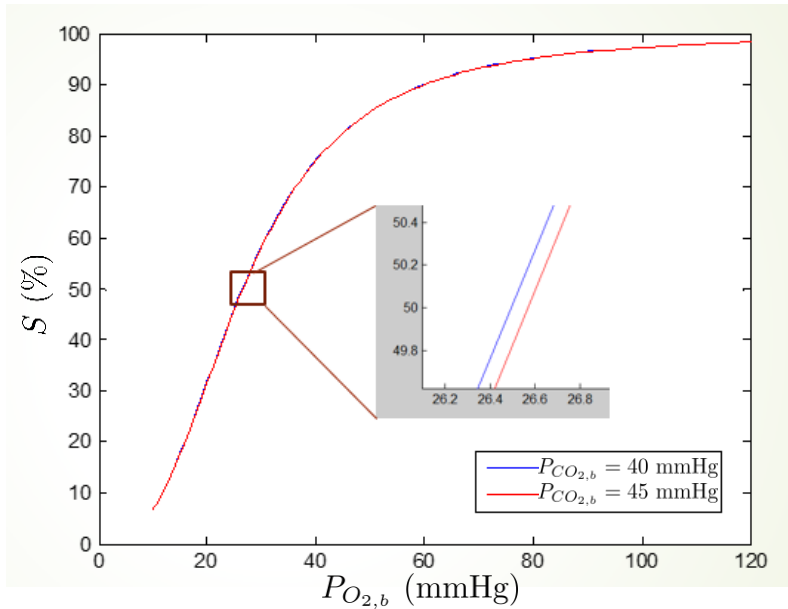


Figure 3-10: Plot of the oxygen dissociation curve as hemoglobin saturation versus oxygen partial pressure for typical values of carbon dioxide partial pressure. The magnification shows the Bohr effect, a leftward shift with lower partial pressure of carbon dioxide

pressure ( $10 \text{ mmHg} < P_{CO_{2,b}} < 80 \text{ mmHg}$ ) and was at first expressed at a 97.5% typical saturation of hemoglobin with oxygen. A correction to the change of saturation was then added to the expression that consists of a negative and a positive exponent:

$$CO_{2,b} = f(P_{CO_{2,b}}, P_{O_{2,b}}) = 462e^{0.00415P_{CO_{2,b}}} - 340e^{-0.0445P_{CO_{2,b}}} + 0.62(97.5 - S) \quad (3.80)$$

$CO_{2,b}$  is expressed in mL/L and  $S$  is the hemoglobin saturation with oxygen found in equation 3.77.

In figure 3-11 below, the carbon dioxide dissociation curve is plotted for two typical saturations of hemoglobin. We can see that as the saturation of oxygen increases, the dissociation curve shifts to the right. This is the Haldane effect, and it is more significant than the Bohr effect which validates the literature.

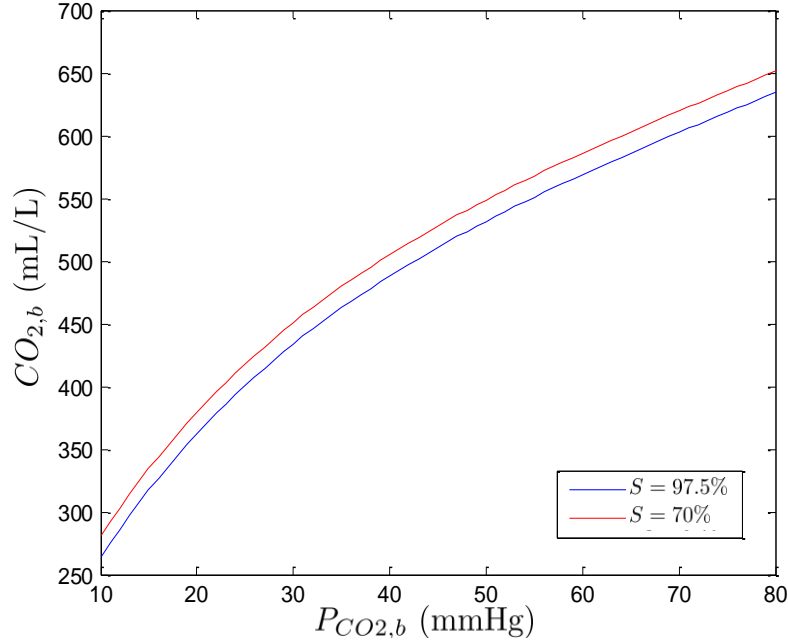


Figure 3-11: Plot of the carbon dioxide dissociation curve as concentration versus partial pressure for typical values hemoglobin saturation with oxygen. The Haldane effect is shown, a leftward shift with lower hemoglobin saturation.

### 3.4.4 Model and governing equations

the pulmonary capillaries are in contact with the alveoli to ensure gas exchange. Each alveolus is surrounded by several capillaries in which the red blood cells travel at the blood speed. In the blood side, models are needed for the blood flow and the capillary distribution around the alveoli before stating the governing equations.

The blood flow model: This model takes as an input, the percent contact area between the alveoli and the capillaries ( $CA$ ), and the resident time of the blood in the pulmonary capillaries, or in other words, the time of gas exchange ( $t_{res}$ ).  $CA$  is a controlled variable in the model,  $t_{res}$  is taken to be constant at 0.8 sec, a typical resident time in the capillaries. The maximum blood volume that can enter the blood can be calculated if the capillaries of diameter  $D_{cap}$  surround the totality of each alveolus' surface area:

$$V_{b,max} = N_{alv} 4\pi (R_{alv}^0)^2 D_{cap} \quad (3.81)$$

The blood volume entering the pulmonary capillaries is then based on the percent of contact area:

$$V_b = CAV_{b,max} \quad (3.82)$$

From the blood volume and the resident time, the volume flow rate of blood entering the pulmonary capillaries is calculated:

$$\dot{V}_b = \frac{V_b}{t_{res}} \quad (3.83)$$

The flow rate of blood entering a single alveolus is:

$$\dot{V}_b^{alv} = \frac{\dot{V}_b}{N_{alv}} \quad (3.84)$$

The capillary distribution model: This model assumes that a single capillary surrounds half of the alveolar perimeter ( $L_{cap} = \pi R_{alv}^0$ ) with a contact length equal to the capillary diameter ( $W = D_{cap}$ ). From the given information, the number of capillaries  $N_{cap}^{alv}$  surrounding a single alveolus, and the contact area  $A_{CA}$  between a single alveolus and the surrounding capillaries can be found:

$$N_{cap}^{alv} = \frac{\frac{V_b}{N_{alv}}}{A_{cap}L_{cap}} \quad (3.85)$$

$$A_{cap} = \pi D_{cap}^2$$

$$A_{CA} = N_{cap}^{alv}L_{cap}W \quad (3.86)$$

Now, the speed of blood in a single capillary can be calculated as follows:

$$U_b = \frac{\dot{V}_b^{alv}}{N_{cap}^{alv}A_{cap}} \quad (3.87)$$

The governing equations of the blood perfusion model are derived by taking a control volume in a single capillary around one alveolus as shown for the case of oxygen in figure 3-12 below:

Similar to the airways, the governing equations consist of a diffusion and an ad-

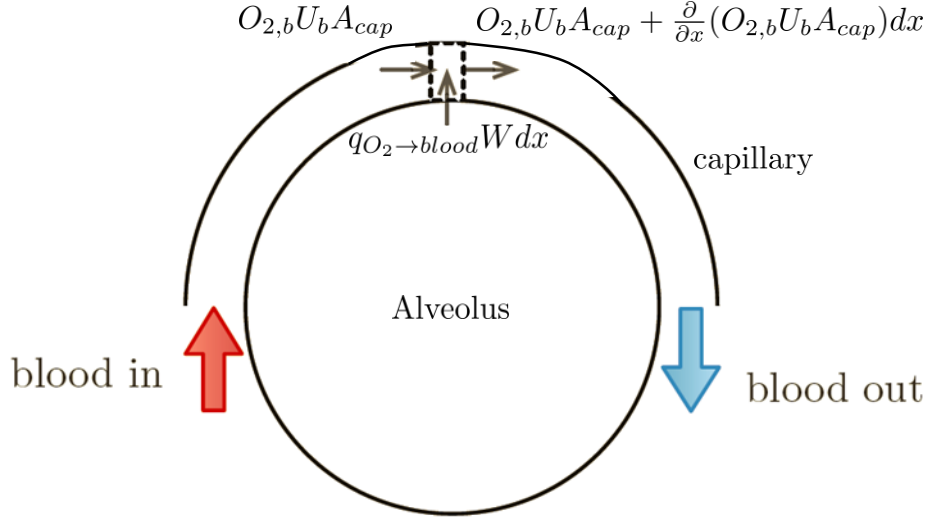


Figure 3-12: schematic showing the control volume taken to derive the advection diffusion equation for oxygen in the pulmonary capillary

vection term and are shown below. The boundary condition of these equations is the content of the blood with oxygen and carbon dioxide at the entrance of the blood. We know that entering blood is rich in  $CO_2$  and poor in  $O_2$  ( $P_{O_{2,b}} = 40\text{mmHg}$  and  $P_{CO_{2,b}} = 45\text{mmHg}$ ). The partial pressures are converted to blood concentrations using the dissociation curves (equations 3.79 and 3.80).

$$\frac{\partial O_{2,b}}{\partial t} + U_b \frac{\partial O_{2,b}}{\partial x} = \frac{W}{A_{cap}} q_{O_2 \rightarrow blood} \quad (3.88)$$

$$\frac{\partial CO_{2,b}}{\partial t} + U_b \frac{\partial CO_{2,b}}{\partial x} = \frac{W}{A_{cap}} q_{CO_2 \leftarrow blood} \quad (3.89)$$

In the blood, equations 3.88 and 3.89 are solved in a Lagrangian frame, by basically discretizing the capillary to similar adjacent Lagrangian particles of length  $X = U_b \Delta T$  where  $\Delta T$  is the time step. Therefore, it is more convenient to write the governing equations as follows:

$$\frac{dO_{2,b}}{dt}(X, t) = \frac{W}{A_{cap}} q_{O_2 \rightarrow blood} \quad (3.90)$$



$$\frac{dCO_{2,b}}{dt}(X, t) = \frac{W}{A_{cap}} q_{CO_2 \leftarrow blood} \quad (3.91)$$

The building blocks of the model are now complete. In the coming chapter, a brief overview on the iterative solution is shown, followed by model testing and validation.

# Chapter 4

## Solution Approach and Validation

The solution approach is based on a first guess of oxygen and carbon dioxide content, followed by several iterations until convergence. In a single iteration, the governing equations of the lung mechanics, the airways, the alveoli, and the blood are numerically solved. The results are displayed in terms of lung mechanics and gases transport in the respiratory system.

### 4.1 Iterative solution

At each time step  $\Delta t$ , the iterative solution has the following steps:

1. Start with given values at time  $t$ , and guess oxygen and carbon dioxide concentrations in the alveolar space. The starting guess can be taken as:

$$\bar{O}_2(t + \Delta t) = \bar{O}_2(t)$$

$$C\bar{O}_2(t + \Delta t) = C\bar{O}_2(t)$$

2. Solve for the mean oxygen and carbon dioxide concentrations ( $O_{2,b}$  and  $CO_{2,b}$ ) and partial pressures ( $P_{O_{2,b}}$  and  $P_{CO_{2,b}}$ ) in the blood using equations 3.90 and 3.91. This step requires iteration and coupling with the nonlinear explicit relations of the dissociation curves (equations 3.79 and 3.80).

3. Solve the advection diffusion equations of oxygen and carbon dioxide in the airways (equations 3.53 and 3.54). Having the mixed boundary coefficients, the spatial and temporal distribution of the respiratory gases can be solved in the airways.
4. Update the oxygen and carbon dioxide concentrations in the alveolar space based on the solution of step 3.

$$\bar{O}_2(t + \Delta t) = O_2(L)$$

$$C\bar{O}_2(t + \Delta t) = CO_2(L)$$

5. Check the convergence of the solution. If the concentrations converge, we move to the next time step and repeat the process. If not, we go back to step 2.

## 4.2 Model Description

The designed lung model can be used in two different directions: normal breathing and imposed breathing.

Normal breathing emulates the natural breathing of an individual that is driven by the difference in intrapleural pressure that nominally oscillates between -5 and -10 cmH<sub>2</sub>O. The frequency of respiration is the nominal value from subsection 3.1.1. Normal breathing is helpful for the validation of the model with pulmonary physiology (subsection 4.3.2).

Imposed breathing allows the user of the model to ventilate an individual by imposing a pressure signal at the mouth that operates similar to the intrapleural pressure oscillation. The intrapleural pressure is assumed to be constant at -5 cmH<sub>2</sub>O, meaning that respiration is fully artificial. This mode gives control over the frequency and the amplitude of the pressure signal. Note that imposing a pressure signal identical to the signal generated by the nominal oscillation of the intrapleural pressure, gives the same results as the normal breathing mode. Imposed breathing is useful to study

oxygenation and ventilation over a range of respiration frequencies (chapter 5). It is also used to perform a treatment for a baby suffering a lack of surfactant (chapter 6)

### 4.2.1 input needed

The model's inputs are classified as follows:

- The individual's identity in terms of age  $A$  and gender. Through the growth charts, an individual's nominal body weight and height are given. Body weight  $BW$  and height  $h$  can also be considered as controlled inputs.
- Parameters taken from the background on respiration physiology, and considered as constants, mainly, the minimum and maximum intrapleural pressure  $P_{ip,min}$  and  $P_{ip,max}$ , the nominal thickness of the pulmonary membrane  $h^0$ , and the diameter of the capillary  $D_{cap}$ .
- Physical constants defining the physics used in the building blocks of the model, mainly, the surface tension of water  $\gamma_{water}$ , Henry's constants  $k_h^{pc}$  and  $k_h^{cc}$ , the universal gas constant  $R$ , the body temperature  $T$ , and the diffusion coefficients of oxygen and carbon dioxide in air and water  $\mathfrak{D}_{O_2,air}$ ,  $\mathfrak{D}_{O_2,water}$ ,  $\mathfrak{D}_{CO_2,air}$ ,  $\mathfrak{D}_{CO_2,water}$ .
- Dissociation curve related parameters all defined in appendix B.
- Inlet boundary conditions to the airways  $O_{2,in}$  and  $CO_{2,in}$ , and to the blood  $P_{O_2,b,in}$  and  $P_{CO_2,b,in}$
- Surfactant fraction  $SF$  used for modeling lack of surfactant in an individual.
- Parameters related to modeling the blood volume and volume flow rate: the contact area percent  $CA$ , an input that needs to be controlled to get optimal oxygenation and ventilation, and the resident time  $t_{res}$  taken to be constant.
- The perturbation frequency  $f$ , pressure amplitude  $\Delta P$ , and mean airway pressure  $MAP$  that are controlled inputs in the imposed breathing mode.

- Inputs related to the numerical solution such as the size of the spatial grids and the number of time steps per respiration cycle.

### 4.2.2 output generated

The output is generated as plots that change in time when a simulation is running. In other words, the respiration cycles of an individual can be monitored throughout a simulation. The plots indicate the behavior of the lung mechanics and the gases transport in the respiratory system. They are described as follows:

- Lung mechanics
  - The intrapleural pressure oscillation and alveolar pressure oscillation as a function of time. The equivalent pressure signal at the mouth is also displayed.
  - The lung volume oscillation as a function of time. The nominal values of the functional residual volume and tidal volume are also shown for the sake of comparison with respiration physiology.
  - The pressure versus volume curve otherwise called the compliance diagram or hysteresis curve.
- Gases transport
  - The spatial distribution of oxygen and carbon dioxide concentrations in the airways at any given time.
  - The spatial distribution of oxygen and carbon dioxide partial pressures in the pulmonary capillaries at any given time.
  - The variation of the mean partial pressure of oxygen and carbon dioxide in the alveoli and the blood as a function of time.

## 4.3 Validation

Validating the obtained lung model with literature on pulmonary physiology is substantial before any results or conclusions can be generated. The calculated lung compliance and airway resistance in the model, need to be checked with available values in literature at first. Then, the results of a breathing simulation are compared with expected results based on the background on respiration physiology and the building blocks of the model.

### 4.3.1 Compliance and airway resistance

The nominal compliance is calculated from the nominal tidal volume  $TV_{nom}$  and intrapleural pressure difference  $P_{ip,max} - P_{ip,min}$ . Both of these values are used from pulmonary physiology, therefore, the nominal compliance is validated. The tissue compliance  $C_{tissue}$  takes into account the surfactant fraction  $SF$ . When an individual lacks surfactant, the lung compliance is supposed to decrease. Using the surfactant model of the previous chapter 3.1.4, the tissue compliance of a preterm infant decreases by about 32 % from normal condition ( $SF=1$ ) to worst condition ( $SF=0$ ). This leads to a tissue compliance of about 2 mL/cmH<sub>2</sub>O. However, compliance values for a sick preterm infant can be much lower than that in literature. For example, the compliance of a preterm infant suffering lack of surfactant reaches 0.17 to 0.68 mL/cmH<sub>2</sub>O [8]. Henceforth, the current implemented model overestimates the tissue compliance of a severely sick preterm infant.

The calculated airway resistance using the implemented lung mechanics model (refer to 3.1.5), is plotted against age from a preterm infant to a 20 years old adult in figure 4-1 below. The airway resistance of a preterm infant is about 22 cmH<sub>2</sub>O.s/L. In a study, infants breathing at the nominal frequency of respiration have an airway resistance between 25 and 41 cmH<sub>2</sub>O.s/L [5]. The calculated value is very close to the lower boundary. For an adult, the calculated resistance decreases to 2 cmH<sub>2</sub>O.s/L. In literature, the airway resistance in healthy adults is around  $1.67 \pm 0.61$  [17]. Consequently, the values for airway resistance lie within a physiological range which

validates their use.

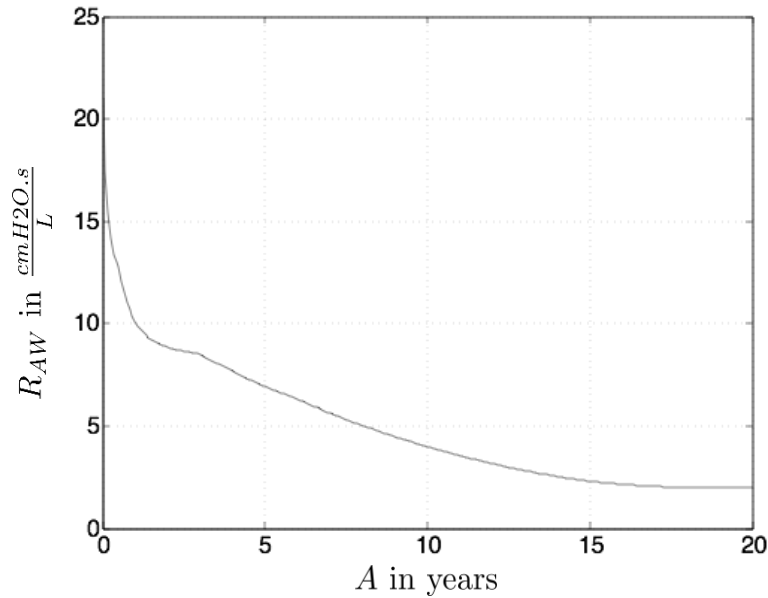


Figure 4-1: Calculated airway resistance versus age from a preterm infant to a 20 years old adult

### 4.3.2 Lung mechanics in normal breathing

The model is first tested using normal breathing simulation for a preterm infant (girl) and an adult 20 years old male. Results related to lung mechanics are shown in figure 4-2 below. The inspiration to expiration time ratio is  $\frac{1}{2}$  as typical for normal breathing. Inspiration is characterized by a decrease in the intrapleural pressure from -5 to -10 cmH<sub>2</sub>O. Expiration takes double the time of inspiration and is characterized by the increase of the intrapleural pressure back to -5 cmH<sub>2</sub>O (the blue curve in the first graph). The green curve is the oscillation of the alveolar pressure bounded by -1 and 1 cmH<sub>2</sub>O. The magenta curve shows the equivalent pressure signal of the blue curve, generated on the openings of the airways. The lung volume in the second graph oscillates between the two lines  $FRC$  and  $FRC + TD$  where  $TD = TV_{nom}$ . As seen, the amplitude of the lung volume is very close to  $TV_{nom}$  which validates the model. The  $p - v$  hysteresis curve is similar to the curves shown in pulmonary physiology books, depicting that the p-v relation is different between inspiration and expiration.

The difference between the preterm infant and the adult is apparent through the tidal volume difference (15 mL versus 500 mL respectively) and the period of a respiration (1.33 s versus 4 s respectively). Consequently, the lung mechanics agree with the physiological characteristics of respiration.

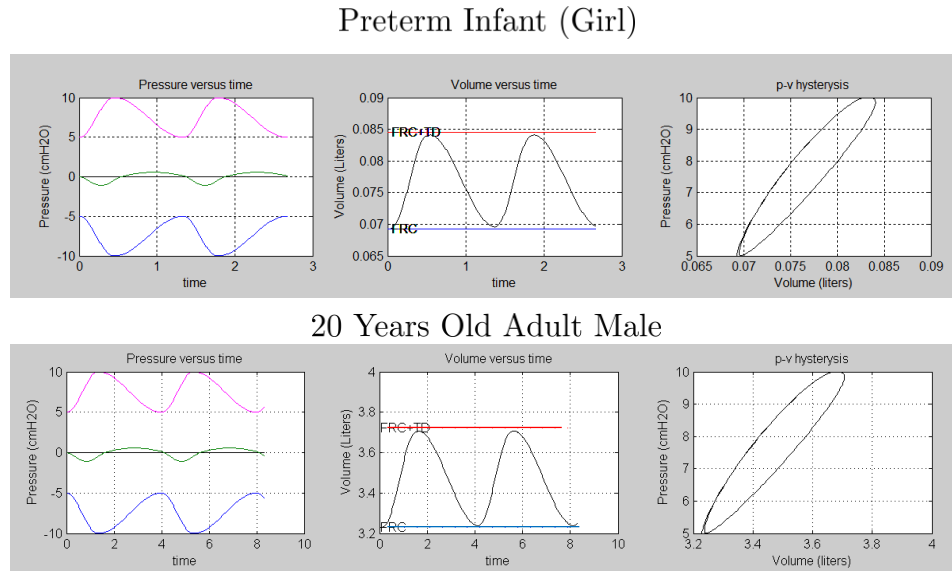


Figure 4-2: Lung mechanics results for a normal breathing case of a preterm infant (girl) and a 20 years old male. The plots on the left show the intrapleural pressure signal (blue), the alveolar pressure signal (green), and the airways' pressure signal (magenta). The plots in middle show the lung volume with the nominal values of FRC (blue) and tidal volume (red). The plots on the right show the pressure versus volume hysteresis curves. 2 respiration cycles are shown.

### 4.3.3 Tuning contact area and getting the blood volume

Specifying the contact area  $CA$  is important for the gases transport solution of the model. Since  $CA$  is a controlled input, it is tuned such that gas exchange across the pulmonary membrane is optimal. In other words, at a given age,  $CA$  is set such that the blood in the pulmonary capillaries saturates with oxygen ( $P_{O_{2,b}} = 102$  mmHg) and has appropriate carbon dioxide ( $P_{CO_{2,b}} = 40$  mmHg). The process is done by trial an error at every age from 0 years till 20 years. From 20 years onward, the contact area is assumed to be invariable. As stated in chapter 3-12, the blood volume



is calculated from the contact area:

$$V_b = CA V_{b,max}$$

In our model, we take  $CA$  to be a function of gender while tuning. Figure 4-3 below, shows the results of tuning  $CA$  as a function of gender and age. A preterm infant has the highest contact area (25 to 30 %). As one grows older, the contact area falls abruptly then acceptably stabilizes around 10 %. In adults, the contact area in females is slightly higher than that in males.

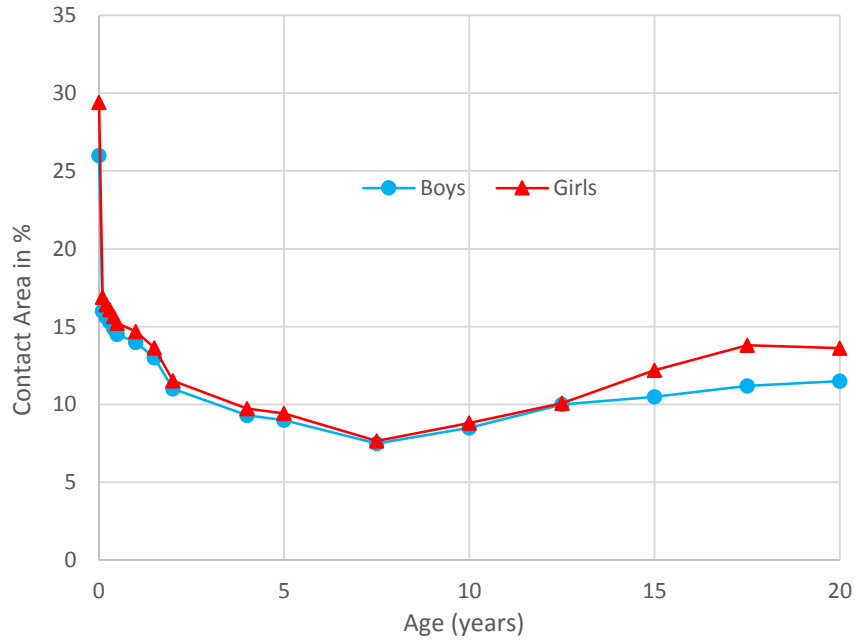


Figure 4-3: The variation of contact area  $CA$  for optimal gas exchange, with age and gender.  $CA$  is a controlled input of the model, and the data point plotted are the fine-tuned values of  $CA$  to yield in an optimal gas exchange.

The maximum blood volume  $V_{b,max}$  is also a function of gender (see equation 3.81) such that the resulting blood volume generated is independent of gender. Therefore our model assumes that the volume of blood entering the pulmonary capillaries is the same for males and females, it is the contact area that is slightly different. The blood volume is plotted versus age in figure 4-4 below:

The resulted blood volume follows a logical trend: it increases slightly from the age

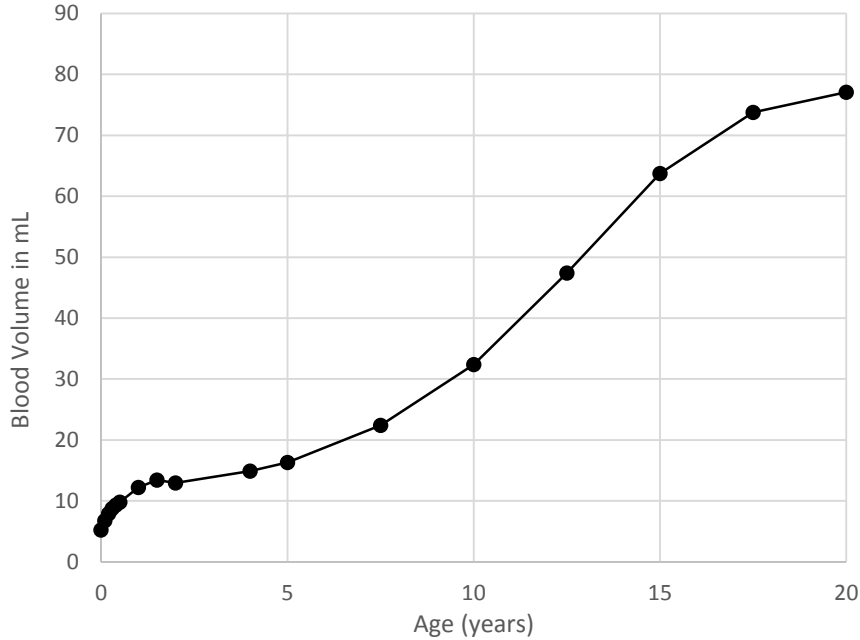


Figure 4-4: The variation of blood volume  $V_b$  with age. The plot is similar for both genders

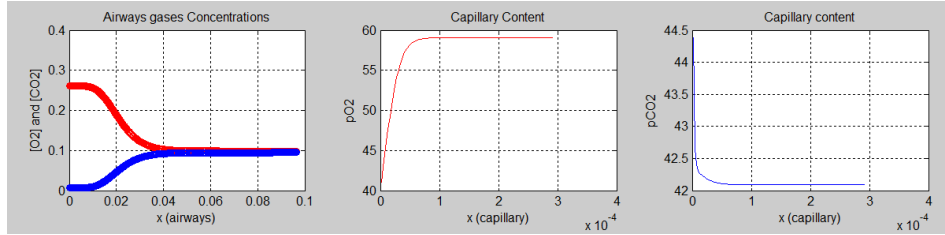
of 0 to 2 years, then increases sharply between 2 and 15 years, then starts stabilizing after 15 years. No physiological data is found on the blood volume for preterm infants and children. However, some research determines the blood volume in adults to be around  $78 \pm 13.2$  mL [13]. At the age of 20, the blood volume in the model is 77 mL which is in accordance with literature. Therefore it can be argued that the obtained blood volume is valid to use in the gases transport solution of the model.

#### 4.3.4 gases transport in normal breathing

After determining the blood volume, the simulation of gases transport can be done with optimal expected oxygenation and ventilation. Results related to gas transport can be displayed spatially and temporally. Figure 4-5 below shows the spatial distribution of oxygen and carbon dioxide in the airways and the capillaries.

Starting an inspiration gradually increases the oxygen concentration and decreases the carbon dioxide concentration with the airway length. This behavior observed in the left plots of figure 4-5, is helpful to visualize the opening and closing of the lungs.

### Starting an inspiration



### starting an expiration

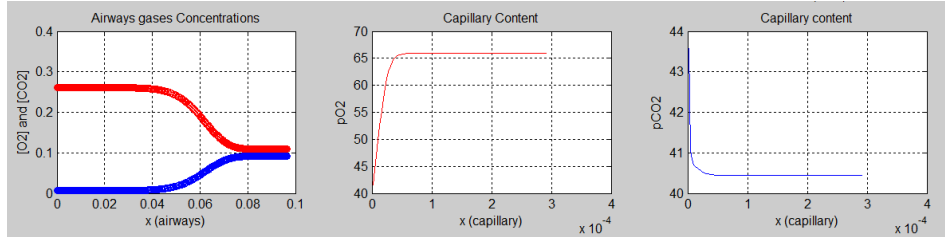


Figure 4-5: The spatial distribution of oxygen (red) and carbon dioxide (blue) in the airways (left plot) and the capillaries (middle and right plots) at the beginning of an inspiration and the beginning of the following expiration for a preterm infant (girl). The third respiration cycle is considered.

For instance, the red and blue thick curves seem to be the lining of the lungs. They are gradually opening with inspiration, then gradually closing with expiration. The model requires some time to reach a quasi-steady behavior where oxygen and carbon dioxide reach their physiological values in the blood. Figure 4-5 shows the third respiration cycle in which oxygen and carbon dioxide reached 65 and 40.5 mmHg respectively, in the capillaries. For oxygen, the value is reached at about one third the distance crossed as it is seen in the background (chapter 2), however, the value is reached at an earlier distance for carbon dioxide. In order to understand the evolution of gases transport with repeated cycles of respiration, we need to investigate the temporal distribution of oxygen and carbon dioxide. This is shown in figure 4-6 below.

The quasi-steady behavior is reached after 12 to 15 respiration cycles. By then, oxygen and carbon dioxide reach their physiological mean partial pressure in the blood. Figure 4-6 displays 10 respiration cycles with the evolution of  $O_2$  and  $CO_2$  both in the alveoli and the blood. The partial pressures of  $O_2$  and  $CO_2$  in the blood follow

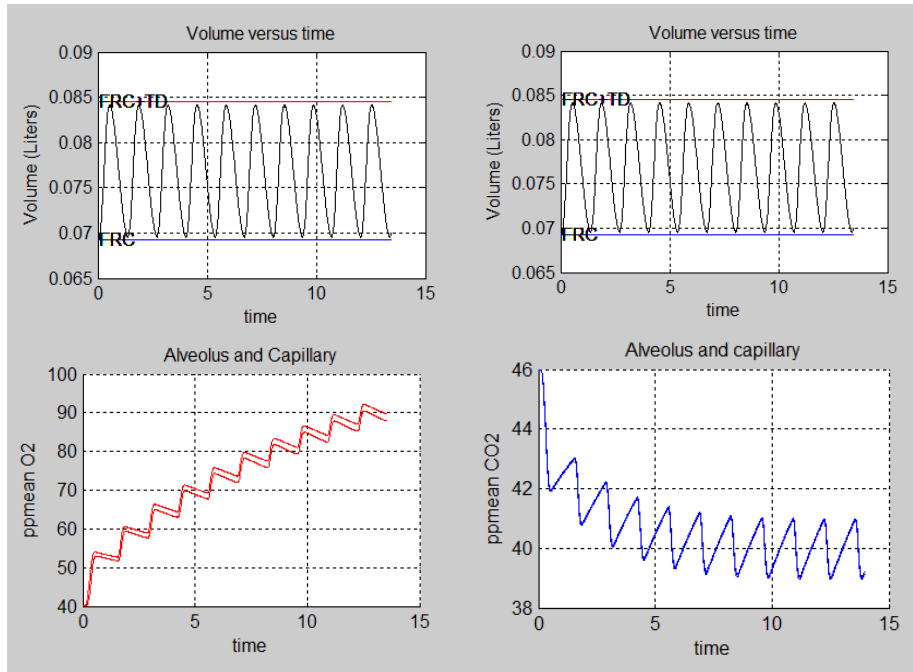


Figure 4-6: The variation of oxygen mean partial pressure  $P_{O_{2,b}}$  (red) and carbon dioxide mean partial pressure  $P_{CO_{2,b}}$  (blue) with time, coupled with the lung volume variation (two similar top plots) for a preterm infant (girl). 10 respiration cycles are shown.

the partial pressures of  $O_2$  and  $CO_2$  in the alveoli, so the two curves are almost the same for both cases. An interesting observation to mention here is the oscillation of the gases partial pressures with time. This oscillation can be explained by inspecting the change of lung volume. Let's consider the first respiration cycle of figure 4-6. During inspiration, air rich in oxygen is entering the lungs for exchange; and since the time scale of diffusion is very small, blood will be enriched with oxygen and deprived of carbon dioxide during the inspiration process. This is why oxygen partial pressure sharply increases and carbon dioxide partial pressure sharply decreases with an inspiration. During expiration, no exchange is really happening, but blood poor in oxygen and rich in carbon dioxide is entering the pulmonary capillaries. This is why we have a decrease in oxygen partial pressure and increase in carbon dioxide partial pressure. This behavior is less significant than the one observed during inspiration and takes more time. With the simulation of several respiration cycles, the oscillations will be less important thus reaching a steady state with 102 mmHg oxygen and 40 mmHg

carbon dioxide at the exit of the capillaries. We can also see that the oscillations for  $CO_2$  are more important than the oscillations for  $O_2$ . This observation is validated by the coupled relationship of oxygen and carbon dioxide in the blood through the dissociation curves. It is mentioned in physiology that the Haldane effect is way more important than the Bohr effect. This means that a change of  $P_{O_{2,b}}$  yields a larger change of  $P_{CO_{2,b}}$ . Henceforth, a larger number of respiration cycles is needed to reach steady partial pressures for both  $O_2$  and  $CO_2$ .

Through the above testings and validations, the built model is capable of capturing most of the respiration physiology observations in literature. The implementation of more sophisticated models for the lung mechanics and airways, and some refinements in the numerical solving method will improve the robustness of the model. Nevertheless, the model in its current status is strong enough to provide insight and investigation in respiration physiology. The next two chapters will make use of the model to come up with conclusions on parameter sensitivity and treatment approaches.

# Chapter 5

## Sensitivity Analysis

This chapter analyzes the performance of an individual in terms of gas exchange, when several respiratory parameters are varied, namely, the frequency of respiration  $f$ , the pressure amplitude  $\Delta P$ , the tissue compliance  $C_{tissue}$ , and the airway resistance  $R_{AW}$ .

### 5.1 Frequency sweep plots

Oxygenation and ventilation are recorded as the mean partial pressure of oxygen and carbon dioxide in the blood respectively ( $P_{O_{2,b}}$  and  $P_{CO_{2,b}}$ ), after a long enough time of respiration for these values to stabilize. These values are an indicator of gas exchange: When  $P_{O_{2,b}}$  is around 100 mmHg, the hemoglobin of the blood is saturated with oxygen, and when  $P_{CO_{2,b}}$  is 40 mmHg or lower, the blood is ventilated from carbon dioxide. This indicates a proper gas exchange. However, an under saturation with oxygen ( $P_{O_{2,b}} < 100$ ) or an accumulation of carbon dioxide ( $P_{CO_{2,b}} > 40$ ) in the blood, is an altered gas exchange that indicates either a pulmonary disease or an abnormal physiological condition. In this section, oxygenation and carbon dioxide removal, otherwise called ventilation, are investigated with the variation of respiration frequency, for two different individuals, a preterm infant (girl) representing the respiration of preterm infants, and a 20 years male representing the respiration of adults.

### 5.1.1 Preterm infant

The preterm infant breathes with an intrapleural pressure difference of 5 cmH<sub>2</sub>O, at the normal operational compliance and resistance. All the respiratory parameters are identical to the normal breathing case, meaning that the preterm infant is healthy. Gas exchange is recorded as the frequency of respiration varies, in figure 5-1 below.

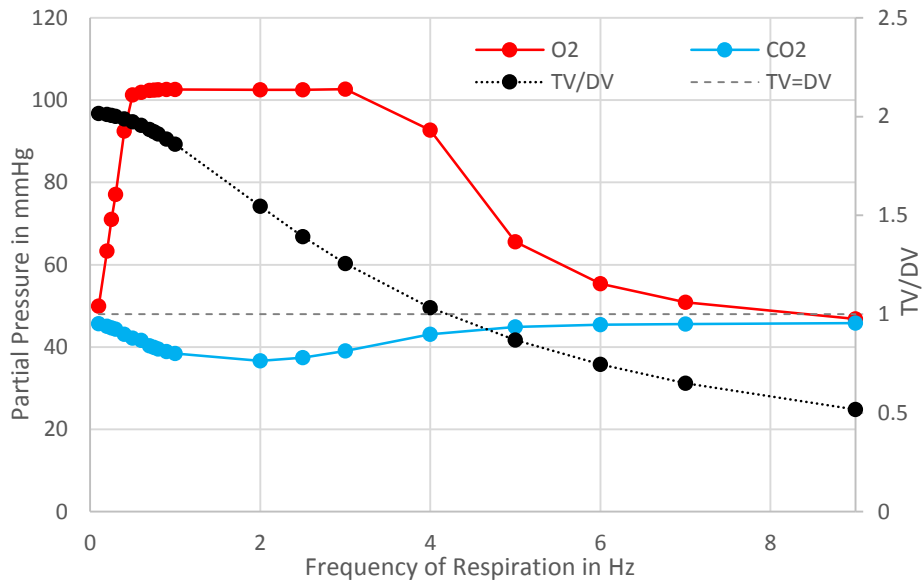


Figure 5-1: Dependence of oxygenation and ventilation on the frequency of respiration for a preterm infant, at nominal values of pressure amplitude, compliance, and resistance. The black curve is the ratio of the tidal volume to the dead space volume (right vertical axis) as a function of the frequency. The dashed horizontal line indicate a tidal volume equal to the dead space volume

The frequency of respiration is swept from 0.1 Hz to 9 Hz. Gas exchange is altered at low frequencies of respiration (0.1 - 0.6 Hz), then oxygen saturates at 102 mmHg and carbon dioxide goes below 40 mmHg to a minimum of 36.6 mmHg (0.6 - 3 Hz). At frequencies higher or equal to 4 Hz, gas exchange is altered again, and as frequency increases from that point, less oxygen is delivered to the blood and less carbon dioxide is removed from the blood to reach, eventually zero exchange. To explain such behavior, the lung mechanics model needs to be considered. The simulated tidal volume ( $TV$ ) is recorded at a given frequency, and the ratio of the

tidal volume to the dead space volume ( $DV$ ) is plotted with gas exchange. The dimensionless number  $\frac{TV}{DV}$  indicates whether fresh air is reaching the gas exchange area during a respiration cycle, since  $DV$  is the volume of gas filling the airways and not subject to gas exchange. When  $\frac{TV}{DV} > 1$ , the fresh air entering the lungs is able to reach the alveoli, thus promoting gas exchange mainly by advection. When  $\frac{TV}{DV} < 1$ , the fresh air doesn't reach the alveoli, meaning that gas exchange is only possible through the diffusion of oxygen and carbon dioxide particles in the airways. From figure 5-1, we can see that when the frequency reaches 4 Hz,  $\frac{TV}{DV} \leq 1$ , meaning that when the tidal volume becomes smaller than the dead space volume, the gas exchange becomes altered, and worsens as  $\frac{TV}{DV}$  decreases. Therefore, the observed behavior at the onset of 4 Hz is justified by the decrease of the tidal volume to an extent where fresh air cannot reach the exchange barrier anymore. The levels of oxygen and carbon dioxide don't immediately collapse after 4 Hz due to the slight gas exchange that is happening through diffusion. However, as the frequency increases, the period of a single respiration decreases, thus fresh air has less time to reach the alveoli. This is why, there will be no gas exchange anymore at a high enough frequency. This analysis goes in parallel with the characteristic frequency explained and derived from the small signal dynamic model in chapter 3.1.6. In fact, the characteristic frequency is nothing but the point corresponding to  $\frac{TV}{DV} = 1$  (refer to section 5.3).

The tidal volume analysis doesn't, however, explain the altered gas exchange at low frequencies. The lung mechanics model implemented is equivalent to an RC circuit. The impedance of the tissue compliance can be written as follows:

$$Z_C = \frac{1}{\omega C_{tissue}} = \frac{1}{2\pi f C_{tissue}} \quad (5.1)$$

for very low frequencies:

$$f \ll \frac{1}{2\pi R_{AW} C_{tissue}} \ll 2.39 Hz$$

The impedance approaches infinity and there will be no airflow to the lungs ( $\frac{dV}{dt} \approx 0$ ). For small enough frequencies, the air flow equation (equation 3.38) can be simplified



to:

$$\frac{dV}{dt} = 2\pi f C_{tissue} \frac{\Delta P}{2} \sin(2\pi f t) \quad (5.2)$$

From equation 5.2, the airflow is zero when the frequency is zero, and no gas exchange can occur with no air flowing to the lungs. Then, as the frequency increases, the amplitude of the airflow increases (with decreasing impedance) and gas exchange is improved. At the onset of 0.7 Hz (figure 5-1), the airflow becomes high enough to enter the alveoli and yield an optimal gas exchange. This explains the behavior of gas exchange at low frequencies.

### 5.1.2 Adult male

Similarly for a 20 years adult male, gas exchange is plotted along with the dimensionless number  $\frac{TV}{DV}$  as a function of the frequency of respiration, for a healthy subject (figure 5-2).

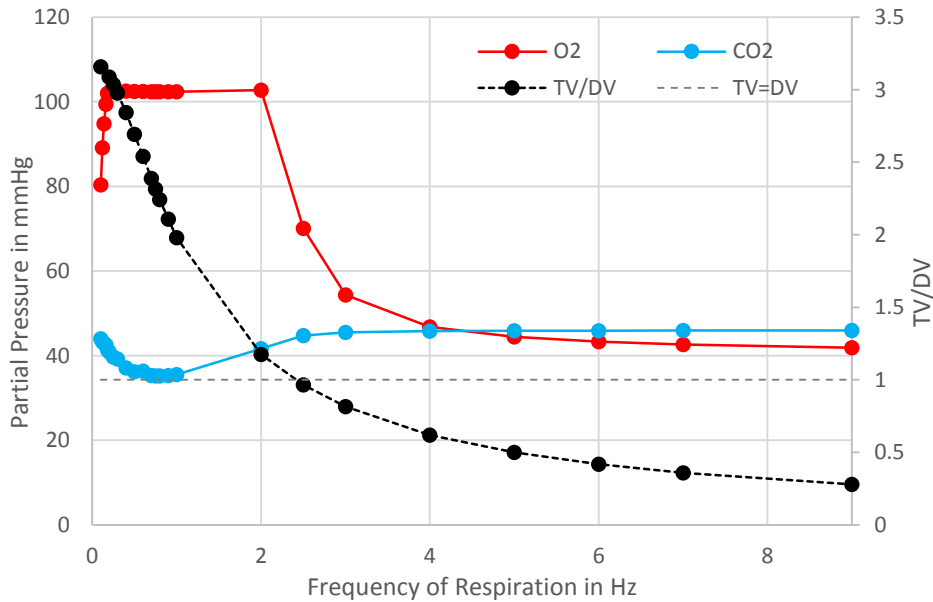


Figure 5-2: Dependence of oxygenation and ventilation on the frequency of respiration for a 20 years old male, at nominal values of the pressure amplitude, the compliance, and the resistance. The black curve is the ratio of the tidal volume to the dead space volume (right vertical axis) as a function of the frequency. The dashed horizontal line indicates a tidal volume equal to the dead space volume.

The frequency range under which an adult can breathe with proper gas exchange is smaller than that of a preterm infant (0.2 - 2 Hz against 0.6 - 3 Hz). These results also show that adults usually breathe at lower frequencies than preterm infants. The same analysis used for infants can be carried out for adults. For instance, fresh air cannot reach the exchange barrier at the onset of 2.5 Hz (the characteristic frequency), where gas exchange starts to be altered. For adults, the frequency of no gas exchange is close to 9 Hz since oxygen and carbon dioxide partial pressures values are close to those entering the capillaries (40 and 45 mmHg respectively). These results confirm the fact that the characteristic frequency of adults is lower than that of preterm infants (chapter 3.1.6). The high impedance at low frequency ( $f \ll 0.8$  Hz for the case of an adult) also explains the altered gas exchange below 0.2 Hz.

## 5.2 Parameter variation

So far, a healthy subject was considered, and the effect of frequency of respiration on gas exchange was explained. This section takes the adult male case, and performs a sensitivity analysis to deduce the effect of altering the pressure amplitude, the tissue compliance and the airway resistance on gas exchange. These parameters are chosen upon others, because they are typical indicators of pulmonary diseases: a low pressure amplitude means an altered intrapleural pressure difference that can originate from defected respiratory muscles, a high resistance indicates lung obstructive diseases, and a low compliance is related to constrictive lung diseases (for more details, see appendix A). A low compliance is typical also in infant respiratory distress syndromes (IRDS) characterized by the lack of surfactant in preterm infants. This scenario is investigated in chapter 6.

### 5.2.1 Pressure amplitude

The pressure amplitude  $\Delta P$  is equivalent to the difference in intrapleural pressure that is the driving force of a respiration cycle. Figures 5-3 and 5-4 show the effect of decreasing the pressure amplitude on oxygenation and ventilation, for a range of

respiration frequencies (0.1 - 7 Hz).

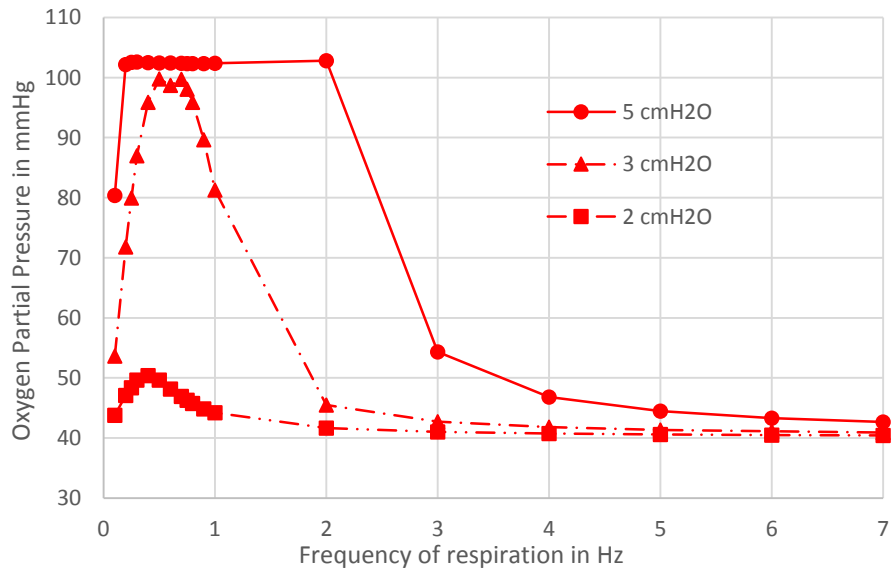


Figure 5-3: Sensitivity of oxygenation on the pressure amplitude over a frequency sweep at nominal values of compliance, and resistance, for an adult male (20 years old).

Gas exchange is highly sensible to the pressure amplitude. Looking at oxygenation in figure 5-3, decreasing the pressure amplitude to 3 cmH<sub>2</sub>O results in poor oxygenation over the frequency range except between 0.5 and 0.7 Hz. Going down to 2 cmH<sub>2</sub>O leads to almost no oxygenation for all the frequency range. An interesting observation is the shift of the optimal oxygenation frequency to the left. The optimal oxygenation frequency is the frequency at which the maximum oxygenation level occurs for a given pressure amplitude. This suggests that a sick subject with a reduced pressure amplitude, tends to breath at a lower frequency than the nominal one. Looking at ventilation in figure 5-4, carbon dioxide accumulates in the blood with a decreasing pressure amplitude. The graph shows that at pressure amplitudes lower than 3 cmH<sub>2</sub>O, there is no frequency for which proper gas exchange occurs, since the minimum  $CO_2$  level is at 42 mmHg at  $\Delta P = 3$  cmH<sub>2</sub>O. Carbon dioxide is almost at its initial level for  $\Delta P = 2$  cmH<sub>2</sub>O. Defining the optimal ventilation frequency as the frequency at which the minimum ventilation level occurs for a given

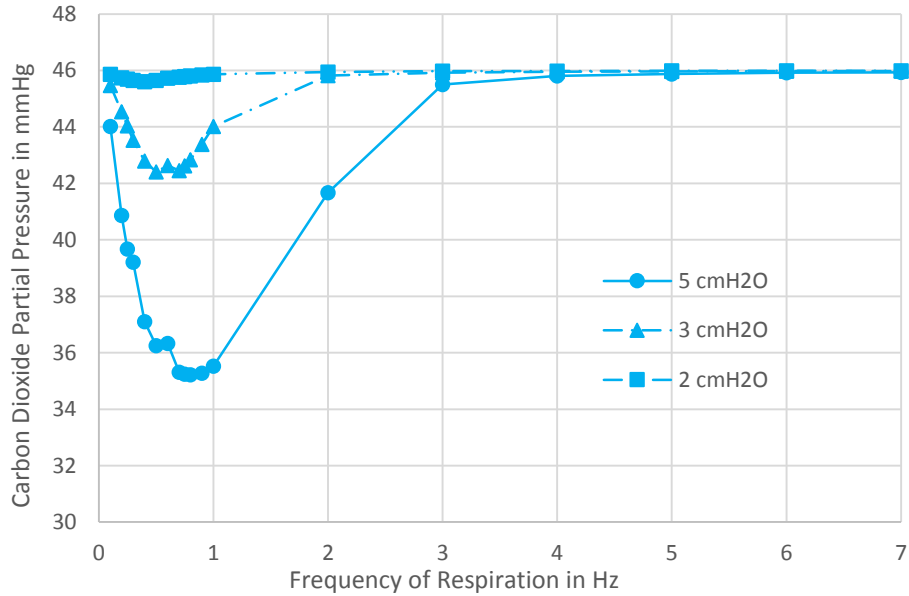


Figure 5-4: Sensitivity of ventilation on the pressure amplitude over a frequency sweep at nominal values of compliance, and resistance, for an adult male (20 years old).

pressure amplitude, we can see that it also shifts to the left. Therefore, oxygenation and ventilation are altered in the same direction with decreasing pressure amplitude.

## 5.2.2 Compliance

The tissue compliance  $C_{tissue}$  tends to decrease in a pulmonary disease, causing the lungs to become stiffer. Figures 5-5 and 5-6 show the effect of decreasing the tissue compliance on oxygenation and ventilation, for a range of respiration frequencies (0.1 - 7 Hz).

A small decrease of the tissue compliance has no or little effect on gas exchange as it can be seen from the -10 % lower value. The effect on gas exchange is more pronounced when the compliance decreases by 50 %. Considering oxygenation in figure 5-5, the range of frequencies for blood saturation with oxygen is significantly narrowed from 0.2 - 2 Hz to 0.7 - 1.8 Hz. As for ventilation in figure 5-6, the minimum  $CO_2$  level is at 42 mmHg meaning that no proper ventilation occurs if the compliance decreases by 50 %. The optimal ventilation frequency is slightly shifted to the right

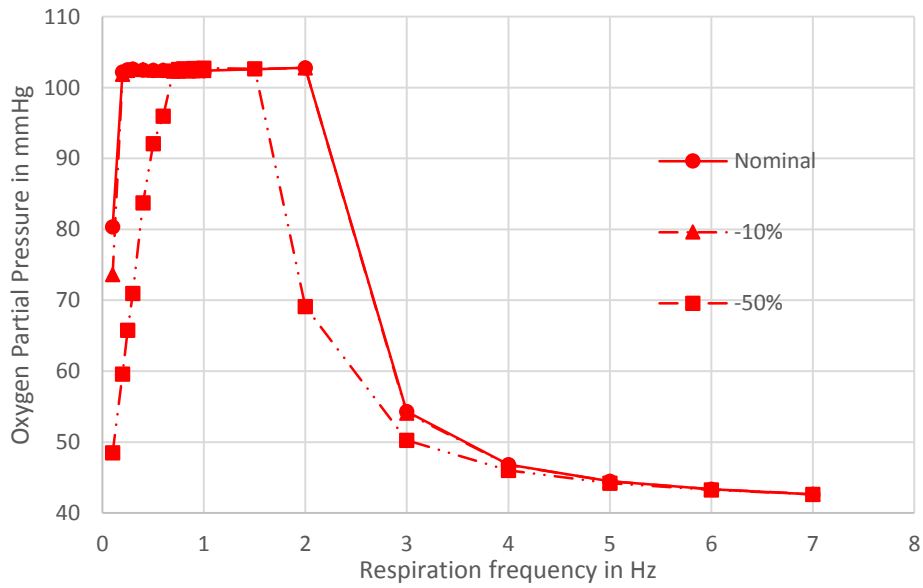


Figure 5-5: Sensitivity of oxygenation on the tissue compliance over a frequency sweep, at nominal values of pressure amplitudes and resistance, for an adult male (20 years old).

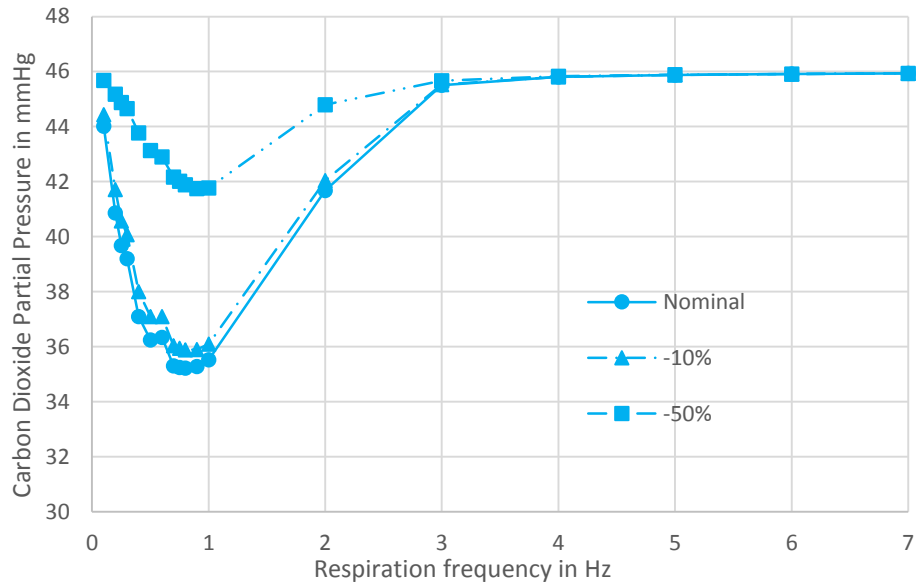


Figure 5-6: Sensitivity of ventilation on the tissue compliance over a frequency sweep, at nominal values of pressure amplitudes and resistance, for an adult male (20 years old).

with decreasing compliance. This suggests that a sick subject with less compliant lungs tends to breath faster than normal subjects. An interesting observation for compliance sensitivity is what happens before oxygen reaches saturation. The lung impedance is also a function of the tissue compliance (equation 5.1), and it increases with lower values of compliance. That's why we need a higher frequency to reach oxygen saturation when the compliance is decreased by 50 %.

### 5.2.3 Airway resistance

The airway resistance  $R_{AW}$  tends to increase in a sick person who suffers obstruction in the airway canals. Figures 5-7 and 5-8 show the effect of decreasing the airway resistance on oxygenation and ventilation, for a range of respiration frequencies (0.1 - 7 Hz).

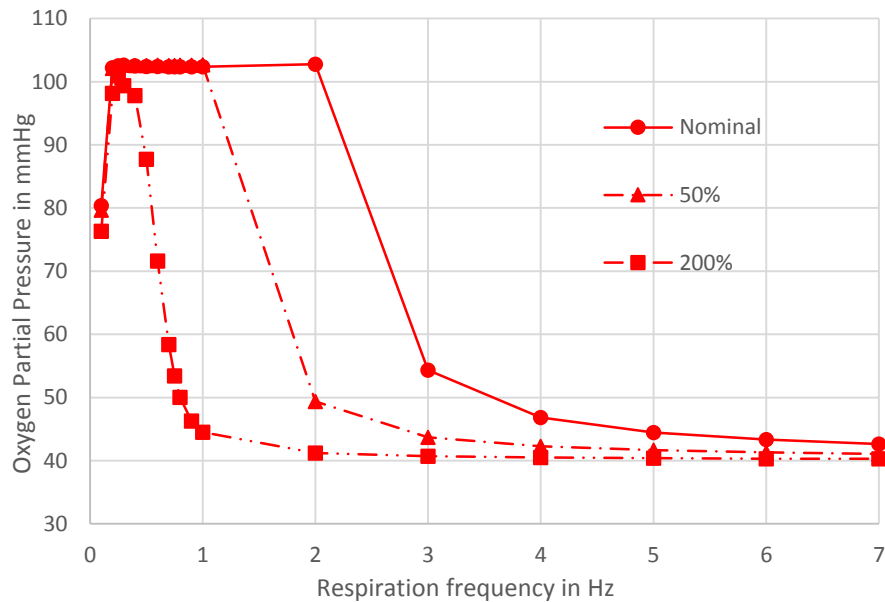


Figure 5-7: Sensitivity of oxygenation on the airway resistance over a frequency sweep, at nominal values of pressure amplitude and compliance, for an adult male (20 years old).

As the airway resistance increases, the range of frequencies for optimal oxygenation decreases as seen in figure 5-7. The optimal oxygenation frequency shifts to the left meaning that a subject suffering an obstructive disease tends to breaths slower

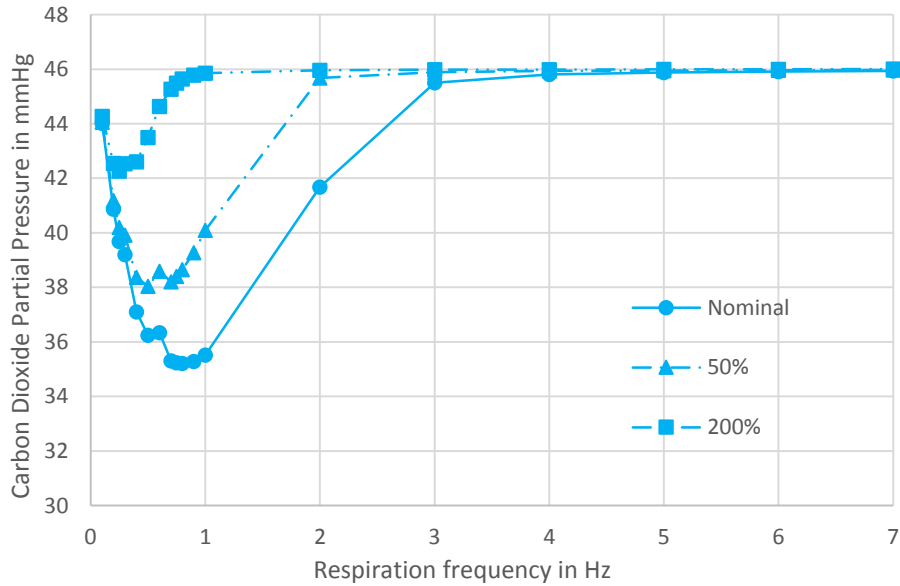


Figure 5-8: Sensitivity of ventilation on the airway resistance over a frequency sweep, at nominal values of pressure amplitude and compliance, for an adult male (20 years old).

than a normal subject. Increasing the resistance by 50 % is not a problematic since the subject can still breath at certain frequencies with an optimal gas exchange. This range can be determined from figure 5-8 to be 0.25 - 1 Hz. So the subject can be qualified as any normal subject breathing at the nominal 12 breaths per minute. However, he might suffer when doing a physical activity since his frequency of respiration can be higher than 1 Hz during exercise. This can be the case of a person with asthma. When the airway resistance increases significantly ( 200 % and more), gas exchange will be altered for all frequencies. This can be the case of a severe obstructive disease. Finally, the optimal ventilation frequency also shifts to the left as expected.

We have seen the effect of the pressure amplitude, the tissue compliance and the airway resistance on the gas exchange. Although the results are physiological, we didn't provide an explanation for the observed behavior. The justification resides in going back to the lung mechanics and inspecting the change in the characteristic frequency. In the next section, an analytic expression of the tidal volume will be

derived using the derived solution of the lung mechanics model in chapter 3.1.5. The tidal volume expression will associate the characteristic frequency to the point of altered gas exchange

### 5.3 Derived Tidal Volume

The solution of the small signal dynamic model is presented in equation 3.34, and rewritten below:

$$V(t) = FRCe^{\frac{-t}{R_{AW}C_{tissue}}} + \frac{1}{R_{AW}} \int_0^t e^{\frac{-(t-\tau)}{R_{AW}C_{tissue}}} \delta P(\tau) d\tau$$

Evaluating the integral and simplifying the solution to only consider the quasi-steady behavior, we get the following:

$$V(t) = C_{tissue}(-P_{ip,max} + \frac{\Delta P[-2C_{tissue}f\pi R_{AW}\cos(2\pi ft) + \sin(2\pi ft)]}{1 + 4C_{tissue}^2 f^2 \pi^2 R_{AW}^2}) \quad (5.3)$$

The solution is the sum of two sinusoidal functions, depicting the oscillation of the lung volume. The tidal volume is the peak to peak value of the volume signal. To calculate it, we need to find adjacent maximum and minimum, and evaluate their difference. This can be done by finding the times  $t^*$ , for which the derivative of  $V(t)$  is zero. Using an efficient mathematical tool, the solution of the null derivative is as follows:

$$t^* = \frac{\text{Arctan}[2\pi f C_{tissue} R_{AW}] + k\pi}{2\pi f} \quad (5.4)$$

Where  $k$  is an integer. For  $k = 0$  and  $k = 1$ , we locate two successive minimum and maximum at  $t_1^*$  and  $t_2^*$ . An analytic expression of the tidal volume can then be calculated:

$$TV = |V(t_1^*) - V(t_2^*)|$$

This expression simplifies to the following:

$$TV = \frac{C_{tissue}\Delta P}{\sqrt{1 + 4C_{tissue}^2 f^2 \pi^2 R_{AW}^2}} \quad (5.5)$$



If we refer back to chapter 3.1.6, we deduce that:

$$TV = A_p L^* \quad (5.6)$$

The characteristic frequency is the solution of the following equation:

$$L^* = L_{pipe} \quad (5.7)$$

Multiplying both sides of the equation by  $A_p$  leads to the following:

$$A_p L^* = A_p L_{pipe}$$

$$TV = DV$$

$$\frac{TV}{DV} = 1$$

This proves that the cutoff in gas exchange ( $\frac{TV}{DV} = 1$ ) is equivalent to the characteristic frequency.

To explain the observed behavior of gas exchange in the previous section, we can plot the variation of the characteristic frequency as a function of  $\Delta P$ ,  $C_{tissue}$ , and  $R_{AW}$  for an adult male. Figures 5-9, 5-10, and 5-11 show the plots respectively.

From figure 5-9, when the pressure amplitude decreases, the characteristic frequency decreases, which explains the shift of the optimal oxygenation and ventilation frequency to the left in figures 5-3 and 5-4. Furthermore, the airflow expression at low frequency (equation 5.2) depends on the pressure amplitude (the airflow decreases with lower pressure amplitude), which explains the alteration of gas exchange at a given low frequency. From figure 5-10, we can see that a decrease of the compliance by 10 % does not significantly affect gas exchange since the characteristic frequency doesn't change significantly. However, gas exchange is expected to be significantly altered with very low tissue compliance as the shape of the curve indicates. The optimal frequencies of oxygenation and ventilation shift to the right with decrease in tissue compliance, because the effect of lung impedance on air flow is a more im-

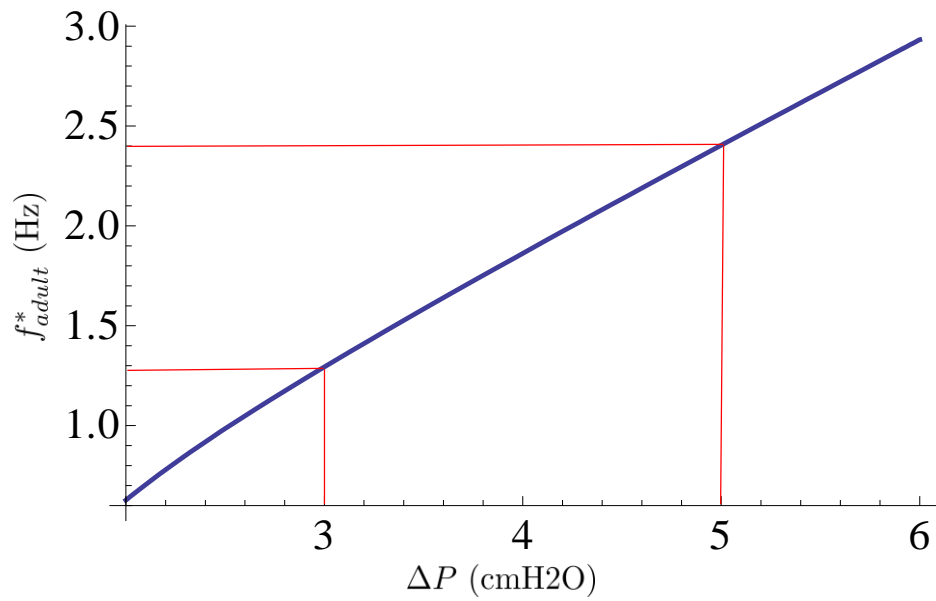


Figure 5-9: The characteristic frequency versus the pressure amplitude for an adult male. the red lines indicate the characteristic frequency at 5 cmH<sub>2</sub>O and 3 cmH<sub>2</sub>O.

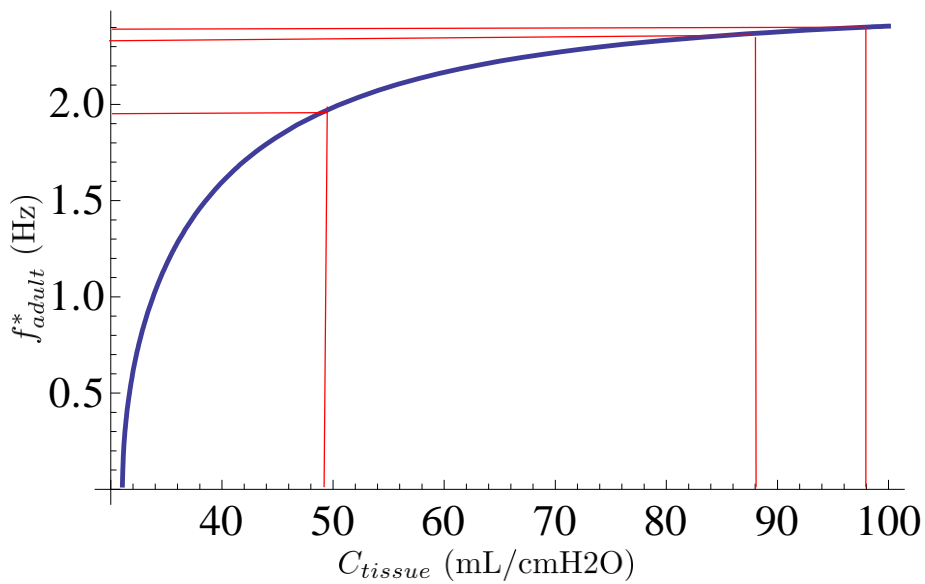


Figure 5-10: The characteristic frequency versus the tissue compliance for an adult male. The red lines indicate the characteristic frequency at nominal compliance, 10 % decrease, and 50 % decrease.

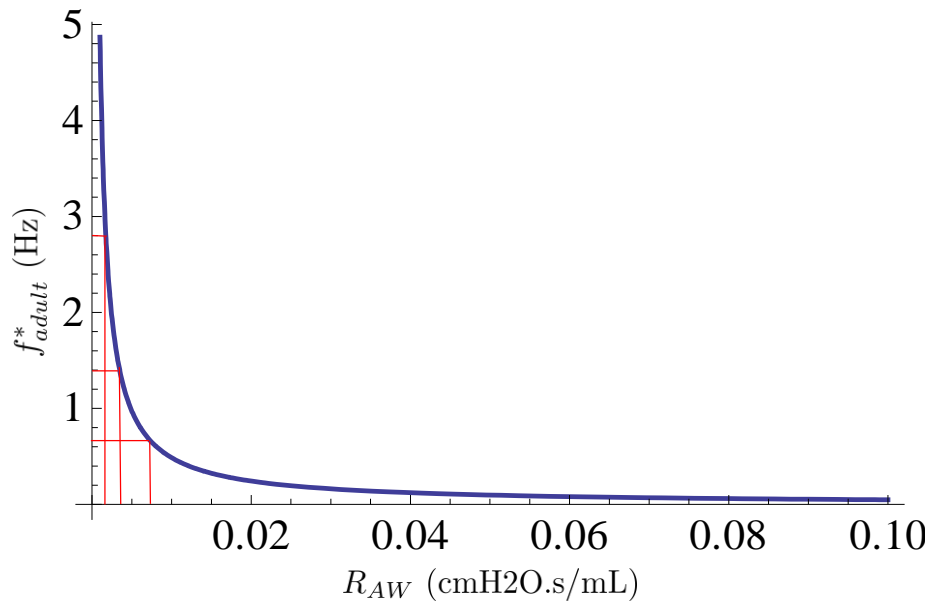


Figure 5-11: The characteristic frequency versus the airway resistance for an adult male. The red lines indicate the characteristic frequency at nominal resistance, 50 % increase, and 200 % increase.

portant effect than the characteristic frequency. In other words, when compliance decreases, the minimum frequency of optimal gas exchange shifts to the right more than the characteristic frequency shifts to the left (figure 5-5). From figure 5-11, the increase in airway resistance results in a decrease of the characteristic frequency which explains the shift of the optimal frequencies of oxygenation and ventilation to the left. At low frequencies, gas exchange remains unchanged, since the expression of the airflow rate doesn't depend on airway resistance.

Running a sensitivity analysis on an adult male, enables us to see the effects of some simplistic pulmonary diseases associated to a decrease in compliance or increase in resistance, on gas exchange. The coming chapter will consider the case of preterm infants suffering from a lack of surfactant, and will show the importance and significance of the high frequency oscillatory ventilation (HFOV) treatment.

# Chapter 6

## Scenario investigation

The main objective of the built physically-based lung model, is to investigate lung abnormalities and understand treatment approaches. Taking the case of preterm infants suffering respiratory distress syndrome (IRDS) due to the lack of surfactant in the linings of the alveoli, clinical practice heads to a treatment by high frequency oscillatory ventilation (HFOV), when the disease is severe enough. This chapter shows the physical reason behind adopting HFOV as a treatment, and its impact on oxygenation and ventilation.

### 6.1 Lack of surfactant in preterm infants

Infant respiratory distress syndrome (IRDS) is a serious disease that affects 1% of the preterm infants population [25]. The disease is characterized by the lack, or absence of surfactant in the linings of the alveoli, causing the lungs to collapse which eventually leads to the death of sick infants. Recall that the surfactant is a chemical substance that has the role to reduce the surface tension caused by the fluid surrounding the alveoli. This surface tension tends to close the alveoli, thus blocking fresh air to reach the gas exchange barrier. Preterm infants usually suffer lack, or absence of surfactant more than adults because the formation of surfactant in the lungs comes at the final stages of gestation, which means that a preterm infant has an increased chance of undeveloped surfactant in the alveoli.

Using the built model, consider a preterm infant (girl) suffering from absence of surfactant. This is the case of a severe IRDS where the surfactant concentration in the alveoli is zero. In the model, this corresponds to  $SF = 0$ . When there is no surfactant, the excess pressure on the alveoli due to surface tension is maximal. This means that the pressure needed to open the lungs is higher than 5 cmH<sub>2</sub>O. Therefore, a minimum airway pressure (MAP) is always needed to open the lungs in the absence of surfactant. Figure 6-1 below, shows the variation of  $P_{open}$  and the needed  $MAP$ , along with the decrease in tissue compliance  $C_{tissue}$  as a function of  $SF$  for the implemented model.

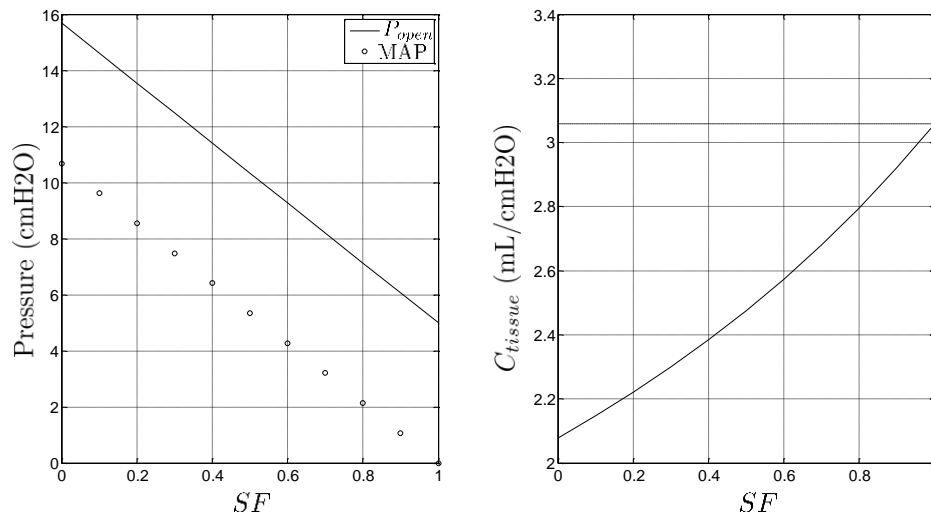


Figure 6-1: The implemented surfactant model. The left plot shows the open pressure (solid line) and the needed minimum airway pressure (line with circles) versus the surfactant fraction. The right plot shows the decrease in compliance with surfactant fraction (the nominal compliance level is at 3.05 mL/cmH<sub>2</sub>O).

The MAP needed for the considered case is about 10.7 cmH<sub>2</sub>O. The compliance decreases by about 32 % (2.07 mL/cmH<sub>2</sub>O) which is an underestimation of the possible decrease of compliance in preterm infants suffering the absence of surfactant (0.17 to 0.68 mL/cmH<sub>2</sub>O [8]). Nevertheless, the compliance can be controlled independently to mimic the IRDS cases found in literature.

An important consideration is the pressure volume model implemented in this scenario. Figure 6-2 shows a comparison between the p-V model for normally breathing preterm infant (shown in figure 3-1) and the one used for the sick preterm infant.

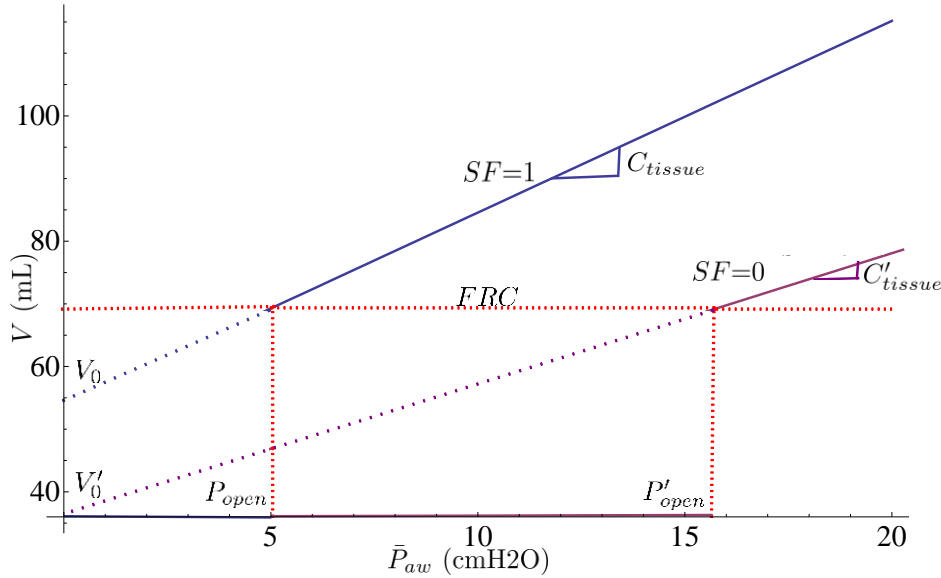


Figure 6-2: The implemented P-V model for the cases of normal presence of surfactant ( $SF=1$ ) and absence of surfactant ( $SF=0$ ). Sick Preterm infants have a higher open pressure equal to  $5 \text{ cmH}_2\text{O} + MAP$ , and a lower compliance shown in the flatter violet curve.

A linear relationship is assumed throughout the operating range of pressure. The lungs are considered blocked before  $P_{open}$ , and opened with  $FRC$  at the open pressure. The decrease in compliance corresponds to the change in the slope of the linear curve ( $C'_{tissue} < C_{tissue}$ ).

The sick preterm infant has definitely an altered gas exchange: Oxygen partial pressure in the blood is  $P_{O_{2,b}} = 74 \text{ mmHg}$ , and carbon dioxide partial pressure is  $P_{CO_{2,b}} = 44.5 \text{ mmHg}$ . The tidal volume of the sick preterm infant is  $TV = 10.14 \text{ mL}$ , giving  $\frac{TV}{DV} = 1.34$ . The reason behind altered gas exchange here is the increase of the impedance of the lungs and not the characteristic frequency. Equation 5.1 shows that the impedance of the lungs not only increase with low frequencies, but also with decreasing tissue compliance. Next, the sick preterm infant is treated with applied

oscillatory ventilation, and the reason behind using HFOV is explained.

## 6.2 High frequency oscillatory ventilation

High frequency oscillatory ventilation (HFOV) is a treatment approach that is based on mechanically ventilating a patient at frequency levels higher than 150 breaths per minute (or 2.5 Hz) [23]. In clinical practice, HFOV is considered as a mode of treatment used for unique patients suffering severe lack of surfactant that drastically disrupts gas exchange in the lungs. It is usually used for preterm infants with very little evidence of its usage for adults. Preterm infants are usually treated around 12 Hz with a sinusoidal flow waveform. It is claimed that HFOV operates at tidal volumes that go lower than the dead space volume. However, the mechanisms of gas exchange are not fully understood yet. An HFOV treatment is controlled with four different settings:

- The mean airway pressure  $P_{mean}$  which is a static pressure component around which the pressure signal oscillates. This component helps with the steady opening of the lungs at a given level where air can enter and reach the alveoli.
- The frequency of oscillation  $f$  which is the frequency at which the pressure signal is operating. The frequencies used for preterm infants is 12-15 Hz or less.
- The pressure amplitude  $\Delta P$  which is the amplitude of the oscillating pressure signal. In a typical HFOV,  $\Delta P$  swings around the mean airway pressure  $P_{mean}$
- The fraction of oxygen breathed  $f_{i,O_2}$  which is usually at 21 % in volume in the atmosphere. In HFOV, the ventilation provides a larger fraction of oxygen to improve oxygenation.

$P_{mean}$  and  $\Delta P$  are critical settings that needs to be minimized because high pressures can destroy the already weak and sick lung tissue. Since the physical mechanisms of HFOV are not yet fully understood, it is only used in clinical practice when it is found to promote gas exchange at acceptable levels of  $P_{mean}$  and  $\Delta P$ .

Back to our scenario of the sick preterm infant with no surfactant, the HFOV parameters in the present model are defined in a way to mimic the actual treatment: The frequency, pressure amplitude, and oxygen fraction can be directly controlled. However, the pressure signal oscillates just above the level of  $P_{open}$  so that the lungs will remain opened at all times. To have an identical HFOV approach, the mean airway pressure is composed of a static term  $P_{open} = -P_{ip,max} + MAP$ , and also depends on  $\Delta P$  as follows:

$$P_{mean} = -P_{ip,max} + MAP + \frac{1}{2}\Delta P \quad (6.1)$$

$MAP$  can be controlled in order to observe the effect of changing  $P_{mean}$  for a given treatment. The objective of this scenario is to find the physical reason behind adopting an HFOV treatment, by investigating gas exchange and lung mechanics.

### 6.3 Optimal frequency of oscillation

The sick preterm infant requires a  $MAP$  of 10.7 cmH<sub>2</sub>O to properly open the lungs. The question is: Why can't we induce a pressure signal that is oscillating at the nominal frequency of respiration (0.75 Hz) and the nominal pressure amplitude (5 cmH<sub>2</sub>O), given that we have opened the lungs with  $MAP$ ? The answer lies in what happens to the tissue compliance. In fact, the sick preterm infant has a reduced tissue compliance which negatively impacts gas exchange for two cases: increasing the lung impedance at low frequencies ( $f \ll \frac{1}{2\pi f R_{AW} C_{tissue}}$ ), and decreasing the tidal volume at high frequencies ( $f > f_{infant}^*$ ) (see chapter 5). Increasing the pressure amplitude is a necessity in both cases: at low frequencies, a higher pressure amplitude leads to a higher flow rate ( $\frac{dV}{dt} = 2\pi f C_{tissue} \frac{\Delta P}{2} \sin(2\pi f t)$ ) thus lowering the effect of the lung impedance, at high frequencies, a higher pressure increases the characteristic frequency (figure 5-9). It follows that as the frequency increases, the pressure amplitude must decrease when we are operating in the first case, and then increase when we are operating in the second case. Consequently, there should be an optimal frequency of



oscillation for which the pressure amplitude is minimal. To confirm this analysis, a pressure signal is induced on the sick preterm infant with the minimum needed  $P_{mean}$  ( $MAP = 10.7$ ) and the atmospheric oxygen content  $f_{i,O_2} = 21\%$ . Starting with the nominal frequency of respiration (0.75 Hz), the pressure amplitude is swept to find the minimum  $\Delta P$  needed, to rescue the infant by optimizing gas exchange (oxygen at saturation and carbon dioxide at 40 mmHg). Then, the frequency is increased, and the same process is repeated to find the new  $\Delta P$ . The result is plotted in figure 6-3.

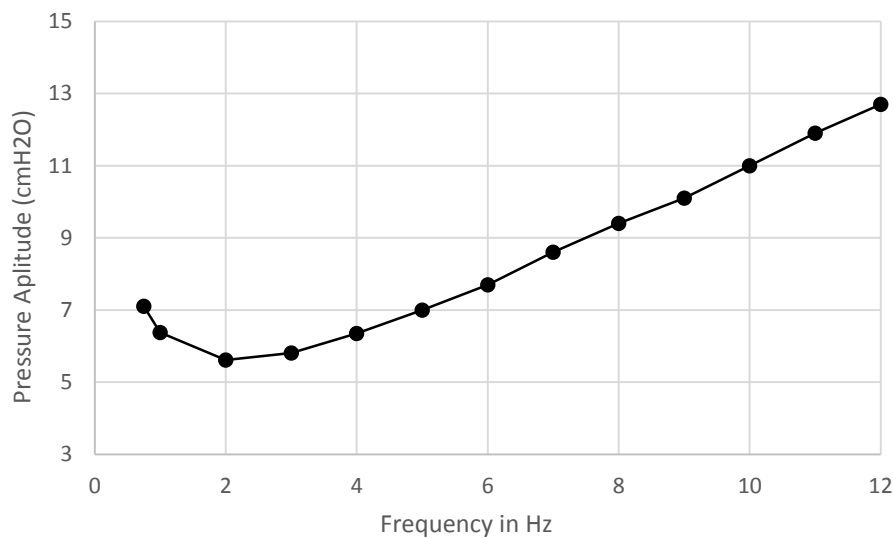


Figure 6-3: Plot showing the pressure amplitude as a function of frequency to yield an optimal gas exchange (proper oxygenation and ventilation) for the sick preterm infant.  $MAP=10.7$  cmH2O  $f_{i,O_2}=21\%$

The plot shows that there is a frequency that is higher than the nominal breathing frequency, for which the needed pressure amplitude for optimal gas exchange is minimal. this frequency is the mentioned optimal frequency of oscillation, and the above analysis is verified. The optimal frequency of oscillation for the sick preterm infant is at 2 Hz, and yields a minimum needed pressure amplitude of 5.6 cmH2O. Recall that the infant's compliance is reduced only by 32 % from the implemented model. In reality, the compliance of a severely sick preterm infant is reduced by 70-90 %. Manually reducing the compliance to such low value, and regenerating plots for

optimal HFOV treatment, shifts the optimal frequency of oscillation to the right (see figure 6-4). The tidal volume  $TV$  and the mean airway pressure  $P_{mean}$  are also plotted for the optimal HFOV treatment in figures 6-5 and 6-6 below.

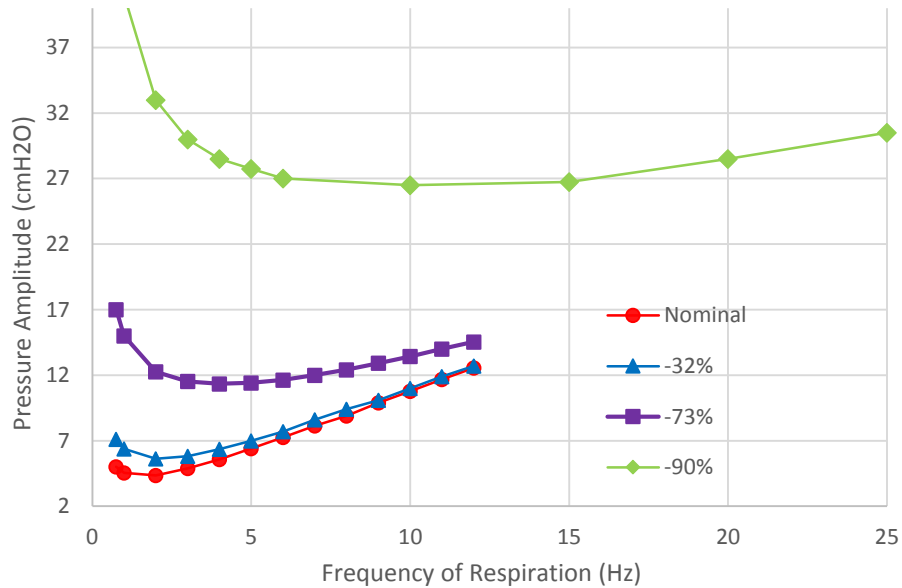


Figure 6-4: Plot showing the pressure amplitude as a function of frequency to yield an optimal gas exchange for several compliance levels.  $MAP=10.7$  cmH<sub>2</sub>O  $f_{i,O_2}=21$  %

For a 73 % decrease of the compliance, the optimal frequency of oscillation is at 4 Hz with a minimal pressure amplitude of 11.3 cmH<sub>2</sub>O. For a 90 % decrease, the optimal frequency is somewhere in the range of 10-15 Hz with a minimal pressure amplitude of 27 cmH<sub>2</sub>O. Figure 6-4 also shows that a sicker subject requires a higher pressure amplitude for HFOV. The results justify the use of HFOV to treat the sick preterm infants. A high frequency of oscillation is needed if the pressure amplitude and the mean airway pressure on the sick lung are to be minimal (figures 6-4 and 6-6). Furthermore, the sicker the baby, the higher the frequency of oscillation, and the higher the minimal pressure amplitude. Interestingly, figure 6-5 shows that the tidal volume of sick infants is only frequency dependent in HFOV treatments and does not depend on the tissue compliance. Based on this finding, an analytic expression that generates an optimal HFOV treatment can be derived. The plots of figure 6-5 are

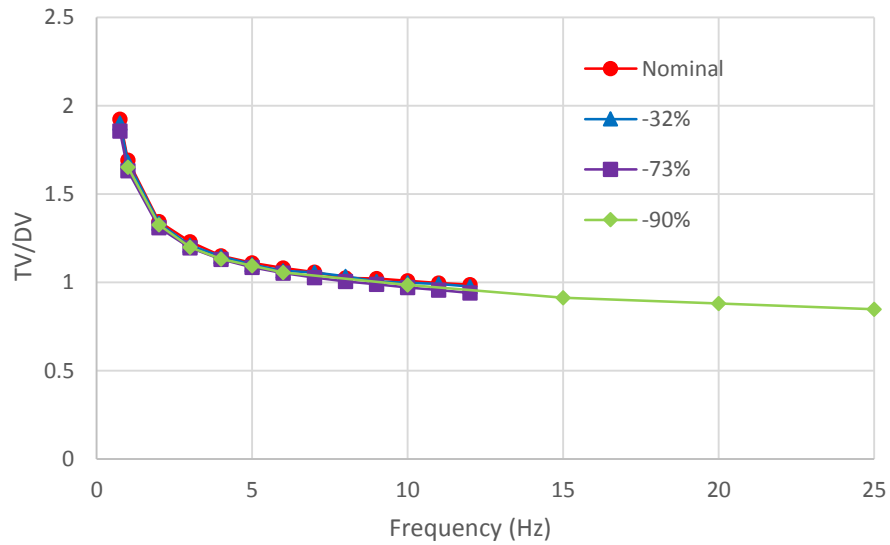


Figure 6-5: Plot showing the ratio of tidal volume to dead space volume as a function of frequency to yield an optimal gas exchange for several compliance levels.  $MAP=10.7 \text{ cmH}_2\text{O}$   $f_{i,O_2}=21 \%$

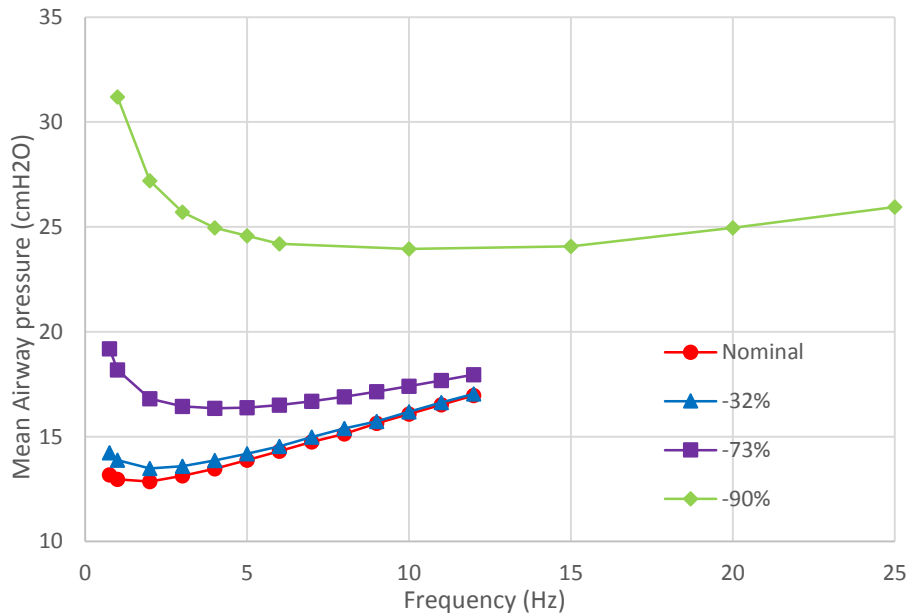


Figure 6-6: Plot showing the mean airway pressure as a function of frequency to yield an optimal gas exchange for several compliance levels.  $MAP=10.7 \text{ cmH}_2\text{O}$   $f_{i,O_2}=21 \%$

well fitted with a power function with 97 % confidence, to give an expression for the tidal volume  $TV^*$  for optimal HFOV treatment:

$$\frac{TV^*}{DV} = 1.5347f^{-0.193} \quad (6.2)$$

The tidal volume is already derived:

$$TV = \frac{C_{tissue}\Delta P}{\sqrt{1 + 4C_{tissue}^2 f^2 \pi^2 R_{AW}^2}}$$

An optimal HFOV treatment occurs for the following expression of pressure amplitude  $\Delta P_{opt}$ :

$$\Delta P_{opt} = \frac{1.5347DVf^{-0.193}}{C_{tissue}} \sqrt{1 + 4\pi^2 f^2 \tau_{RC}^2} \quad (6.3)$$

We can use equation 6.3 to find the optimal frequency of oscillation by solving:

$$\frac{d\Delta P_{opt}}{df} = 0$$

The optimal frequency of oscillation correspond to a tidal volume to dead space ratio higher than unity, for the cases of nominal compliance, 32 % decrease, and 73 % decrease. However, for the severe case of IRDS modeled by a 90 % decrease in tissue compliance (0.3 mL/cmH<sub>2</sub>O), optimal HFOV treatment points start occurring at levels where  $\frac{TV}{DV} \leq 1$ . This validates the fact that HFOV rely on an optimal gas exchange by diffusion, and that is for severe cases of IRDS.

## 6.4 Effect on gas exchange

So far, optimal points of HFOV treatments yielding perfect gas exchange, were shown. The effect of the HFOV settings directly on oxygenation and ventilation is investigated in this section. The sick preterm infant defined in this chapter (-32% compliance), with  $MAP$  of 10.7 cmH<sub>2</sub>O, is considered. To observe the effect of  $f$ ,  $\Delta P$ , and  $f_{i,O_2}$ , oxygenation and ventilation are recorded as a function of  $\Delta p$ , for different values of  $f$  starting from the optimal frequency of oscillation, and for different values of  $f_{i,O_2}$

(figures 6-7 and 6-8):

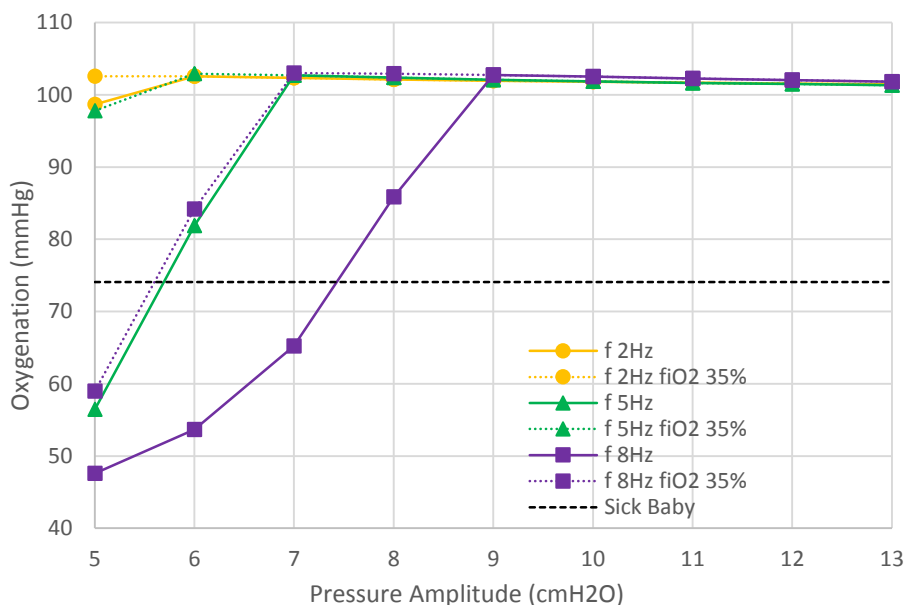


Figure 6-7: The effect of the pressure amplitude (x-axis), frequency (legends) and breathed fraction of oxygen (legend) on oxygenation, for a sick preterm infant (-32 %  $C_{tissue}$ ), with  $MAP=10.7$  cmH2O. The black dashed line indicates the oxygen level of the sick infant

For a given frequency, oxygenation and ventilation are improved with an increasing pressure amplitude. Oxygen reaches a plateau at 102 mmHg meaning that the hemoglobin is fully saturated and no more oxygen is delivered to the blood. Carbon dioxide's partial pressure keeps decreasing below 40 mmHg causing a hyperventilation. In normal breathing, chemical receptors in the blood always prevent hyperventilation by regulating  $P_{CO_{2,b}}$  around 40 mmHg, but, when a forced ventilation is imposed on a sick patient, hyperventilation can be induced. In figure 6-7, all the points reaching a saturation of the blood with oxygen, are determined by  $\frac{TV}{DV} \geq 1$ . Similarly in figure 6-8, point of  $P_{CO_{2,b}} \leq 40$  are determined by  $\frac{TV}{DV} \geq 1$ . For a 32 % decrease in compliance, we can deduce that an optimal HFOV treatment requires the arrival of fresh air to the alveoli, or, in other words, exchange by advection. Gas exchange by diffusion can help the sick preterm infant, however, no such point gives an optimal HFOV. For a given pressure amplitude, oxygen's partial pressure decreases and carbon dioxide's

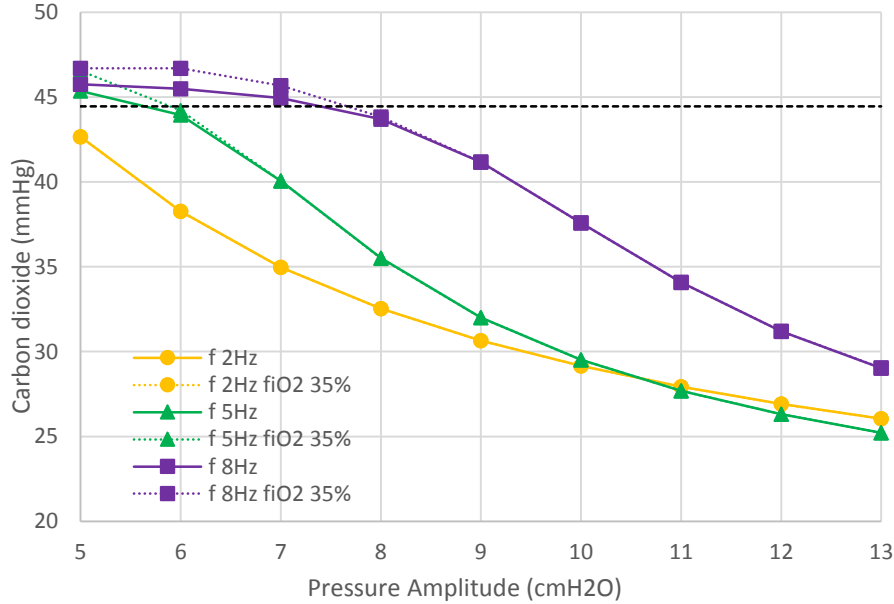


Figure 6-8: The effect of the pressure amplitude (x-axis), frequency (legends) and breathed fraction of oxygen (legend) on ventilation, for a sick preterm infant (-32 %  $C_{tissue}$ ), with  $MAP=10.7$  cmH2O. The black dashed line indicates the carbon dioxide level of the sick infant

partial pressure increases respectively with frequency, when  $\frac{TV}{DV} < 1$ . An interesting exception is seen in figure 6-8, at  $\Delta P = 11$  cmH2O, where carbon dioxide removal is more important at a higher frequency. But this observation cannot lead to any definitive conclusion. Increasing the fraction of inspired oxygen, obviously enhances oxygenation levels for any given pressure amplitude, but has no or little effect on ventilation. In fact, at low pressure amplitude, carbon dioxide removal is further impeded for the enhanced oxygenation. The optimal HFOV treatments plotted in figure 6-3, are determined by ventilation and not oxygenation, because oxygen reaches the plateau of 102 mmHg before carbon dioxide reaches 40 mmHg in the blood. Increasing  $f_{i,O_2}$  can be useful in cases where HFOV is optimal for ventilation but hemoglobin is not fully saturated in the blood, but none of these cases were encountered in the simulated results.

The remaining setting of HFOV is the mean airway pressure  $P_{mean}$ .  $P_{mean}$  in our model has the same effect than  $\Delta P$  if we refer to equation 6.1. But, the static

component of  $P_{mean}$ , which is  $MAP$ , has no effect whatsoever on gas exchange. The reason is simply looking at the solution of lung mechanics for the quasi-steady state of interest; all the static components including  $MAP$  disappear from the solution. But this doesn't mean that  $MAP$  is useless for HFOV treatments, it is a requirement to open the lungs that are otherwise collapsed from lack of surfactant.

# Chapter 7

## Conclusion

### 7.1 Effective summary

In this thesis, a physically-based lung model was constructed for the main purpose of understanding the physical mechanisms underlying respiratory abnormalities and treatments. Besides this, the model is built in a way to cover a wide span of subjects and lung parameters, and can be used as an efficient tool in academics and clinical practice. The model relies on background data from respiration physiology, and is unique in its nature as it solves the spatial and temporal distribution of oxygen and carbon dioxide, from the onset of the airway openings, to the blood in the pulmonary capillaries, where gas exchange occurs. A viscoelastic model accounting for the airway resistance and the tissue compliance, is implemented to cover the lung mechanics by relating the pressure signal to the change in the lung volume. The advection-diffusion equation is solved in its complete form to obtain the spatial distribution of respiratory gases in the airways. The blood content in oxygen and carbon dioxide is determined by solving another advection-diffusion equation in a Lagrangian reference frame, coupled with the non-linear dissociation curves, that relate oxygen and carbon dioxide's concentrations and partial pressures. The air side and the blood side are coupled through the non-steady conservation equation in the alveoli. The equations governing lung mechanics, airways, alveoli, and blood, are solved simultaneously in an iterative numerical approach. Estimating lung parameters such as the lung volumes,



number of alveoli, alveolar membrane, blood flow and capillary distribution, is done by integrating appropriate models verified with literature. The simulation interface of the built model provides the choice to run normal breathing, or imposed breathing simulations. Through normal breathing, the model is validated with knowledge acquired from respiration physiology. The imposed breathing is useful to undergo sensitivity analysis and treatment cases. Two typical subjects representing preterm infants and adults were considered to study the breathing performance in terms of gas exchange. The effect of respiration frequency, pressure amplitude, tissue compliance, and airway resistance on gas exchange was inspected, with a justification from the implemented lung mechanics model. The analysis helped understand the physical mechanisms of simplistic lung abnormalities related to a decrease in tissue compliance (constrictive diseases, IRDS), or increase in airway resistance (obstructive diseases, asthma). Finally, a scenario of a preterm infant suffering from a severe IRDS was considered, to reveal some of the mechanisms behind using HFOV treatment. The need to ventilate at high frequency to try to minimize the applied pressure on the sick lung, is justified through simulations and analysis of the lung mechanics model. The effect of HFOV settings on gas exchange was then studied.

## 7.2 Future directions

Future directions to this project are numerous, since the lung model is comprehensive enough to carry out several research studies and investigations. They can be summarized under two main categories: model refinement and experimentation. The first category enhances the robustness and validity of the model. The second category puts the model into practice in the clinical discipline.

### Model refinement

The lung mechanics model can be extended to include the case of over stretched lungs, where the pressure volume relationship becomes non-linear at a high enough airway pressure. This will lead to solving the small signal dynamic model with a variable tissue compliance. Besides the resistance and compliance, an inductance can

be added to the lung mechanics to show the effect of air density on the breathing performance. This is important in cases of treatments with changed fraction of gases in the inspired air to induce a smoother inspiration. For example, breathing oxygen with helium is less dense than breathing oxygen with nitrogen, hence, the work of the lungs can be reduced. As seen in the scenario of chapter 6, the surfactant model underestimates the decrease in compliance, it needs to be enhanced by investigating other possible parameters that may further reduce the tissue compliance in the absence of surfactant.

The airways are currently modeled as a bundle of parallel tubes of equivalent airway resistances. This model can be changed into a more realistic one that mimics the several generations of the bronchial tree. Each generation consists of a certain compliance and resistance. The work of Ionescu *et al* [16], can support the new model. In reality, the lungs are asymmetric elements. For example, in a case of alveolar collapse, not all alveoli become dysfunctional, the lung can be damaged only in specific regions while it still operates normally in other regions. This asymmetry can be accounted for once the resistance and compliance of an airway generation are not identical.

Regarding the blood side, a cardiovascular model can be integrated to the lung model to enhance the solution of gas contents in the blood. The cardiac output is equivalent to the blood flow rate entering the lungs since all the pumped blood from the heart passes first by the lungs. The cardiac output will be useful to calculate the resident time in the pulmonary capillaries, once the blood volume is found. This can improve the blood flow model currently used in this work. Besides, shunt portions of the blood (subject to no gas exchange) can be considered in the cardiovascular model, thus simulating lung diseases related to blood perfusion.

### Experimentation

Once the physical mechanisms of lung abnormalities are fully understood, a lung disease is accurately simulated, and the built model can be correlated with actual medical records and data for sick subjects. This puts the model in practice for clinicians. Appendix A is a brief introduction to the disease types that can be encountered

in lung physiology. It can be considered as a starting point for disease investigation.

# Appendix A

## An overview on lung diseases

Lung diseases alter the physiological levels of oxygen and carbon dioxide in the blood. The severity of some diseases can cause death if appropriate treatment is not considered. Typical lung diseases will be briefly explained and categorized based on their impact on lung parameters. The information provided in this appendix is highly based on [14].

In general, respiratory disorders come from either an inadequate ventilation (hypoventilation), irregularities in the diffusion process across the pulmonary membrane, or abnormalities on the blood side of the respiratory system. Accordingly, several substantial parameters determines the status of these disorders; some of them are the airway resistance, the tissue compliance, the alveolar membrane or the exchange surface area, the blood flow, and the binding capacity of hemoglobin.

### Diseases that affect airway resistance

Every disease that causes a contraction of the airways (trachea, bronchi, and bronchioles) is one that increases the airways resistance. Asthma is an example in which bronchioles are partially obstructed by spastic contraction of smooth muscles. It belongs to a bigger group of diseases under the name of airway obstructive diseases. They are known for an easy inspiration followed by a harder expiration since, during expiration, there is a positive pressure in the lung tissues that further obtrude the airways. A harder expiration causes air to be trapped in the lungs with time, thus increasing residual volume and total lung capacity. Examples of serious obstructive

diseases are atelectasis and emphysema.

#### Diseases that affect tissue compliance

The lung compliance is the measure of how much the lungs can expand per unit of pressure. In constricted lung diseases, the lung volume can't reach normal values due to a decreased lung compliance. These types of diseases can be fibrotic (tuberculosis, silicosis) or related to the respiratory muscles of the chest cage (kyphosis, scoliosis, fibrotic pleurisy). Atelectasis is another serious disease that, besides closing the airways, causes the alveoli to collapse. It is also characterized by a lack of surfactant in the linings of the alveoli that leads to the filling of alveoli with fluid. Lobes of the lungs can become totally dysfunctional leading to a significant decrease in the lung compliance.

#### Diseases that affect the pulmonary membrane for gas exchange

Some diseases lead to the total destruction of alveolar regions, thus decreasing the surface contact area of gas exchange. An example is pneumonia where the alveolar membrane becomes porous and allows fluid and red blood cells to enter and fill the alveoli. Consequently, parts of lungs will not be aerated properly, and blood will be under-saturated with oxygen ( $S = 60\%$ ). Another dangerous disease originating from long term smoking is the chronic pulmonary emphysema. It leads to the destruction of 50 to 80 % of the alveolar walls yielding in serious lack of oxygen and excess of carbon dioxide.

#### Diseases that affect the blood flow and hemoglobin function

All the above mentioned diseases are based on the air side of the respiratory system. Other diseases such as sickle-cell anemia and cardiac shunts are related to the blood side. In sickle-cell anemia, there is a lack of functional hemoglobin causing a poor transport of oxygen to the tissues. Consequently, the percent of oxygen-saturated hemoglobin in the blood only reaches a maximum of 60 % rather than 97 % in a healthy subject. Cardiac shunts are characterized by a complete or partial blockage of arteries or veins connecting the heart to the pulmonary region. The blood flow in the pulmonary capillaries is reduced in these types of diseases.

Most of the lung diseases cause a lack of oxygen or hypoxia more than an excess

of carbon dioxide or hypercapnia. That's why treatments usually head to oxygen therapy. Oxygen therapy is the treatment of the patient with 100 % oxygen through a mask or in a medical tent. This kind of therapy isn't guaranteed to work expect for the abnormalities that originates from insufficient levels of inspired oxygen in the atmosphere. Other therapies rely on applying a positive pressure on the airway openings, with an oscillating signal, to aid the opening of the lungs and optimize gas exchange. This kind of therapies such as CPAP and HFOV, is proved to be helpful especially for lungs with low compliance.



# Appendix B

## Detailed derivation of the ODC

The derivation of the explicit relation of the ODC is based on the balance equations of the chemical reactions that relate oxygen, carbon dioxide, hydrogen ions, and hemoglobin in the blood [26]. Table B.1 and table B.2 show respectively the needed concentrations and the chemical reactions along with their balance equations.  $k_i$  and  $k'_i$  are respectively the association and dissociation rate constants of reaction  $i$  in table B.2.

Concentration $[X]$	Symbol
$[O_2]$	$C_1$
$[O_2HbNH_3^+]$	$C_2$
$[O_2HbNH_2]$	$C_3$
$[O_2HbNHCOO^-]$	$C_4$
$[CO_2]$	$C_5$
$[HbNHCOO^-]$	$C_6$
$[HCO_3^-]$	$C_7$
$[H^+]$	$C_8$
$[HbNH_3^+]$	$C_9$
$[HbNH_2]$	$C_{10}$

Table B.1: Concentration definition for the derivation of the ODC

The combination of oxygen with hemoglobin is a first step kinetic reaction of order  $n$  to account for the sigmoidal shape of the dissociation curve (balance equation for



$i$	Chemical reaction	Balance equation
1	$HbNH_2 + H^+ \rightleftharpoons HbNH_3^+$	$k_1 C_8 C_{10} = k'_1 C_9$
2	$O_2 HbNH_2 + H^+ \rightleftharpoons O_2 HbNH_3^+$	$k_2 C_8 C_3 = k'_2 C_2$
3	$HbNH_2 + O_2 \rightleftharpoons O_2 HbNH_2$	$k_3 C_1^n C_{10} = k'_3 C_3$
4	$H^+ + HCO_3^- \rightleftharpoons CO_2 + H_2O$	$k_4 C_8 C_7 = k'_4 C_5$
5	$HbNH_2 + CO_2 \rightleftharpoons HbNHCOO^- + H^+$	$k_5 C_5 C_{10} = k'_5 C_6 C_8$
6	$O_2 HbNH_2 + CO_2 \rightleftharpoons O_2 HbNHCOO^- + H^+$	$k_6 C_5 C_3 = k'_6 C_4 C_8$

Table B.2: Chemical reactions and balance equations in the blood

$i=3$  in table B.2). The total hemoglobin concentration  $H$ , in the blood is:

$$H = C_2 + C_3 + C_4 + C_6 + C_9 + C_{10} \quad (B.1)$$

The concentration of oxygenated hemoglobin  $H_{ox}$ , in the blood is:

$$H_{ox} = C_2 + C_3 + C_4 \quad (B.2)$$

Therefore, the hemoglobin saturation with oxygen  $S$  in percent can be written as follows:

$$S = 100 \frac{H_{ox}}{H} \quad (B.3)$$

It is assumed that the uptake of oxygen by hemoglobin is determined by the following relation,  $k$  and  $l$  being constants:

$$k_3 = k C_8^l \quad (B.4)$$

The pH is related to the hydrogen ions concentration  $C_8$ :

$$pH = -\log C_8 \quad (B.5)$$

So

$$C_8 = 10^{-pH}$$

Let  $K_i = \frac{k_i}{k'_i}$ , and  $K' = \frac{k}{k_3}$ , then equation B.4 can be rewritten as:

$$K_3 = K'10^{-pH} \quad (\text{B.6})$$

The partial pressures of oxygen and carbon dioxide in the blood can be related to their respective concentrations through oxygen solubility  $\alpha$  and carbon dioxide solubility  $\gamma$ :

$$C_1 = \alpha P_{O_2,b} \quad (\text{B.7})$$

$$C_5 = \gamma P_{CO_2,b} \quad (\text{B.8})$$

Finally, let  $K = K'\alpha^n$ , using the balance equations and combining all the aforementioned equations, the explicit relation of the ODC is derived:

$$S = 100 \frac{K_0 P_{O_2,b}^n}{1 + K_0 P_{O_2,b}^n}$$

$$K_0 = \frac{(1 + 10^{-pH} K_2 + \frac{\gamma K_6 P_{CO_2,b}}{10^{-pH}}) K 10^{l pH}}{1 + 10^{-pH} K_1 + \frac{\gamma K_5 P_{CO_2,b}}{10^{-pH}}}$$



# Bibliography

- [1] A Athanasiades, F Ghorbel, JW Clark Jr, SC Niranjana, J Olansen, JB Zwischenberger, and A Bidani. Energy analysis of a nonlinear model of the normal human lung. *Journal of Biological Systems*, 8(02):115–139, 2000.
- [2] JM Bogaard, SE Overbeek, AF Verbraak, C Vons, HT Folgering, Th W van der Mark, CM Roos, and PJ Sterk. Pressure-volume analysis of the lung with an exponential and linear-exponential model in asthma and copd. dutch cnsld study group. *European Respiratory Journal*, 8(9):1525–1531, 1995.
- [3] Ibrahim Chamseddine. A model of neonatal oxygenation covering the dynamics of alveolus. Master’s thesis, American University of Beirut, 2013.
- [4] Nicolas W Chbat, Massimo Giannessi, Antonio Albanese, and Mauro Ursino. A comprehensive cardiopulmonary simulation model for the analysis of hypercapnic respiratory failure. *International Conference of the IEEE EMBS*, 2009.
- [5] CD Cook, JM Sutherland, S Segal, RB Cherry, J Mead, MB McIlroy, and CA Smith. Studies of respiratory physiology in the newborn infant. iii. mmeasurement of mechanics of respiration. *Journal of Clinical Investigation*, 36(3):440, 1957.
- [6] M.C. Hart M.M. Orzalesi C>D. Cook. Relation between anatomic respiratory dead space and body size and lung volume. *Applied Physiology*, 18:519–522, 1963.
- [7] Wilburta Q. Lindh Marilyn Pooler Carol Tamparo Barbara M. Dahl. *Delmar’s Comprehensive Medical Assisting: Administrative and Clinical Competencies*. Cengage Learning, 2009.
- [8] HL Dorkin, AR Stark, JW Werthammer, DJ Strieder, JJ Fredberg, ID Frantz, et al. Respiratory system impedance from 4 to 40 hz in paralyzed intubated infants with respiratory disease. *Journal of Clinical Investigation*, 72(3):903, 1983.
- [9] KM Flegal and Tj Cole. Construction of lms parameters for the centers for disease control and prevention 2000 growth chart, August 2009.
- [10] Raymond W Flumerfelt and Edward D Crandall. An analysis of external respiration in man. *Mathematical Biosciences*, 3:205–230, 1968.

- [11] Alan D Freed, JP Carson, DR Einstein, and Rick E Jacob. Viscoelastic model for lung parenchyma for multi-scale modeling of respiratory system phase ii: Dodecahedral micro-model. *Pacific Northwest National Laboratory (Battelle)*, 2012.
- [12] Fabrizio Gaudenzi and Alberto P Avolio. Lumped parameter model of cardiovascular-respiratory interaction. *International Conference of the IEEE EMBS*, 2013.
- [13] H Guenard, N Varene, and P Vaida. Determination of lung capillary blood volume and membrane diffusing capacity in man by the measurement of no and co transfer. *Respiration Physiology*, 70:113–120, 1987.
- [14] John E. Hall Arthur C. Guyton. *Guyton and Hall Textbook of Medical Physiology*. William Schmitt, 2011.
- [15] J Hildebrandt. Comparison of mathematical models for cat lung and viscoelastic balloon derived by laplace transform methods from pressure-volume data. *The Bulletin of mathematical biophysics*, 31(4):651–667, 1969.
- [16] Clara-Mihaela Ionescu, W Kosinski, and Robain De Keyser. Viscoelasticity and fractal structure in a model of human lungs. *Archives of Mechanics*, 62(1), 2010.
- [17] D. W. Kaczka, E. P. Ingenito, B. Suki, and K. R. Lutchen. Partitioning airway and lung tissue resistances in humans: effects of bronchoconstriction. *Journal of applied physiology (Bethesda, Md. : 1985)*, 82(5):1531–1541, May 1997.
- [18] CH Liu, SC Niranjana, JW Clark, KY San, JB Zwischenberger, A Bidani, et al. Airway mechanics, gas exchange, and blood flow in a nonlinear model of the normal human lung. *Journal of applied physiology*, 84(4):1447–1469, 1998.
- [19] K Lu, JW Jr Clark, FH Ghorbel, DL Ware, JB Zwischenberger, and A Bidani. Whole-body gas exchange in human predicted by a cardiopulmonary model. *Cardiovascular Engineering: An International Journal*, 3(1):1–19, 2003.
- [20] Felix Meade. A formula for the carbon dioxide dissociation curve. *British Journal of Anaesthesia*, page 630, 1972.
- [21] SC Niranjana, A Bidani, F Ghorbel, JB Zwischenberger, and JW Clark Jr. Theoretical study of inspiratory flow waveforms during mechanical ventilation on pulmonary blood flow and gas exchange. *Computers and biomedical research*, 32(4):355–390, 1999.
- [22] G.J. Tammeling J.E. Cotes O.F. Pedersen R. Peslin J-C. Yernault Ph.H Quanjer. Lung volumes and forced ventilatory flows. *Eur Respir J*, 6:5–40, 1993.
- [23] Allan Prost. High frequency oscillation ventilation. Lecture, February 2011.

- [24] J. Stocks Ph.H. Quanjer. Reference values for residual volume, functional residual capacity and total lung capacity. *Eur Respir J*, 8:492–506, 1995.
- [25] RJ Rodriguez, RJ Martin, and AA Fanaroff. Respiratory distress syndrome and its management. *Neonatal-Perinatal Medicine. 8th ed. Philadelphia*, pages 1097–185, 2002.
- [26] M Sharan, M.P Singh, and A Aminataei. A mathematical model for the computation of the oxygen dissociation curve in human blood. *BioSystems*, 22:249–260, 1989.
- [27] P. Auld N.M. Nelson R.B. Cherry A.J. Rudolph C.A. Smith. Measurement of thoracic gas volume in the newborn infant. *Journal of Clinical Investigation*, 42(4), 1963.
- [28] William M Thurlbeck. Postnatal human lung growth. *Thorax*, 37:564–571, 1982.
- [29] HR van Genderingen, A Versprille, T Leenhoven, DG Markhorst, AJ van Vught, and RM Heethaar. Reduction of oscillatory pressure along the endotracheal tube is indicative for maximal respiratory compliance during high-frequency oscillatory ventilation: A mathematical model study. *Pediatric pulmonology*, 31(6):458–463, 2001.
- [30] Jonathan P Whiteley, David J Gavaghan, and Clive EW Hahn. Mathematical modelling of pulmonary gas transport. *Journal of mathematical biology*, 47(1):79–99, 2003.

